Temperature and Pressure Effects on Lateral Membrane Organization of Model and Natural Membrane Lipids and Lipid-Peptide and Lipid-Protein Interactions

DISSERTATION

zur Erlangung des akademischen Grades
Doktor der Naturwissenschaften
(Dr. rer. nat.)

vorgelegt von

Nagarajan Periasamy B.Pharmacy., M.E., M.Res.,

aus Mohanur, India

eingereicht bei der
Fakultät Chemie
der Technische Universität Dortmund

Dortmund 2007

Erstgutachter:	Prof. Dr. Roland Winter
Zweitgutachter:	Prof. Dr. Heinz Rehage
Dritter Prüfer:	PD. Dr. Claus Czeslik
Tag der mündlichen Prüfung:	28.01.2008

Dedicated to my dear parents

Acknowledgements

First of all I would like to express my gratitude to my supervisor Prof. Dr. Roland Winter for his continuous support and guidance starting from date first. I am very much pleased to carry out my doctoral research under his supervision and thankful to him for introducing me in the field of liposome research.

My special thanks to PD Dr. Claus Czeslik for his invaluable help in all the experimental part and fruitful discussions throughout this work.
I thank Prof. Dr. Heinz Rehage and PD Dr. Claus Czeslik for being members of the examination committee.

I would like to thank Prof. Dr. Heinz Rehage and Dr. Anuj Shukla for their help and cooperation in carrying out the DLS measurements.

I would like to thank Prof. Dr. Rudi F. Vogel and his group at the Technische Universität München for fruitful collaborations. I thank Holger Teichert at TUM who expressed and purified LmrA protein in order to carry out this project.

I would to thank Prof. Dr. E Gratton and his group at the LFD-University of California, Irvine, in particular Dr. Theodore L Hazlett (Chip), Dr. Susana Sanchez, Dr. Oliver Holub and Claudia Y. Lee for their help and cooperation in carrying out the 2-photon excitation fluorescence microscopy measurements.

I thank Michael Sulc, Vytautas Smirnovas, Shuang Zhao, Christoph Jeworrek, Suman Jha, Matthias Pühse, Christoph Jeworrek, Dr. Nadeem Javid, Dr. Ewa Powalska, Lally Mitra, Diana Radovan, Linus Okoro, Andrea Gohlke, Dr. Rajesh Mishra, Dr. Roland Krivanek, Dr. Jörg Baranski, Dr. Karsten Vogt, Dr. Guido Jackler, Dr. Monika Khurana, Gurpreet Singh, Maximilian Andrews, Oliver Hollmann and Christian Reichhart for providing a co-operative and diversely cultural working environment. I wish to thank Dr. Katrin Weise for performing AFM experiments and Daniel Sellin for translating my thesis summary (Zusammenfassung) in German. I thank my friend Mahesh Kulharia for his support and help.

I thank and appreciate Dr. Werner Horstmann, Andrea Kreusel, Bertina Schuppan, Kirsten Skodzik, Milan Saskovic for their help in official matters. I would like to thank the mechanical and electrical workshop people for their help in fixing and setting up many instruments.

I would like to thank the International Max-Planck Research School in Chemical Biology (IMPRS-CB) and Dr. Jutta Roetter for providing financial support in the beginning of my PhD.

I thank all my friends, living in Aldalbert Str. 149 who make my life more comfortable and giving me pleasant memories of my stay in Dortmund. Particularly I thank my friend Nageswaran Rajendran (Eswar) for his company and stimulating discussion in many topics from physics to philosophy.

I thank my fiancée, Vidyalakshmi Rajendran who is taking care of my personal work and supporting me throughout the last 2 years.

I thank and acknowledge my parents for their endless love and all support throughout my life, which is always driving me. I thank my brother and sister as well for their love which keeps me always happy.

Contents

1. Introduction

1.1 Biomembranes

Cell membranes constitute one of the fundamental structural and functional elements of living organisms. Most fundamentally, the plasma membrane of a cell denotes the outer boundary of the system and distinguishes between the inside and the outside of the system. Besides the plasma membrane, the eukaryotic cells have a number of well defined internal membranes associated with the cell nucleus and the organelles. Membranes thereby become the most abundant cellular structure in all living system. This compartmentalization allows different composition between the inside and outside of the system. Communication across the boundary becomes essential both for transport of nutrients and waste and for the cellular response to the external environments. These demands for a more complex membrane function than just creating the boundaries to system. Biological membranes consist of a macromolecular aggregate of lipids and proteins, their association with each other are governed largely by the hydrophobic effect. Once the membrane is formed it is further stabilized by hydrogen bonds, electrostatic attractions and van der Waals forces.

A simple but often used model which explains the gross organization and structure of the proteins and lipids of biological membranes is known as “fluid mosaic model” [1]. This model considers cell membranes as being a two dimensional fluid bilayer composed of phospholipids in which the proteins that are integral to the membrane are a heterogeneous set of globular molecules. The ionic and highly polar groups of the protein protruding from the membrane into the aqueous phase, and the non-polar groups are largely buried in the hydrophobic interior of the membrane. These globular molecules are partially embedded in a matrix of phospholipids. Hence, the bulk of the phospholipids are organized as a discontinuous, fluid bilayer. According to this model, membranes are a dynamic system in which proteins and lipids can move and interact. Besides proteins, the major components of natural membranes are lipids and cholesterol, with a small amount of other materials such as fatty acids. This model emphasizes that the membrane lipids do not form a homogenous phase consisting of lipids, cholesterol and proteins, but a mosaic of domains with unique compositions. The relative amounts of these components vary from membrane to membrane, and the type of lipids in membranes can also vary.

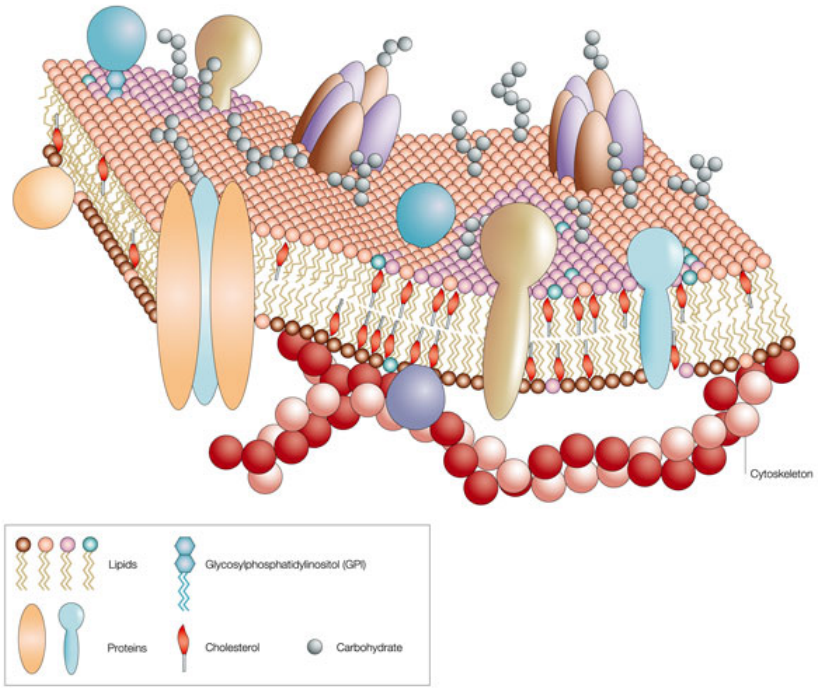

Figure 1.1: The Fluid-Mosaic-Model of the cell membrane [2]

The nature and concentration of lipids varies in both the inner and outer walls of the lipid bilayer in biomembranes [3]. From the current literature, it is evident that cholesterol and sphingolipids are abundant and restricted to the outer leaflet, and also it suggests that these lipids are not distributed uniformly but rather they cluster into domains called as lipid rafts. Lipid rafts have unique physicochemical properties that direct their organisation into liquid-ordered phases floating in a liquid-disordered environment. Lipid rafts have been morphologically characterized as small membrane patches that are tens of nanometers to micrometer in diameter. These lipid rafts may play a vital role in many important biological processes, such as signal transduction, apoptosis, cell adhesion and migration, synaptic transmission, organization of the cytoskeleton and protein sorting [4-11]. Besides these functions, lipid rafts are believed to act as a port of cellular entry for a wide range of viruses, bacteria and toxins [12]. Membrane proteins and lipidated peptides or proteins would either reside in or be excluded from these rafts, depending on their physio-chemical properties. Hence, it is important to study their properties, such as the lateral organization and structure of lipid rafts and their influence on the conformation and activity of membrane proteins. The lateral structure of the membrane controls the mechanical

properties (which is important for the shape of cells). In order to understand how proteins function in a membranes it is necessary to determine the ways in which proteins interact with the lipid bilayer, more specifically how the proteins influence the local structure and composition of the bilayer, and on the other hand, how changes in the lipid-bilayer physical properties modulate the functional state of the proteins.

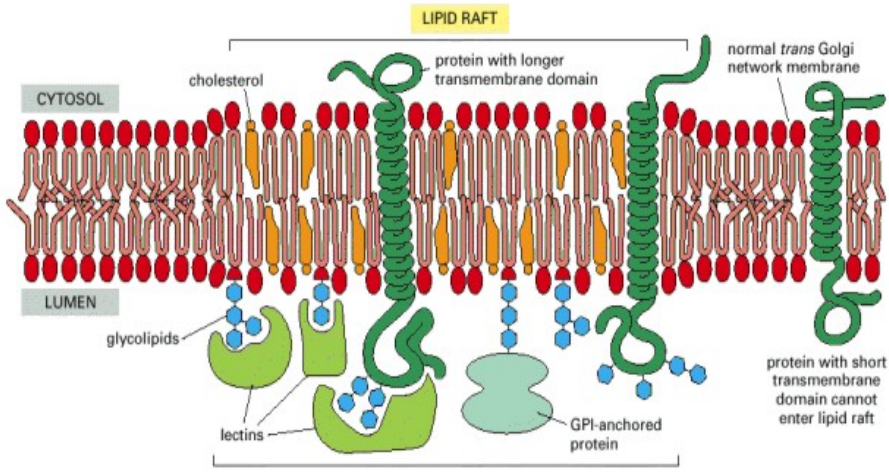

Figure 1.2: Lipid raft or microdomain that is enriched in cholesterol and sphingolipids. (Alberts et al., *The Cell*, 2004)

1.2 Classification of Membrane Lipids

In general, lipid can be defined as a biological material soluble in organic solvents, such as ether or chloroform. Lipids are amphipathic (amphiphilic) molecules - they have two different natures, one is polar (hydrophilic) which is stable in aqueous solution, and the other is non polar (hydrophobic) aliphatic or aromatic hydrocarbon, which is more stable in an non-aqueous environment.

The hydrocarbon chains in the non polar part can contain different numbers of carbon atoms, and the bonds between the carbons atoms can be single (saturated) or double (unsaturated). A hydrocarbon chain can be turned into a *fatty acid* by attaching a carboxylic acid (–COOH) group at the end. The fatty acids are the fundamental building blocks of all lipids in living matter. Plants and animals use a variety of fatty acids with chain lengths ranging from two to thirty-six. The most common chain lengths fall between fourteen and twenty-two. Fatty acids are rarely found free in the cell; instead they are chemically linked to a hydrophobic group like glycerol. Glycerol

acts as the backbone of the lipid molecule. Although biological membranes contain a diverse variety of lipids, we can divide them into three general types as phospholipids, glycolipids and sterols. Based on the shape of each membrane lipid and the coexistence of different lipids phases within the membrane [13], these lipids can be specifically categorized as

- Glycerophopsholipids (GPLs),
- Sphingolipids
- Cholesterol.

1.2.1 Glycerophopsholipids (GPLs)

Glycero-phospholipids (GPLs) are derivatives from *sn*-glycero-3-phosphoric acid with usually two fatty acids esterified in the *sn*-1 and -2 positions of the glycerol moiety. GPLs are the major lipid type in the eukaryotic cells and they constitute the fundamental matrix of natural membranes. GPLs differ from each other with respect to their polar head groups. The main polar head groups are phosphatidylcholine (PC), phosphatidylethanolamine (PE), phosphatidylserine (PS), phosphatidylinositol (PI) and phosphotidylglycerol (PG).

While PC and PE are neutral (zwitter-ionic), PS, PG and PI lipids can be electrically charged. This difference has an important consequence for the capacity of the lipids, when incorporated into a lipid membrane, to bind protein and drugs [14]. Fatty acid at *sn*-1 has a saturated chain with 16 or 18 carbon atoms. At *sn*-2, the fatty acid is generally longer (at least 18 carbon atoms) and is always unsaturated with one or more *cis* double bonds. Each double bond introduces a bend in the fatty acid chain.

1.2.2 Sphingolipids

Nature also uses another strategy to construct lipids with head and tail groups. Instead of using glycerol to bind the fatty acids, *sphingosine,* which is a long chain (up to 24 carbon atoms) amine, is bound to the fatty acid. The simplest version of sphingolipid is ceramide, a PC head group attached to ceramide leading to sphingomyelin. The saturated chains of sphingolipids allow them to pack tightly with GPLs through van der Walls interactions. In addition, sphingolipids may self-associate through hydrogen

bonds between the hydroxyl (OH) groups of the sphingosine base and the α-OH group present in the fatty acid of many sphingolipids, forming a gel-like phase at the physiological temperature. Overall, sphingolipids have a much higher melting temperature (*T*m) than that of GPLs.

1.2.3 Cholesterol

Cholesterol is an important constituent of most mammalian cell membranes and its concentration in various cellular membranes is tightly regulated. Cholesterol is quite different from the GPLs and sphingolipids. In stead of a fatty acid chain as its hydrophobic part, cholesterol has a steroid ring structure with a small hydrocarbon chain at the end and a simple hydroxyl group as its polar head group. So cholesterol has a bulky and stiff tail and a small head as shown in Fig. 1.3.

Eukaryotic plasma membranes contain relatively large amounts of cholesterol ranging between 20-50 % of the total lipids. In contrast, the organelle membranes contain very little: mitochondrial membranes less than 5 %, Golgi membranes about 8 % and ER membranes around 10%. In contrast, sterols are universally absent in the membranes of all prokaryotes [14]. Being an amphiphilic molecule, cholesterol easily incorporates into lipid bilayers. Considering the different type of ordering of the lipid molecules, cholesterol on the one side, due to its hydrophobically smooth and stiff steroid ring structure, has a preference for having conformationally ordered lipid chains next to it because such an arrangement helps for the tightest interactions. From this perspective, cholesterol prefers the solid-order lipid phase. On the other side, the solid-ordered phase is a crystalline phase with dense packing order among the lipid molecules. The cholesterol molecule, with its own peculiar size and shape does not fit well into this packing order, whereas there is plenty of free space into the liquid-disordered phase. From this perspective, cholesterol prefers the liquid-disordered phase. Hence, the cholesterol molecule becomes frustrated when presented with two different lipid phases. In 1987 the Danish biophysicist John Hjort Ipsen proposed as cholesterol releases the frustration by introducing a new phase called *liquid-ordered* phase [15].

This liquid-ordered phase is a genuine liquid with a positional disorder and high lateral mobility of the membrane molecules. The lipid's chains have a substantial degree of

conformational order. Cholesterol makes the membrane thicker and stiffer but retains the fluidity required for membrane function.

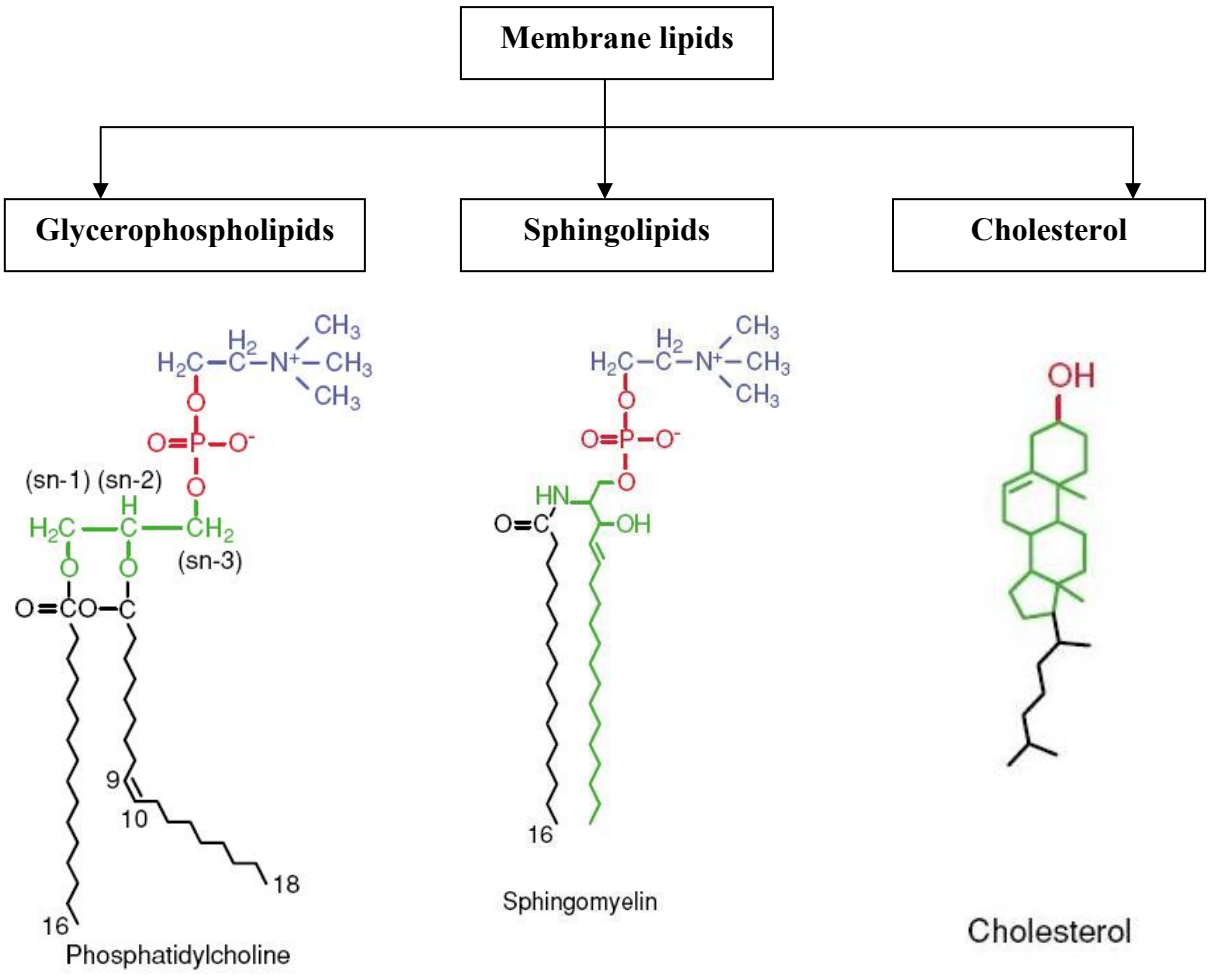

Figure 1.3: Structure-based classification of membrane lipids.

1.3 Lateral Membrane Phases and Phase Transitions

When lipids are mix with water, the hydrophobic effect acts to ensure that the acyl chains of lipid molecules are screened and protected from water. This leads to a whole family of supramolecular aggregates that are formed spontaneously by self assembling the lipids head to head. The simplest and most ideal lipid aggregate is the lipid monolayer where a film of lipids formed on the interface between water and air. The lipid bilayer is considered as two monolayers assembled back to back. The open ends of the bilayers close themselves and form closed structures called *vesicles* or *liposomes*. Several lipid bilayers often organize among themselves to form multi-

lamellar structures. A uni-lamellar liposome constitutes the simplest possible model of a cell membrane.

The lipid aggregates are all characterized by being of planar or lamellar symmetry. This requires that the lipid molecules have a shape that is approximately cylindrical in order to fit in. If the shape is more conical, other non lamellar aggregates symmetries like cubic, hexagonal, inverted hexagonal, micelles and inverted micelles may arise. Non polar lipids like triglyceride oil do not form aggregates in water whereas all polar lipids except cholesterol form aggregates in water.

The effective shape of a lipid molecule is determined by the compatibility between the size of the head group and the size of the hydrophobic tail. Full compatibility results in a cylindrical shape. The effective shape of a lipid molecule as a measure of its ability to fit into a particular lipid aggregate is described by a packing parameter $P = (v / a\ \ l)$, where v, a, and l denotes volume, area of the head group and length of the lipid acyl chain, respectively [14]. Deviation of P from unity suggests that non-lamellar aggregate having different curvatures.

Pure phospholipid bilayers can exist in two states, a solid or gel state, and above their melting temperature (Tm), a fluid or liquid state. At low temperatures, the acyl chains of the lipid bilayers are in an ordered chain conformation typical of a gel phase ($P_{\beta'}$). The solid phase is not thought to be of physiological relevance [9]. Above the melting temperature (Tm) the conformational order is lost and the lipids form a liquid-crystalline phase (L_α). The presence of cholesterol in a system can change the phase behaviour drastically. The gel phase is denoted by s_o, the indices "s" standing for solid in two dimensions and "o" for orientationally ordered chains, the liquid-crystalline phase l_d by the indices "l" for two-dimensional liquid and "d" for disordered chains and, finally, the new liquid-ordered phase (in the presence of cholesterol) is denoted by l_o. An important property of the l_o phase is the enormous increase in mechanical strength over the l_d phase [16], which must be partly due to the increased importance of the van der Waals interaction for the ordered chains in the lipid molecule. This phenomenon, in combination with the increased bilayer thickness, reduces the membrane permeability greatly [17]. It is supposed that the l_o phase is a "biologically relevant" phase [15].

Each and every lipid molecule has a specific transition temperature *T*m. For example DMPC has a *T*m value around 24ºC. When more than one type of lipid molecules are present in a bilayer, thus leads to a complex phase behavior. There will not be a single transition temperature and the transition will take place over a range of temperature where the system separates into more than one phase.

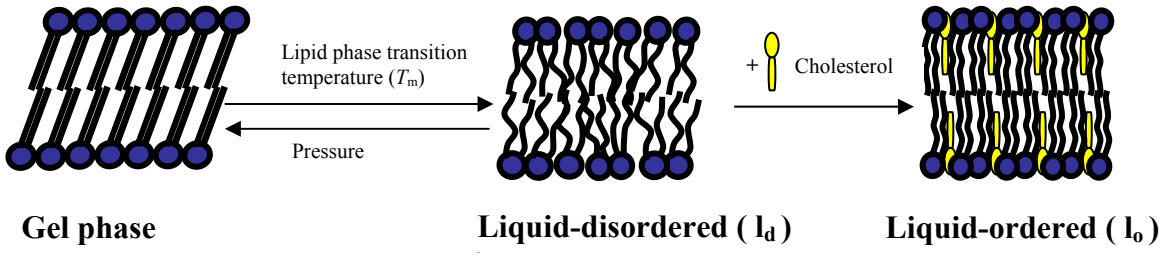

Multi-lamellar vesicle (MLV) Uni-lamellar vesicle

Figure 1.4: Structures and organization of lipid bilayers.

1.4 Lateral Pressure Profile

The lateral pressure profile is a fundamental physical property of lipid bilayers. Fig. 1.5 shows different forces acting to stabilize the bilayer and at equilibrium all these forces sum up to zero. The lateral pressure profile is built up from three contributions, namely 1. a positive pressure created by the repulsion of the head groups, 2. a negative pressure that acts in the interface of the hydrophobic and hydrophilic part (interfacial tension) of the lipid molecules by the hydrophobic effect, and 3. a positive pressure generated from the entropic repulsion between the fatty acid chains (chain pressure). Since the bilayer thickness is so small as about 5 nm, the large interfacial tension has to be distributed over a short range. This implies that the counteracting pressure from

the fatty acid chains, i.e., the chain pressure, should be high, typically around several hundreds of atmospheres. These high pressure densities have an influence on the molecular conformation of the proteins embedded in the membrane and provide a possible non-specific coupling between the lipid membrane and the function of the proteins [14].

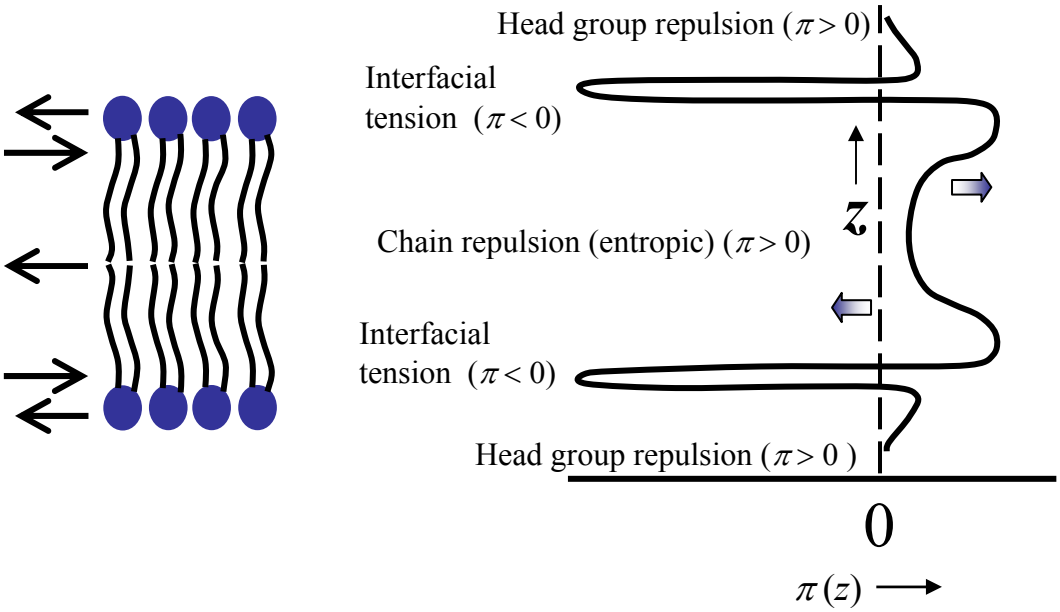

Figure 1.5: Lateral pressure profile and stress profile of lipid bilayer [18]

1.5 Lipid Protein Interactions

Proteins are involved in every step of biological activity. There are different ways in which proteins can interact with membranes namely, a) by spanning the whole membrane called membrane proteins or trans-membrane proteins, b) by electrostatic binding, c) by nonspecific binding through weak physical forces, d) by anchoring to the membrane via a lipid extended conformation, e) by anchoring by lipid attached to the protein, and f) by the amphilic protein partially penetrating the bilayer [14].

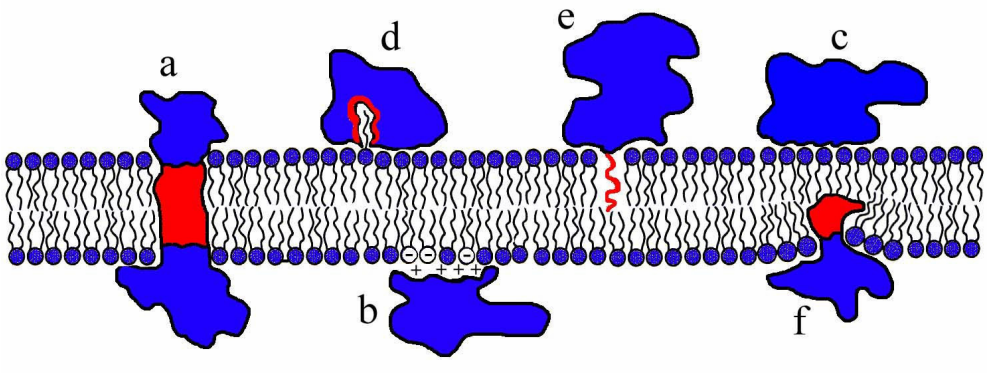

Figure 1.6: Possible interactions of proteins with lipid membrane [18]

There are three constrains that an integral membrane protein has to conform when embedded in a bilayer. Those are 1) Hydrophobic matching – the hydrophobic membrane spanning domain of the protein has to adapt or fix to the hydrophobic thickness of the lipid bilayer [18]. 2) Lateral pressure tolerance – implies that the later pressure exerted by the lipids on the trans-membrane segment of the protein varies through the belayed. 3) Curvature stress releasing – built in curvature stress in the membrane caused by certain non-lamellar forming lipids that have a tendency to form a curved structure which exert a strain on the protein. This strain may be locally released by a conformational change in the protein structure.

The effects of lipids on the function of proteins can be at the microscopic or macroscopic level. The microscopic level includes the hydrogen bonding between lipids and protein, charge-charge interactions and van der Waals interactions. The macroscopic level includes membrane viscosity, membrane pressure, and curvature stress. The distribution of proteins in a bilayer membrane will change as per the molecular structure and composition of the lipids and hence promote lipid mediated protein-protein interactions. Biologically important interactions will be microscopic rather than macroscopic because intrinsic or trans-membrane proteins are designed or adopted such that they are not affected by macroscopic interactions that could occur physiologically [19].

The lipid bilayer is also affected by the encounter of proteins. These include changes in the membrane thickness, changes in the conformational order of the lipid acyl chains, possibly lipid sorting to accommodate different peptides and proteins based on

the composition of the lipid and protein population, protein mediated lipid-lipid interactions, and a change in the lateral organisation and distribution of lipids i.e., lipid domain formation which creates the lipid bilayer heterogeneity [20].

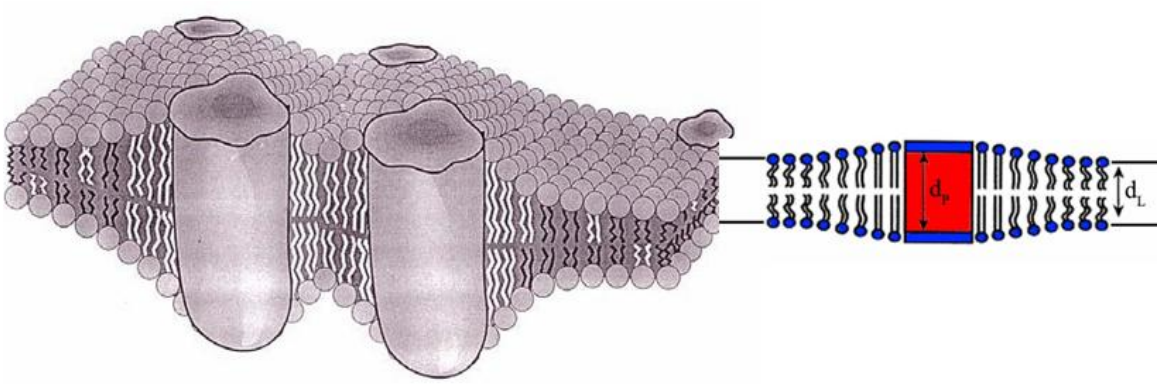

Figure 1.7: Hydrophobic matching, where d_p denotes the hydrophobic thickness of the trans-membrane domain of the protein and d_L denotes the hydrophobic thickness of the lipid bilayer [18].

Lipids around the protein conform to the hydrophobic matching condition either by stretching their acyl chains by increasing the conformation order or by recruiting the best matched lipid species at the interface. Hydrophobic matching may induce lipid mediated protein-protein interactions.

1.6 Lipid-Peptide and Lipid-Protein Interactions in Artificial Cells

Peptide or protein reconstituted in an artificial cell made up of model membrane lipids is an ideal environment to study the individual lipid–peptide and lipid–protein interactions. A reasonable model system for studying biophysical properties of lipid lateral organisation are lipid vesicles composed of three-component lipid mixtures, such as DOPC:DPPC:Chol and POPC:SM:Chol, which exhibit a rich phase diagram, including liquid-ordered/liquid-disordered phase coexistence regions [21], which are thought to be of utmost physiological relevance. Comparing the phase behaviour of ternary system with single or two component lipid mixtures will give us the detailed information about the interactions of an individual lipid with peptide or protein of our concern.

Temperature and hydrostatic pressure are well-known parameters, often used for studying biomolecular systems. Mostly, temperature has been used to study the thermodynamic, structural, and dynamic properties of membranes. A change in temperature of a system leads to changes of the thermal energy and density at the same time, whereas pressure-dependent studies at constant temperature introduce only changes in density and the intermolecular separations of the system, thus providing additional information about the energetics and phase behavior of the system without disturbing thermally activated processes [22-28]. Hydrostatic pressure has not only been used as a physical parameter for studying the stability and energetics of biomolecular systems, but also because high pressure is an important feature of certain natural membrane environments, and because the high pressure phase behavior of biomolecules is of biotechnological interest [24, 28, 29].

In particular the study of membrane-bound proteins using high pressure has the potential to provide novel information regarding molecular interactions that cause a protein to insert into membranes or bind to the membrane surface, and their associations with other proteins on the membrane surface. Compared to other biomolecules, lipid bilayers have been shown to respond most sensitively to hydrostatic pressure [24, 29]. Considerable knowledge exists about pressure effects on simple, one-component lipid bilayer systems, however, very little is known about complex lipid mixtures and lipid bilayer-peptide and -protein interactions under pressure[24, 28, 30-35]. Generally, pressure affects chemical equilibria and reaction rates. For example, the activation volume, $\Delta V^{\neq}$, of a reaction is given by the pressure dependence of the rate of reaction, k. Therefore, $\Delta V^{\neq} = -RT(\partial \ln k/\partial p)_T$. High hydrostatic pressure has also been exploited in diverse areas of biotechnology, including the ability to modify the catalytic specificity of enzymes [24]. Reasons for high hydrostatic pressure-induced changes in the rate of enzyme-catalyzed reactions may be classified into three main groups: (i) changes in the structure of the enzyme, (ii) changes in the reaction mechanism or changes in the overall rate by affecting a particular rate-determining step, and (iii) the effect of pressure on the function of membrane proteins, which might also be due to an increase in lipid packing density or a change in phase state, which might lead to a change in the conformation and dynamics of the embedded protein [36].

1.7 Model Peptide – Gramicidin D

The linear polypeptide antibiotic gramicidin D is capable of transporting ions through biological membranes by forming ionophores [37, 38]. Naturally occurring gramicidin D contains approximately 80-85% of gramicidin A, 6-7% of gramicidin B, and 5-14% of gramicidin C. Gramicidin A is a linear polypeptide with the sequence formyl-L-Val-Gly-L-Ala-D-Leu-L-Ala-D-Val-L-Val-D-Val-(L-Trp-D-Leu)$_3$-L-Trp-ethanolamide [37-39]. Either phenylalanine or tyrosine is replacing tryptophan at position 11 in case of gramicidin B and gramicidin C, respectively. The primary sequence of gramicidin consists of 15 amino acid residues of alternative L and D chirality, and all side-chains are non polar. As a consequence, the peptide is able to adopt conformations of β-helices, which would be unacceptable for an all L-amino acid peptide. The helices can be right or left handed and they can differ in the number of amino acid residues per turn and hence in length and diameter [37, 38]. A common form is the head-to-head dimer of two right-handed single-stranded β-helices. The conformation with 6.3 residues per turn ($\beta^{6.3}$-helix) is one of the possible active ion channel structures; it has a hydrophobic length of ~24 Å (channel diameter 4 Å) (Fig. 1.8b). A further form is the left-handed antiparallel double-stranded $\beta^{5.6}$-helix, being approximately 31 Å long (Fig. 1.8b), which has been observed in particular organic solvents and long-chain or gel phase lipid bilayer systems [30, 37, 38].

a)

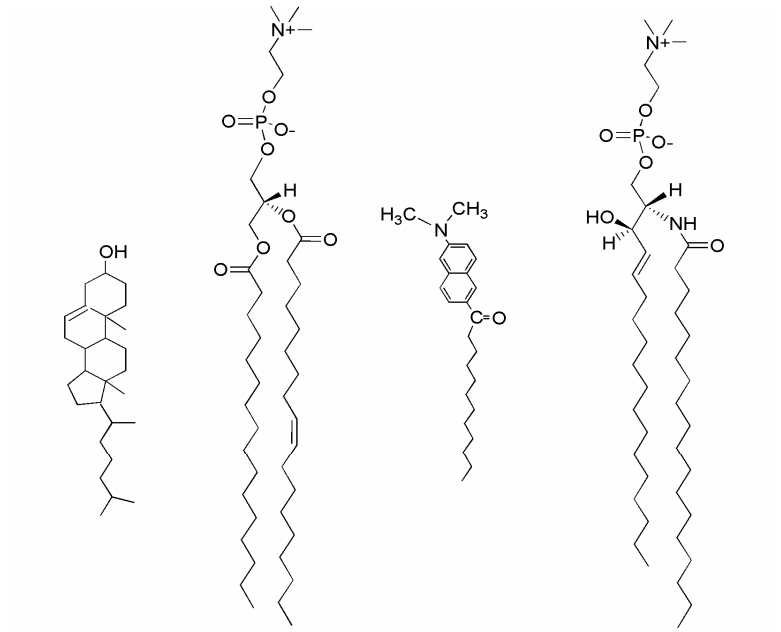

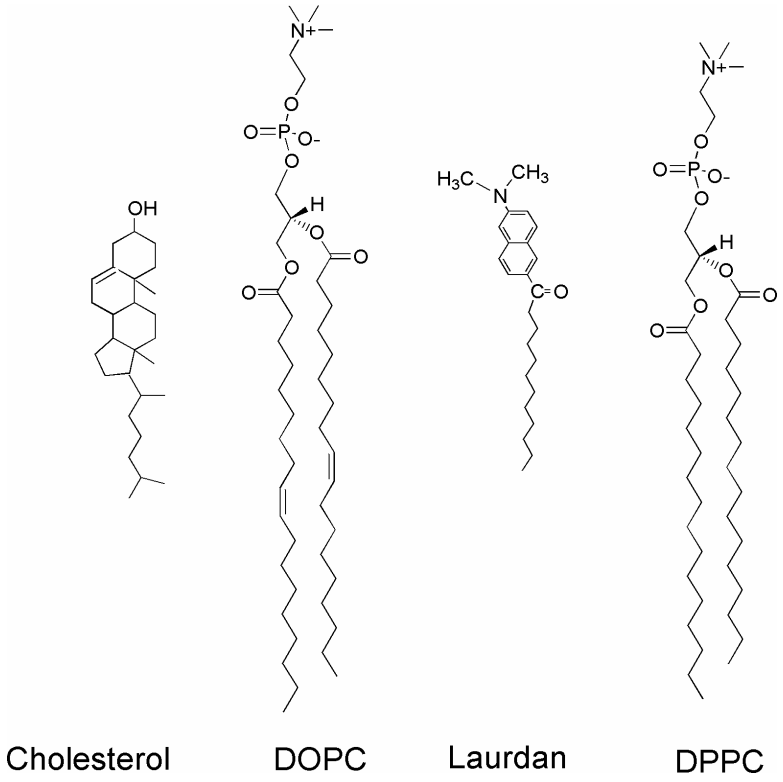

b)

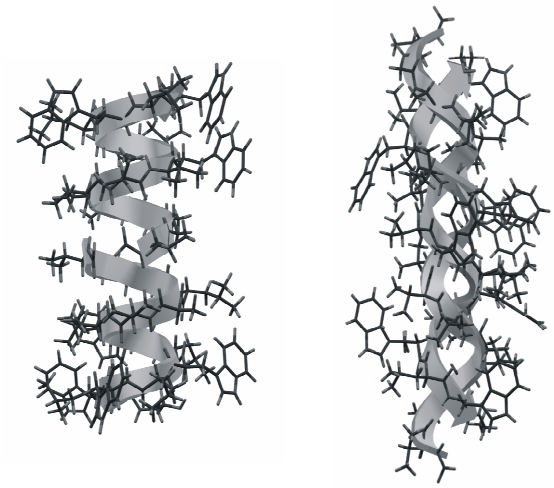

Figure 1.8a) Chemical structure and location of the fluorescence probe Laurdan in lipid bilayers made up of POPC:SM:Chol and DOPC:DPPC:Chol ternary systems. b) Schematic representation showing the polypeptide backbone of a helical dimer (left) and double-helical (right) form of gramicidin.

1.8 Multi-Drug Resistance

Microorganisms have developed different mechanisms to prevent the toxic effects of many antibiotics and other drugs [40, 41]. One of the general mechanisms of resistance is the inhibition of drug entry into the cell. Some transporters are dedicated to extrude only specific drug or a class of compounds such as the tetracycline efflux proteins [42, 43]. In contrast to these selective transporters, so called multi-drug resistance transporters can efflux a wide variety of structurally unrelated compounds [44-47].

On the basis of bioenergetic and structural criteria, multidrug transporters can be divided into two major classes [48]. Those are 1) secondary multidrug transporters that utilize the transmembrane electrochemical gradient of protons or sodium ions to drive the extrusion of drugs from the cell, and 2) ATP-binding cassette (ABC)-type multidrug transporters that use the free energy of ATP hydrolysis to pump drugs out of the cell (Fig. 1.9).

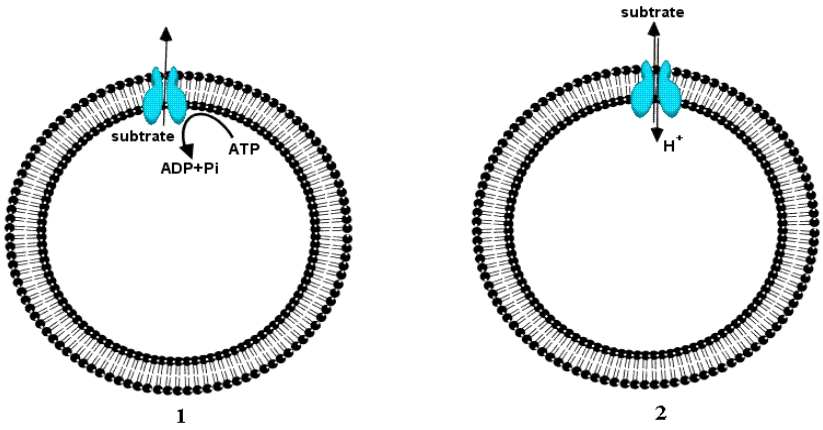

Figure 1.9: Two major classes of multidrug transporters; 1) ABC type and 2) secondary multidrug transporters.

1.8.1 LABs and Multidrug Resistance

Lactic acid bacteria (LABs) belong to a group of gram-positive anaerobic bacteria that excrete lactic acid as their main fermentation product into the culture medium. LABs play crucial roles in the manufacturing of fermented milk products, vegetables and meat, as well as in wine and beer. LABs can be beer spoilage bacteria. They produce

turbidity, acidity and unfavorable taste in beers. In LABs hop resistance is of importance for them to grow in beer. Hop compounds, e.g. hops iso-α-acids in beer, have an anti bacterial activity against gram-positive bacteria. Hops act as ionophores which dissipate the pH gradient across the cytoplasmic membrane and reduce the proton motive force (pmf). Therefore the pmf depended nutrient uptake is inhibited, resulting in cell death [49].

In the LAB *Lactococcus lactis*, two multidrug-resistance transporters were mainly found to confer resistance to cationic lipophilic cytotoxic compounds [43]. The two best investigated are LmrP as a representative of the secondary MDR transporters [50], and LmrA as a representative of the ABC transporter family [51], which can also be found in *Lactobacillus plantarum* and in the strain TMW 1.460.

In another LAB *Lactobacillus brevis*, a homolog of LmrA was found that confers resistance to hop [52]. This LmrA homolog is encoded by the gene called horA. LmrA and HorA contribute to the intrinsic drug resistance of the organisms in which they are expressed.

1.9 Model Protein – LmrA

LmrA causes antibiotic resistance by expelling amphiphilic compounds from the inner leaflet of the cytoplasmic membrane [53, 54]. Unlike other bacterial multidrug-resistance proteins, LmrA is the first ABC-transporter found in bacteria to confer multidrug resistance [55]. It is a 590 amino acid protein with an N-terminal hydrophobic domain, consisting of six transmembrane helices, followed by C-terminal hydrophilic domain, containing the ATP-nucleotide binding site. The membrane topology of LmrA is shown in Fig. 1.10. Although it's topology in the lipid membrane had been predicted from its primary structure, a well defined tertiary structure is not known. LmrA has the broadest substrate specificity reported for MDRs. The human multidrug-resistance P-glycoprotein, encoded by the *MDR1* gene, is also an ABC transporter.

The most commonly accepted topology model suggests these MDR proteins are constituted of two homologous halves composed of an ATP-binding domain and a membrane-embedded domain [56]. LmrA has about 50% similarity with each half of a

plasma membrane glycoprotein (P-glycoprotein or P-gp) and functions as a homologous dimmer [53]. Hence functional crosstalk between two LmrA monomers in the lipid matrix is essential for its activity [57]. LmrA exhibits specificity for phospholipid head groups and may be involved in the lipid sorting in *L. lactis* [51]. Bacterial LmrA and human P-glycoprotein are functionally interchangeable and this type of MDR nature is conserved from bacteria to man [53].

The mechanism of extrusion of cytotoxic compounds by LmrA has been studied in whole cells, isolated membrane vesicles and proteoliposomes. These studies revealed that the lipophilic substrates intercalate rapidly in the outer leaflet of the membrane. Subsequently, the substrate flips over slowly to the inner leaflet from where it is picked up by LmrA and extruded in an ATP-dependent process to the external medium [54].

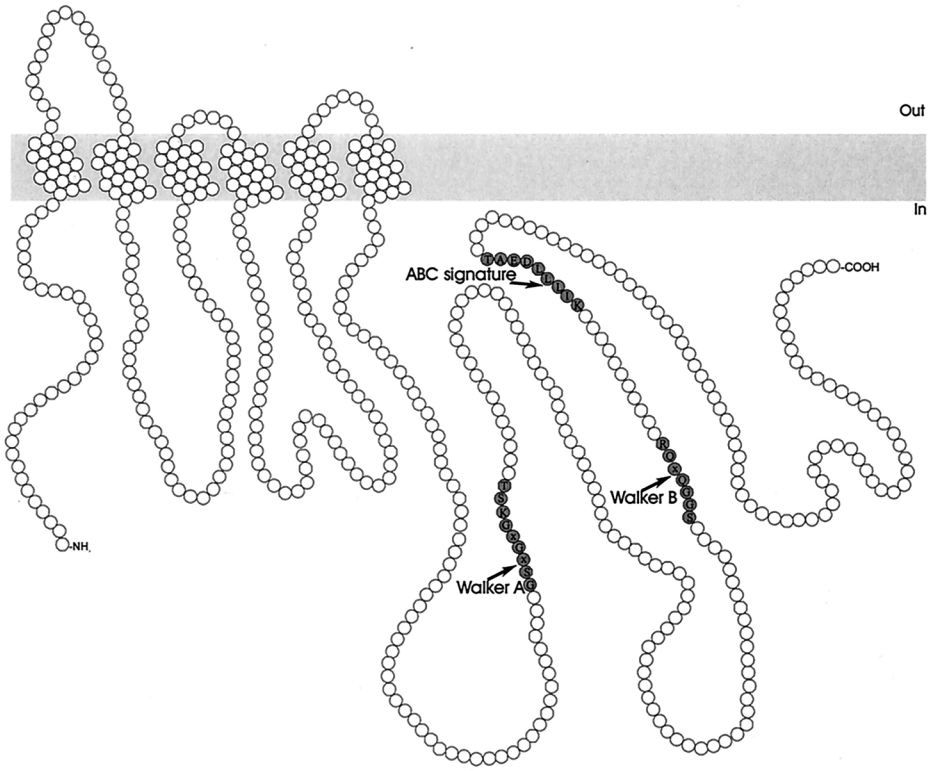

Figure 1.10: Proposed membrane topology of LmrA [48].

1.10 Aim of this Research

Cell membranes constitute one of the fundamental structural and functional elements of living organisms. There is considerable evidence that lateral inhomogeneities in lipid composition in the both inner and outer layer exist in biological membranes. Lipids and proteins are often organized into microdomains, lipid rafts. These rafts are composed of mainly cholesterol and saturated lipids, which form a l_o phase. These lipid rafts may play an important role in many important biological processes. Almost fifty percent of the proteins in our cells are attached to lipid membranes, some of them are transmembrane proteins, bound to the membrane head groups or interacting to the membrane for some time during their function. Membrane proteins and lipidated peptides or proteins would either reside in or be excluded from these rafts, depending on their physical-chemical properties. Hence, it is important to study their properties, such as the lateral organisation and structure of lipid rafts and their influence on the conformation and activity of membrane proteins. The lateral organisation controls the mechanical properties (which is important for the shape of cells) of the membrane. In order to understand how proteins function in membranes it is necessary to determine the ways in which proteins interact with the lipid bilayer, specifically how the proteins influence the local structure and composition of the bilayer, and on the other hand, how changes in the lipid-bilayer physical properties modulate the functional state of the proteins.

The primary goals of this work are to study the lateral membrane organization and lipid-peptide and lipid-protein interactions using different lipid mixtures. In the first part of this thesis, the lateral membrane organization of a typical lipid raft mixture, such as POPC/sphingomyelin/cholesterol, and its phase segregation originating from compositional fluctuations as a function of concentration, temperature (from ~2 up to 70 °C) and pressure (from 1 up to 2000 bar) are studied by Laurdan fluorescence spectroscopy. Lipid-peptide interactions are studied using Gramicidin D as a model peptide along with this lipid mixture.

In the second part of this thesis, lipid-protein interactions are studied using LmrA as a model protein. Laurdan fluorescence spectroscopy was used to follow the lateral organisation of the membrane made of different model membrane lipids such as

- single component lipid systems containing DMPC, DOPC
- two-component system containing DMPC with 10 mol% cholesterol
- ternary lipid raft systems containing DOPC/DPPC/Chol mixtures
- natural membrane lipids extracted from *Lactobacillus plantarum.*

Except the DOPC bilayer and the natural membrane system all other lipid systems were also examined by atomic force microscopy (AFM).

In the third part of the thesis, changes in the secondary structure of non-reconstituted LmrA was analysed as a function of temperature from 30 to 70 °C by using circular dichroism (CD) spectroscopy.

The fourth part of this thesis deals with a consensus description of the lateral inhomogeneity of DOPC/DPPC/Chol mixtures, studied by various biophysical methods in addition to Laurdan fluorescence spectroscopy, such as 2-photon excitation fluorescence microscopy using giant unilamellar vesicles (GUV) and atomic force microscopy (AFM). The GUV studies allow direct microscopic visualization of domains and their topology in the micrometer range. AFM allows checking the lateral inhomogeneity and domain topology in nanometer range. Furthermore fluorescence anisotropy measurements were performed for both raft mixtures using the TMA-DPH fluorescent probe.

The final part of the thesis deals with the transport activity and ATPase activity of LmrA reconstituted in pure DMPC and DOPC/DPPC/Chol systems under different pressures.

2. Materials and Methods

2.1 Materials

POPC	1-palmitoyl-2-oleoyl-*sn*-glycero-3-phosphocholine	Avanti Polar Lipids
DOPC	1,2-dioleoyl-*sn*-glycero-3-phosphocholine	Avanti Polar Lipids
DPPC	1,2-dipalmitoyl-*sn*-glycero-3-phosphocholine	Avanti Polar Lipids
SM	sphingomyelin, brain porcine	Avanti Polar Lipids
Chol	cholesterol	Sigma-Aldrich
GD	gramicidin D	Sigma-Aldrich

Rhodamine DHPE	Lissamine™ rhodamine B 1,2-dihexadecanoyl-sn-glycero-3-phosphoethanolamine, triethylammonium salt	Molecular Probes
C_5-ganglioside G_{M1}	BODIPY® FL C_5-ganglioside G_{M1}	Molecular Probes

Laurdan	1-dodecanone, 1-(6-(dimethylamino) -2-naphthalenyl)	Molecular Probes
TMA-DPH	1-(4-trimethylammoniumphenyl)-6-phenyl -1,3,5-hexatriene p-toluenesulfonate	Molecular Probes
Hoechst	Hoechst 33342, trihydrochloride, trihydrate 10 mg/mL solution in water	Molecular Probes
DDM	Dodecyl maltoside	GERBU Biochemicals GmbH
Biobeads	DM-2 adsorbent	Bio-Rad
HEPES	HEPES buffer	Sigma

All chemicals were used without further purification.

All other materials were reagent grade and obtained from commercial sources.

LmrA protein was expressed and purified by Holger Teichert (Prof. Dr. Rudi F. Vogel group) from the Technische Universität München, Germany.

2.2 Fluorescence Spectroscopy

Luminescence is the emission of light from any substance and occurs from electronically excited states. Depending on the nature of the excited state, it is divided into fluorescence and phosphorescence. Fluorescence is the emission of light from an excited singlet state and the electron in the excited orbital is paired (of opposite spin) to the second electron in the ground-state orbital. The emission rates of fluorescence are typically 10^8 s^{-1}, hence the typical fluorescence lifetime is nearly 10 ns. The life time (τ) of a fluorophore is the average time between its excitation and its return to the ground state. Phosphorescence is emission of light from triplet excited states, in which the electron in the excited orbital has the same spin orientation as the ground-state electron. The emission rates are slow, $10^3 - 10^0$ s^{-1}, so that phosphorescence lifetimes are typically milliseconds to seconds. Fluorescence spectroscopy is a powerful technique for studying molecular interactions. The technique has become quite popular because of its exquisitely sensitivity to the immediate environment of the probe and high signal to noise ratio [58].

2.2.1 Basic Theory of Fluorescence

The processes which occur between the absorption and emission are usually illustrated by the Jablonski diagram. In Fig. 2.1, the singlet ground, first, and second electronic states are depicted by S_o, S_1 and S_2, respectively. At each of these electronic energy levels, the fluorophores can exist in a number of vibrational energy levels, denoted by 0, 1, 2, etc. The transitions between states are depicted as vertical lines. Transitions occur in about 10^{-15} s, a time too short for significant displacement of nuclei. This is known as Franck- Condon principle. Following light absorption, several processes usually occur. A fluorophore is usually excited to some higher vibrational level of either S_1, or S_2. With a few rare exceptions, molecules in condensed phases rapidly relax to the lowest vibrational level of S_1. This process is called internal conversion (IC) and generally occurs in 10^{-12} s or less. Since fluorescence lifetimes are typically near 10^{-8} s, IC is generally complete prior to emission. Hence, fluorescence emission generally results from a thermally equilibrated excited state, that is, the lowest-energy vibrational state of S_1, return to the ground state typically occurs to a higher excited vibrational ground-state level, which then quickly (10^{-12} s) reaches thermal

equilibrium. An interesting consequence of emission to higher vibrational ground states is that the emission spectrum is typically a mirror image of the absorption spectrum of the $S_0 \rightarrow S_1$ transition. Molecules in the S_1 state can also undergo a spin conversion to the first triplet state, T_1. Emission from T_1 is termed phosphorescence. Conversion of S_1 to $T_1$is called intersystem crossing (ISC). The transition from T_1 to the singlet ground state is forbidden.

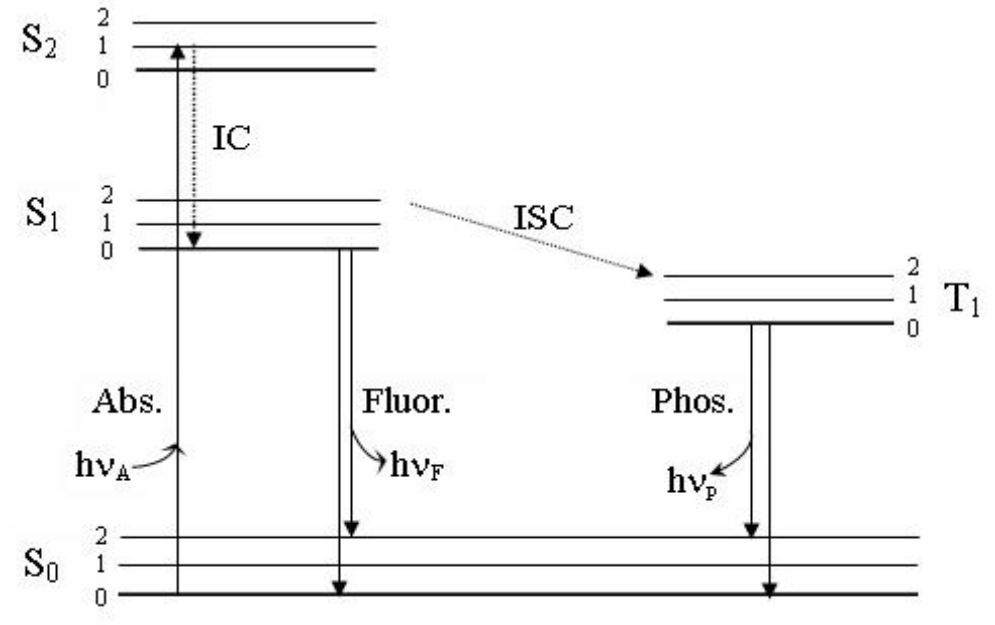

Figure 2.1: Jablonski diagram.

2.3 Fluorescence Anisotropy

Anisotropy measurements provide information on the size and shape of proteins or the rigidity of various molecular environments. Anisotropy measurements have been used to measure protein-protein associations and the fluidity of membranes and immunoassays of numerous substances.

Anisotropy measurements are based on the principle of photoselective excitation of fluorophores by polarized light. Fluorophores preferentially absorb photons whose electric field vectors are aligned parallel to the transition moment of the fluorophore. The transition moment has a defined orientation with respect to the molecular axes. In an isotropic solution, the fluorophores are oriented randomly. Upon excitation with polarized light, one selectively excites those fluorophore molecules whose absorption

transition dipole is parallel to the electric vector of the excitation. This selective excitation results in a partially oriented population of fluorophores (photoselection) and in partially polarized fluorescence emission.

The fluorescence anisotropy (r) and polarization (P) are defined by

$$r = \frac{I_{\parallel} - I_{\perp}}{I_{\parallel} + 2I_{\perp}}$$

$$p = \frac{I_{\parallel} - I_{\perp}}{I_{\parallel} + I_{\perp}}$$

where $I_{\parallel}$ and $I_{\perp}$ are the fluorescence intensities of the vertically ($\parallel$) and horizontally ($\perp$) polarized emission. Several phenomena can decrease the measured anisotropy to values lower than the maximum theoretical values. The most common cause is rotational diffusion. Such diffusion occurs during the lifetime of the excited state and displaces the emission dipole of the fluorophore. Measurement of this parameter provides information about the relative angular displacement of the fluorophore between the times of absorption and emission. In fluid solution, most fluorophores rotate extensively in 50-100 ps. Hence, the molecules can rotate many times during the fluorescence lifetime (1-10 ns) and the orientation of the polarized emission is randomized. For this reason, fluorophores in aqueous non-viscous solution typically display anisotropies near zero. Transfer of excitation between fluorophores also results in decreased anisotropies. The effects of rotational diffusion can be decreased if the fluorophore is bound to a macromolecule. As a result, measurements of fluorescence anisotropy will be sensitive to any factor which affects the rate of rotational diffusion. The rotational rates of fluorophores in cell membranes also occur on the nanosecond timescale, and the anisotropy values are thus sensitive to the membrane composition. For these reasons, measurements of fluorescence polarization are widely used to study interactions of biological macromolecules.

2.3.1 Experimental Part - Sample Preparation for Anisotropy Measurements

Lipid and cholesterol stock solutions were prepared in chloroform. TMA-DPH was dissolved in ethanol at a concentration of 1 mmol/L. Vesicles containing the desired molar ratio of POPC, SM and Chol and DOPC, DPPC and Chol were prepared together with the TMA-DPH fluorophore. After co-dissolving the lipids, cholesterol and fluorophore, the solvents chloroform and ethanol were removed by a flow of nitrogen gas. Then the samples were dried under high vacuum pumping for several hours to completely remove the remaining solvent. The remaining dry film was then resuspended in buffer, vortexed and sonicated for 15 min in a bath-type sonicator (Bandelin SONOREX RK100SH). Large unilamellar vesicles were produced by five freeze-thaw cycles (freezing in liquid nitrogen and slow-thawing in a warm water bath). The final concentration of lipid vesicles in the sample used for the fluorescence measurements was 0.3 mmol/L (0.2 mg/mL) and that of the fluorescent probe was ~0.6 μmol/L. The final vesicle solution contained a 1:500 fluorophore to lipid ratio on a molecular basis.

Measurements of the temperature dependence of the steady-state fluorescence anisotropy r_{ss} were carried out in a K2 multifrequency phase and modulation fluorometer with photon counting mode equipment (ISS Inc., Champaign, Ill), aligned to the "L"-format light path and equipped with polarizers. The excitation and emission wavelength were 338 nm and 446 nm respectively.

2.4 Laurdan Fluorescence Spectroscopy

The emission spectrum of the environmentally sensitive fluorescence probe Laurdan (6-dodecanoyl-2-dimethyl-aminonapthalene) was used to decipher the phase behavior of the lipid bilayer system. Laurdan is a naphthalene-based, membrane probe that displays spectral sensitivity to the polarity of the environment. It possesses both an electron donor and acceptor, so that fluorescent excitation induces a large excited state electrical dipole moment, which tends to locally align surrounding polar molecules (e.g., water) by dissipating a small fraction of the excited state energy and shifting the emission spectrum towards the red [59, 60] in aqueous environment. When inserted into a membrane, Laurdan aligns its lauroyl tail with the lipid moiety and locates its

naphthalene ring near the phospholipid glycerol backbone (Fig. 1.8a). It is virtually non-fluorescent in aqueous environments with a fluorescence lifetime of less than 100 ps, while in organic solvents and in membranes, it displays a strong fluorescence signal with an average lifetime of about 4-8 ns, depending on the solvent. Laurdan distributes equally into fluid and gel phase lipid membranes and does not have a specific affinity towards any phospholipid head group [61]. The spectral changes of the emission spectrum of Laurdan is generally quantified by the so-called generalized polarization function, which is defined as $GP = (I_B\text{-}I_R)/(I_B+I_R)$, where I_B and I_R are the fluorescence intensities at 440 nm (characteristic for a gel phase state environment) and 490 nm (characteristic for a fluid, liquid-crystalline lipid state), respectively. Hence, *GP* values range from -1 to +1. In phase coexistence regions, the *GP* values exhibit values typical for fluid (liquid-disordered) and gel-type (liquid-ordered) domains. Hence the measured *GP* values of our systems reflect the overall phase behavior and fluidity of the membranes as a function of lipid concentration, temperature and pressure.

2.4.1 Experimental Part – Sample Preparation for Lipid-Peptide Interactions

Lipid and cholesterol stock solutions were prepared in chloroform. Laurdan was dissolved in chloroform at a concentration of 1 mmol/L. Vesicles containing the desired molar ratio of POPC, SM and Chol were prepared together with the Laurdan fluorophore. After co-dissolving the lipids, cholesterol, fluorophore and GD (5 mol% with respect to lipid for the peptide containing sample), the solvent chloroform was removed by a flow of nitrogen gas. Then the samples were dried under high vacuum pumping for several hours to completely remove the remaining solvent. The remaining dry film was then resuspended in water, vortexed and sonicated for 15 min in a bath-type sonicator (Bandelin SONOREX RK100SH). Large unilamellar vesicles were produced by five freeze-thaw cycles (freezing in liquid nitrogen and slow-thawing at warm water bath) followed by 13 passages through two stacked nucleopore polycarbonate membranes of 100 nm pore size in a mini-extruder. The samples were kept at high temperature ($>T_m$) during the extrusion procedure. Fig 2.2 illustrates the liposome preparation. The final concentration of lipid vesicles in the samples used for the fluorescence measurements was 0.3 mmol/L and that of the fluorescent probe was

~0.5 µmol/L. The final vesicle solution contained a 1:550 fluorophore to lipid mixture on a molecular basis.

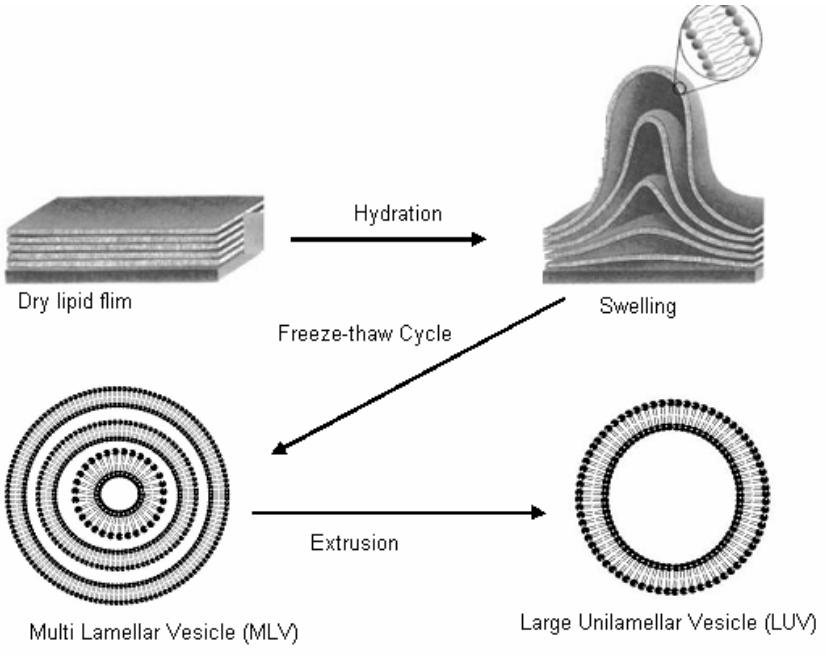

Figure 2.2: Liposome preparation.

2.4.2 Experimental Part – Sample Preparation for Lipid-Protein Interactions

Proteoliposome of LmrA with DMPC, DOPC, DMPC+10 mol% cholesterol, natural lipid extract and the raft mixture DOPC:DPPC:Chol-(1:2:1) along with Laurdan were prepared by the successive detergent removal method [62]. Liposomes of the desired single- or multi-component lipid mixture was prepared by sonication-freeze thaw cycles. The required amount (1.5 mM) of detergent dodecyl maltoside (DDM) to destabilize different liposomes was determined by light scattering measurements. Liposomes were destabilized by the slow addition of 1.5 mM detergent DDM and kept stirring at room temperature for 15 min. For reconstitution, the purified LmrA was mixed with DDM-destabilized liposomes in a 1:20 wt ratio and incubated for 30 min at room temperature under gentle stirring. The detergent was removed by two successive extractions with SM2 biobeads. These polystyrene beads are thoroughly washed with methanol and water for 3 times before use. A wet weight of 80 mg biobeads/mL of liposomes was used to extract the detergent each time. First extraction was performed at room temperature for 2 hrs and the second extraction at 4 ºC for 16

hr. Finally, proteoliposomes were collected by centrifugation (280000 g, 30 min, 20 ºC) and resuspended in 20 mM HEPES buffer, pH 7.2 at a final lipid concentration of 1 mg/mL and the protein to lipid ratio is 1:20 wt/wt. For the AFM studies and the measurement of the ATPase activity of LmrA reconstituted in pure DMPC and DOPC/DPPC/Chol systems, the proteoliposome, were prepared without the Laurdan fluorophore. Figure 2.3 illustrates the proteoliposome preparation protocol.

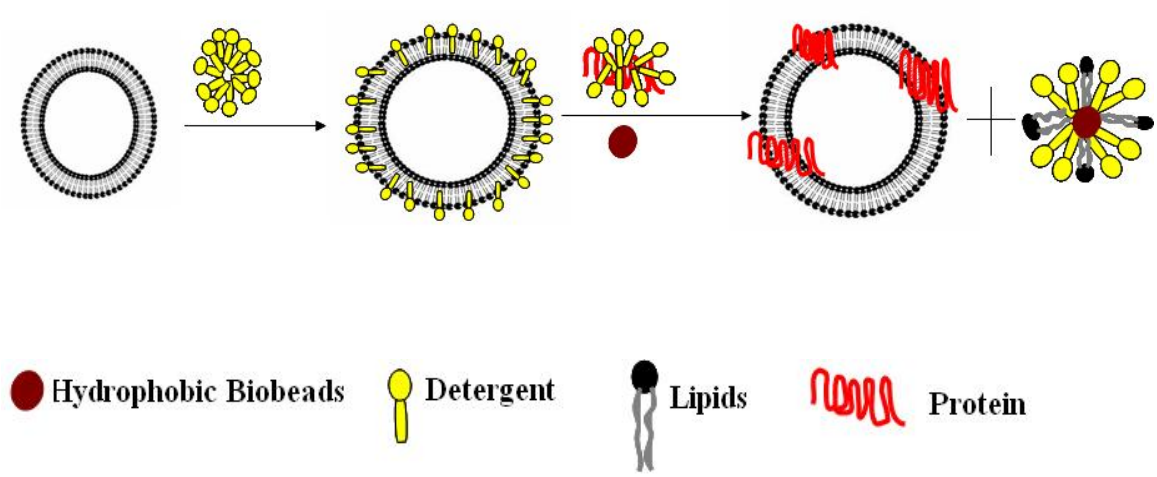

Figure 2.3: Proteoliposome preparation.

2.4.3 Fluorescence Spectrometer Setup

The fluorescence spectroscopic measurements were performed using a K2 multifrequency phase and modulation fluorometer with photon counting mode equipment (ISS Inc., Champaign, Ill). The detailed operational principle of the multifrequency fluorometer has been described in detail elsewhere [63, 64]. A schematic illustration of the K2 fluorescence spectrometer is shown in Fig. 2.4. The instrument has a xenon arc lamp as the source of excitation light. Such lamps are generally useful because of their high intensity in wavelengths range between 250 and 1100 nm. Xenon arc lamps emit a continuum of light as a result of the recombination of electrons with ionized Xe atoms. These ions are generated by collisions of Xe atoms with the electrons which flow across the arc.

The emitted light is focused with the help of lenses on the entrance slit of the excitation monochromator. A monochromator accepts incoming light and disperses it

into the various colors of the spectrum. This dispersion can be accomplished using prisms or diffraction gratings. In the K2 spectrometer the spectral dispersion in the monochromator takes place in the concave, holographic gratings with 1200 grooves per millimeter. The spectral region is in the range of λ = 200-800 nm with allowance of $\Delta\lambda$ = 0.25 nm. Both monochromators are equipped with a set of interchangeable slits. The slit handles are marked with the width of the slits: 2, 1, 0.5 mm. Since the linear dispersion of the monochromator is 8 nm/mm, slits have a bandwidth of 16, 8, and 4 nm. The monochromatic light is stirred afterwards over a mirror which is fastened to the corner of a two-way polarizer, directly on a beam splitter. A beam splitter is provided in the excitation light path and reflects part of the excitation light to a reference cell, in this case Rhodamine-B, a stable reference fluorophore. Excitation spectra are distorted primarily by the wavelength dependence of the intensity of the exciting light. This intensity can be converted to a signal proportional to the number of incident photons by the use of a "quantum counter". This concentrated solution absorbs virtually all incidents light from 200-600 nm. The quantum yield and emission maximum (~630 nm) are essentially independent of excitation wavelength from 220-600 nm. Rhodamine-B remains the most generally reliable and convenient "quantum counter".

Polarizer's are present in the both excitation and emission light paths. Generally polarizers are removable so that they can be inserted only for the measurement of fluorescence anisotropy or when it is necessary to select for particular polarized components of the emission and/or excitation. In the sample space there are two possibilities, the temperature cell might be placed or the high-pressure autoclave. In the right emission channel light emitted by the sample is spectrally divided by the emission monochromator in the optical path. Just like the excitation monochromator, this also contains concave holographic gratings with 1200 grooves per millimeter as a dispersive element. The emission monochromator grating is maximized for fluorescence light detection in the region λ = 350-800 nm. Additionally slits for optical filter are indicated in both detection ways directly behind the polarizer. Optical filters are used to compensate for the less than ideal behavior of monochromators.

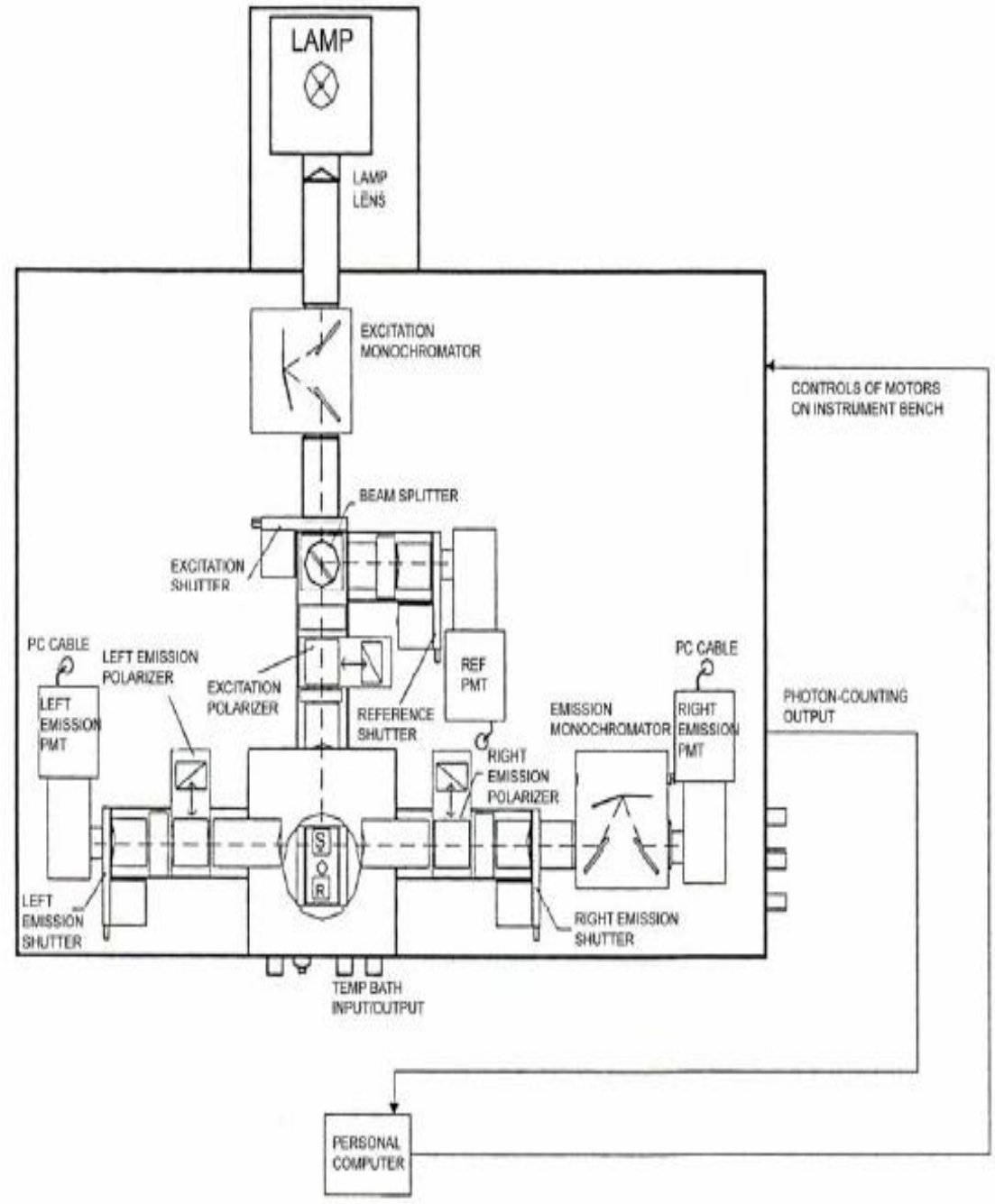

Figure 2.4: Schematic illustration of the K2 fluorescence spectrometer.

The detection of the emission can be made by the two photomultipliers, on the left and on the right side of the sample area. The emitted fluorescence radiation is bundled first by a lens. The bundled emission radiation arrived then nonpolarized to the detector. Almost all fluorometers use photomultiplier tubes as detectors. A PMT is best

regarded as accurate source, the current being proportional to the light intensity. Although a PMT responds to individual photons, these individual pulses are generally detected as an average signal.

2.4.4 High Pressure Cell

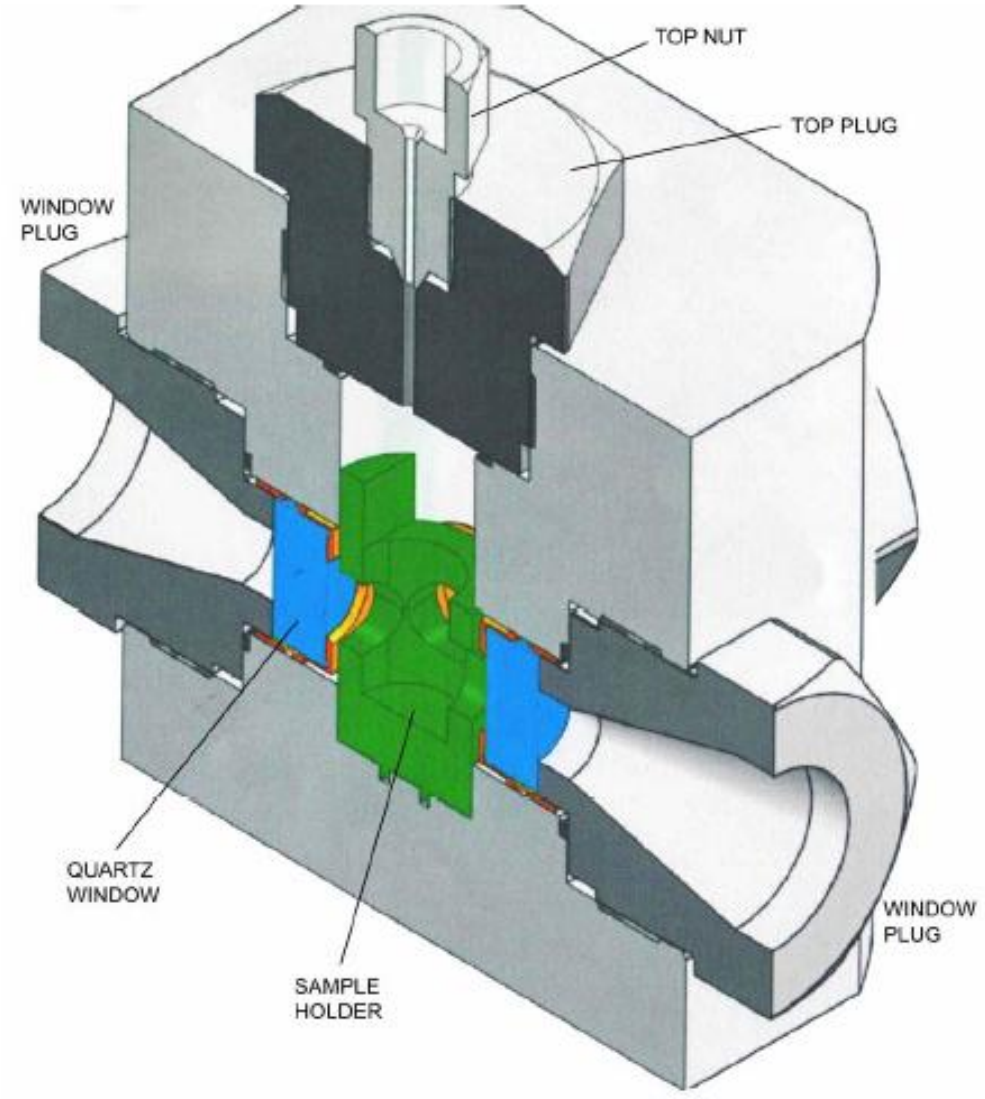

Figure 2.5: Cross section image of the high pressure fluorescence cell.

To accomplish high pressure measurements, sample was pressurized by ethanol in a high pressure cell system made by the ISS company. The high pressure cell construction is presented in Fig. 2.5. It has been specifically designed for high pressure

fluorescence studies up to pressures of about 3000 bar. The cell can work up to 4 kbar, if sapphire windows are used**.** Three 19 mm diameter and 8.5 mm thickness quartz windows have been placed allowing the use of the fluorescence format either with laser or with xenon lamp sources. The cell is made of a stainless steel alloy which has excellent thermal conductivity. The cell also includes a built-in circulation path for temperature control through an external liquid circulation bath. The cell pressure was generated through a manual pump system limited to 4 kbar (HP Technology Frankfurt, Germany). The accuracy of the manual pump system is indicated as 10 bar.

2.5 Circular Dichroism Spectroscopy

Unpolarized light has electric and magnetic field vectors that point in random directions perpendicular to its axis of travel. In case of *linearly polarized* (also called *plane polarized)* light, the electric and magnetic field vectors all point in the same direction. There is another kind of polarization of light, called *circular polarization*. In this case, the light vector propagates as a helix, as shown in Figure 2.6, from both side view and an end view. The helix can be right-handed or left-handed, so we can have right-circularly polarized light and left-circularly polarized light.

CD spectroscopy is used to measure the interaction of polarized light with optically active (i.e., asymmetric) molecules. Asymmetry can result from chiral molecules such as the peptide backbone of proteins, a non-chiral molecule covalently attached to a chiral molecule (aromatic amino acid side chains), or a non-chiral molecule in an asymmetric environment (e.g., a chromophore bound to a protein). Proteins are CD active (all amino acids except glycine contain a chiral carbon), and the resulting CD signals are sensitive to the protein's secondary and tertiary structure. The secondary structures of proteins interact preferentially with one circular polarization, allowing one to follow the changes in protein structure using circular dichroism spectroscopy

Side view End view

Figure 2.6: Circularly polarized light, side view and end view.

By definition, CD is a measure of the differential absorbance between the left circularly polarized (lcp-l) and right circularly polarized (rcp-r) light. According to the Beer-Lambert law, we can define the absorbance for lcp as

$$A = \log_{10} (I_o / I) = \varepsilon_l cl$$

Where I_o and I are, respectively, the intensities of lcp light incident on the sample and after traveling a distance l through a medium containing the molar concentration C of the chiral solute, and ε_l is the molar extinction coefficient of the solute for lcp light. Corresponding definitions can be formulated for rcp light, leading to the definition of CD as

$$\Delta A = A_l - A_{r=} \varepsilon_l cl - \varepsilon_r cl = \Delta\varepsilon cl$$

where $\Delta\varepsilon$ is the molar CD, defined as

$$\Delta\varepsilon = \varepsilon_l - \varepsilon_r$$

Therefore it would be logical to use $\Delta\varepsilon$ as CD data. However, for most historical and instrumental reasons, the CD data are often expressed not as $\Delta\varepsilon$ but in terms of the molar ellipticity, i.e., $\theta(\lambda)$, which has units of deg cm^2 $dmol^{-1}$. When plane polarized light passes through a solution containing an optically active substance, the left and right circularly polarized components of the plane polarized light are absorbed by different amounts. When these components are recombined, they appear as elliptically polarized light. The ellipticity is the angle θ, the tangent of which is the ratio of the minor to the major axis of the ellipse.

CD spectra of proteins and peptides are usually measured in two spectral regions. In the far-UV region (approximately 180-250 nm), the measured bands represent the electronic transitions of the amide groups of the protein backbone. The sign, magnitude, and position of these bands are strongly dependent on the φ and ψ angles of the peptide bond. From this region of the spectrum it is possible to obtain

information about the secondary structure of the protein. The analysis of the bands in near UV region (approximately 250-350 nm) is influenced by the side chains of aromatic amino acids and by disulfide bonds. The CD-spectra depend on the local environment of the aromatic amino acids and on their orientation with respect to the backbone, thus providing a fingerprint of the tertiary structure of the protein molecule.

2.5.1 Far UV CD Spectra and Protein Secondary Structure

The most stable and abundant elements of regular, periodic secondary structures are α-helices and parallel and antiparallel β-sheets [65]. All proteins can be grouped into five classes according to their secondary structures: 1) All α protein, which show a strong double minimum at 222 and 208-210 nm and a strong maximum at 191-193 nm. 2) All β proteins usually have a single negative minimum between 210 and 225 nm and a single positive maximum between 190 and 200 nm. In contrast a highly distorted β-sheet or β-sheets made up of short irregular β-strands show a strong negative band near 200 nm similar to unordered forms [66]. 3) α+β proteins have α-helices and β-sheets often in separate domains. 4) α/β proteins have intermixed segments that often alternate along with polypeptide chain. For α+β and α/β proteins, the intensities of α-helices usually predominate those of β-sheets. Sometimes a single broad minimum CD band may appear between 210 and 220 nm because of overlapping of various α-helices and β-sheets. For α + β proteins, the 208- to 210-nm band usually has a larger intensity than the 222 nm band, and the reverse is true for the α/β proteins [67]. 5) Unordered or denatured proteins that have little ordered structures show a strong negative band near 200 nm and some week bands between 220 and 230 nm which can have either positive or negative signs.

The estimation of the secondary structure of a protein from its CD spectrum remains an empirical task despite many proposed methods of analysis, simple as well as sophisticated. This is because of the lack of a unique solution for the deconvolution of a CD spectrum. Most of these approaches assume that the secondary structure of the measured protein can be obtained by fitting the experimental spectrum with reference spectra believed to represent pure components of the secondary structures. However, the analyses of CD data based on the use of reference spectra of model polypeptides, when applied to proteins may result in disadvantages, because of the difference in the

percentage of secondary structure present in the reference and sample of interest. In contrast, the convex constraint analyses (CCA) are based on an algorithm that uses only experimental CD curves, without any reference spectra. A relatively new method based on the theory of neural networks has been introduced as an alternative to the statistical methods. Direct comparison of different methods is also not possible because of different reference proteins and numbers of proteins used as well as different wavelength truncations.

2.5.2 Experimental Part – Sample Preparation for Far UV CD Measurements

Stock solutions of purified LmrA are prepared in 50 mM HEPES-KOH, pH 7.0, 300 mM Nacl, 10% glycerol, 250 mM Imidazole, pH 7.0, and 0.05% DDM. This stock solution is diluted to 5 μM with 20 mM HEPES buffer, pH 7.0, and used for the CD spectroscopy measurements. CD spectra were recorded in a cylindrical thermocell (0.01 cm path length) from 190 to 260 nm in 1 nm steps on a JASCO J-715 (Easton, MD) under constant nitrogen flush. Each spectrum is an average of 20 scans taken with a scan speed of 20 nm per minute. An external water thermostat was used to control the temperature within ±0.1 ºC. Temperature-dependent CD scans were carried out from 30 to 70 ºC by stepwise increase of 5 ºC. Samples were equilibrated at each temperature for 15 min. CD data are expressed as the mean residual ellipticity (MRE) [θ] in degrees cm^2 $dmol^{-1}$. The secondary structure content of the protein was determined using the CDNN software [68] and DichroWeb [69, 70].

2.6 2-Photon Excitation Microscopy

Two-photon fluorescence excitation has many advantages including not only the 3-D resolution without using detection pinholes, but also the unique properties like localized photobleaching and photodamage to a sub-micron region at the focal point and not to the entire sample. The excitation of fluorophore happens not by absorption of a single photon of visible light, but by simultaneous absorption of two photons in a very short space of time, 10^{-16} s, each having half the energy needed for the excitation transition [71]. Giant unilamellar vesicle (GUV) studies allow direct microscopic visualization of domains and their topology in the μm range.

2.6.1 Experimental Part – GUV Preparation

Stock solutions of phospholipids, cholesterol, along with the fluorophore Lissamine rhodamine B rhodamine DHPE, and a raft marker Bodipy labeled fatty acid analogue C_5-ganglioside G_{M1} were prepared in chloroform solution. Rhodamine DHPE has preference to localise in the liquid-disordered domains of the lipid membrane. The ganglioside G_{M1} preferentially partitions into a ordered phases known as lipid rafts [72]. The concentration of the lipid stock solutions was 0.2 mg/mL, and the molar ratio DOPC/DPPC/chol was 1:2:1. For preparing giant unilamellar vesicles (GUVs), the electroformation method developed by Angelova and Dimitrov was followed [73]. To grow the GUVs, a special temperature controlled chamber was used, which was previously described [74]. The experiments were carried out in the same chamber after vesicle formation, using an inverted microscope (Axiovert 35; Zeiss, Thornwood, NY).

The following steps were used to prepare the GUVs. (1) The lipid solution (3 µL) was spread on each platinum (Pt) wire under a stream of N_2. To remove residues of the organic solvent, the samples were lyophilized for 1 h. (2) Pt wires are heated up to 65 °C by a circulating water bath. (3) In order to add the aqueous solvent into the chamber (Millipore water), the bottom part of the chamber was sealed with a cover slip. The water was previously heated to 65 °C and then a sufficient amount was added to cover the Pt wires. After this step, the Pt wires were connected to a function generator (Hewlett-Packard, Santa Clara, CA), and a low frequency AC field (sinusoidal wave function with a frequency of 10 Hz and an amplitude of 3 V) was applied for 90 min. After vesicle formation, the AC field was turned off and the temperature scan (from high to low temperatures) was initiated. A CCD color video camera (CCD-Iris; Sony, Tokyo) attached to the microscope was used to follow the vesicle formation and to select a target vesicle. The temperature was measured inside the sample chamber with a digital thermocouple (Model 400B; Omega, Stamford, CT) with a precision of 0.1 °C. After selecting a particular vesicle, the temperature was reduced slowly (5°C / 15 min) and the image was captured. The fluorescent probes were premixed with lipids in chloroform; the *N*-Rh-DPPE/lipid ratio was 1:400 (mol/mol) and the C_5-ganglioside G_{M1}/lipid ratio was 1:100 (mol/mol). Figure 2.7 illustrates the electroformation method of GUV cultivation.

2.6.2 Experimental Setup – Two-Photon Excitation Microscopy

The two-photon excitation fluorescence microscopy experiments were performed at the Laboratory of Fluorescence Dynamics (University of California, Irvine). The high photon densities required for two-photon absorption are achieved by focusing a high peak power laser light source on a diffraction-limited spot through a high numerical aperture objective. Therefore, in the areas above and below the focal plane, two-photon absorption does not occur because of insufficient photon flux. This allows a sectioning effect without the use of emission pinholes as in confocal microscopy. Another advantage of two-photon excitation is the low extent of photobleaching and photodamage above and below the focal plane. For our experiments, we used a scanning two-photon fluorescence microscope [75] with an LDAchroplan 20X long working distance air objective (Zeiss, Homldale, NJ) with a numerical aperture of 0.4. A titanium-sapphire laser (Mira 900; Coherent, Palo Alto, CA), pumped by a frequency-doubled Nd:vanadate laser was used as excitation light source. The excitation wavelength was set at 780 nm. The laser was guided by a galvanometer driven *x-y* scanner (Cambridge Technology, Water-Town, MA) to achieve beam scanning in both the *x* and *y* directions. The scanning rate was controlled by the input signal from a frequency synthesizer (Hewlett-Packard, Santa Clara, CA), and the frame rate of 200 μs was used to acquire the images (256 X 256 pixels). The fluorescence emission was observed through a broad band-pass filter from 350 to 600 nm (BG39 filter; Chroma Technology, Brattleboro, VT). For detecting 2 fluorophore emissions simultaneously in two channels, a fluorescein/Texas red filter set was used to collect fluorescence in the green and red regions, respectively. The green emission filter was a Chroma HQ525/50 (500-550 nm), the red was a Chroma HQ610/75 (573-648 nm), and the dichroic was a Q560LP. Both of the emission filters were coated for multiphoton work. A miniature photomultiplier (R5600- P; Hamamatsu, Brigdewater, NJ) was used for light detection in the photon counting mode.

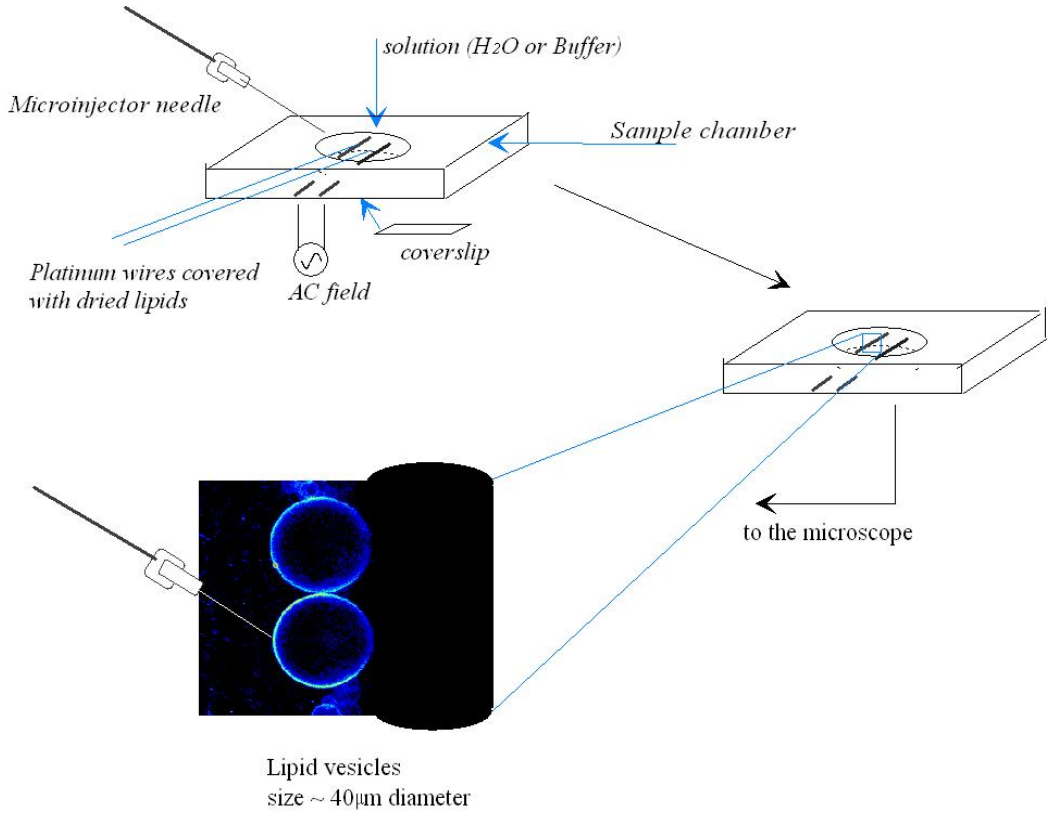

Figure 2.7: Electroformation method of GUV cultivation.

2.7 Atomic Force Microscopy (AFM)

AFM is a method of measuring surface topography on a scale from angstroms to 100 microns. The technique involves imaging a sample through the use of a probe, or tip, which is mounted at the end of a small flexible cantilever. The tip is the heart of the instrument because it is brought in closest contact with the sample and gives rise to the image through its force of interactions with the surface. The tip-cantilever assembly typically is fabricated from silicon or silicon nitride. The standard tip is usually a 3 μm tall pyramid with approximately 30 nm end radius. There are essentially two designs for cantilevers, the "V" shaped and the single arm kind which have different torsional properties. AFMs can generally measure the vertical deflection of the cantilever with picometer resolution. A laser beam is reflected from the backside of the cantilever (often coated by a thin metal layer to make a mirror) onto a position-sensitive photodetector consisting of two side-by-side photodiodes. A small deflection of the cantilever will tilt the reflected beam and change the position on the photodetector. Images are formed by recording the effects of the interacting forces between the

oscillating tip and sample surface as the cantilever is scanned over the sample. The scanner is an extremely accurate positioning stage used to move the tip over the sample to form an image, and generally the scanner is made from a piezoelectric tube. The scanner and the electronic feedback circuit together with sample, cantilever, and optical lever form a feedback loop setup to alter the stage height while scanning.

Figure 2.8 illustrates the AFM setup. AFM provides superior topographic contrast in addition to direct measurements of true three-dimensional surface features providing quantitative height information. The AFM technique offers a number of special features: very high magnification with very high resolution using a minimum amount of samples at physiological condition.

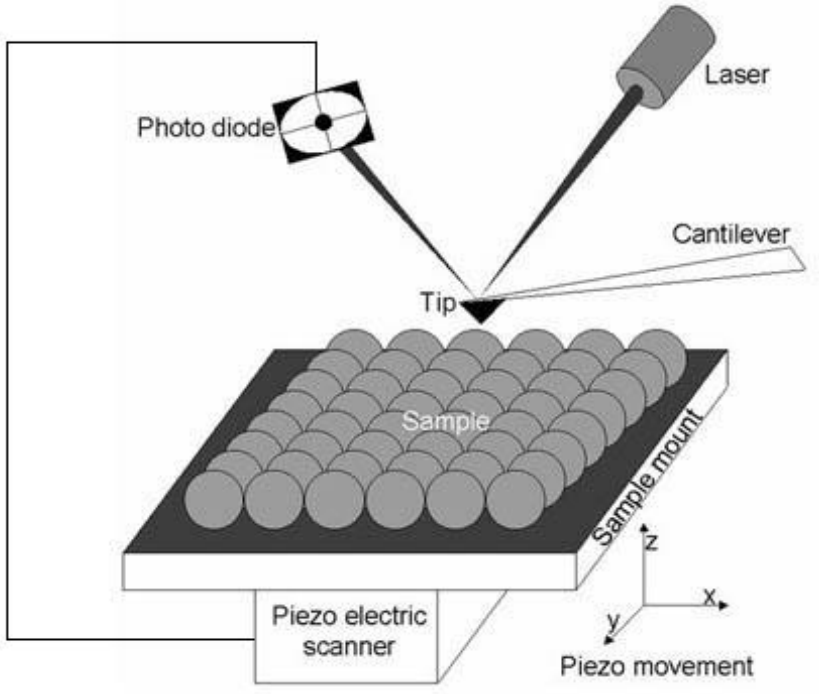

Figure 2.8: Schematics of an AFM setup

2.7.1 Experimental Part – Sample Preparation

For AFM studies, a freshly prepared LmrA proteoliposome sample (lipid-protein ratio 50:1 wt/wt, $c_{(lipid)}$ = 1 mg/mL) was extruded at 40 °C using an Avanti Mini-extruder (Avanti Polar Lipids, Alabaster, AL) with polycarbonate membrane filters of 100 nm pore size to yield large unilamellar vesicles. Supported lipid bilayers for AFM measurements were produced by depositing 60 µL of the LmrA proteoliposome solution together with 30 µL of buffer (20 mM HEPES, 10 mM $MgCl_2$ pH 7.2) on a freshly cleaved mica and incubation in a wet chamber overnight at 37 °C for DMPC and DMPC+Chol membranes and 45 °C for DOPC:DPPC:Chol membranes. After incubation, the sample was allowed to cool to room temperature, carefully rinsed with buffer and placed on the AFM stage.

2.7.2 AFM Setup

Measurements were conducted on a MultiMode scanning probe microscope with a NanoScope IIIa controller (Digital Instruments, Santa Barbara, CA) and using a J-Scanner (scan size 125 µm x 125 µm). Images were obtained by applying the Tapping Mode with oxide-sharpened silicon nitride probes (DNP-S, Veeco Instruments, Mannheim) mounted in a fluid cell (MTFML, Veeco Instruments, Mannheim). Tips with nominal force constants of 0.32 N/m were used at driving frequencies around 9 kHz and drive amplitudes between 200 and 400 mV corresponding to the softness of the sample. Height and phase images of sample regions were acquired with resolutions of 512 x 512 pixels and scan frequencies between 0.5 and 1.5 Hz. All measurements were carried out at room temperature. Images were processed by using NanoScope software version 5.

2.8 Transport Activity of LmrA in Different Reconstituted System

2.8.1 Hoechst-33342 Transport in Proteoliposomes

The ATP-binding cassette (ABC) transporter LmrA is a primary drug transporter in *Lactococcus lactis.* Primary-active transporters are dependent on ATP hydrolysis. LmrA uses the free energy of ATP hydrolysis to expel a wide variety of structurally unrelated compounds from the membrane. The fluorescent substrate Hoechst-33342 was used to assess the transport activity of the reconstituted LmrA in DMPC model

membrane system. Hoechst-33342 is non fluorescent in aqueous environment while in the membrane environment it displays a strong fluorescence signal [51]. This compound has been used for activity measurements of reconstituted systems with P-glycoprotein [76] and LmrP [77]. The ATP depended decrease of the fluorescence intensity of Hoechst-33342 will indicate that the reconstituted LmrA is functionally active.

2.8.2 Experimental Part – Sample Preparation for Transport Activity Assay

Proteoliposomes were constructed in DMPC bilayer by the successive detergent removal method and resuspended in 50 mM potassium phosphate buffer, pH 7.2. The weight ratio between LmrA and lipid is 1:20. The concentration of lipid is 1mg/mL. The sample containing 250 μL proteoliposomes were added to 2 mM $MgSO_4$, 8.5 mM NaCl, 50 mM HEPES, 50 mM KOH. After 75 s of data collection, 1.25 μM Hoechst-33342 was added. Mg-ATP was added 100 s after the Hoechst-33342 addition. The fluorescence intensity was followed for 15 min with the K2 multi phase fluorometer, using excitation and emission wavelengths of 355 and 457 nm, respectively.

2.9 ATPase Activity Using Coupled Enzyme ATPase Assay

ATP hydrolysis by the action of LmrA is also checked by a coupled enzyme ATPase assay [78, 79]. The coupled enzyme ATPase assay is based on the conversion of phosphoenolpyruvate (PEP) to pyruvate by pyruvate kinase (PK) coupled to the conversion of pyruvate to lactate by lactate dehydrogenase (LDH). The latter step requires NADH which is oxidized to NAD^+. NADH absorbs strongly at 340 nm but NAD^+ does not absorb, enabling the utilisation of NADH to be followed by monitoring the absorbance at 340 nm with time. A decrease in NADH absorbance at 340 nm is a measure of the ATPase activity of the reconstituted system. The pressure effect on the activity of LmrA is followed by checking the ATPase activity of LmrA using the coupled enzyme assay in different lipid environments at different pressures.

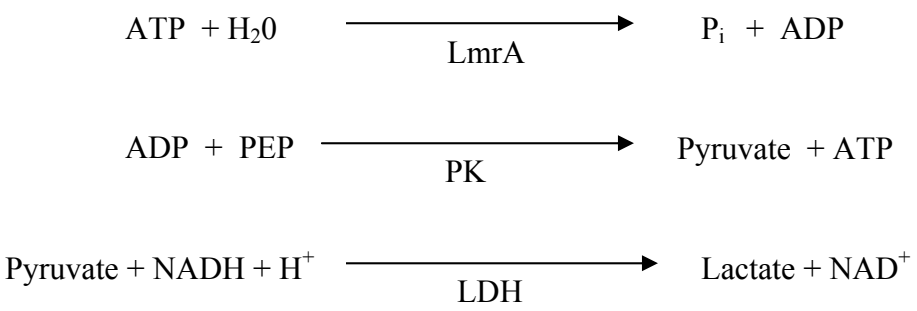

The ATPase reaction is started with addition of 3 mM mg-ATP. If the reconstituted LmrA retains its ATPase activity, results in the conversion of ATP to ADP. Using this ADP, phosphoenolpyruvate is converted to pyruvate in the presence of pyruvate kinase, and regenerate the ATP in order to reuse. Finally, pyruvate is converted to lactate by lactate dehydrogenase and this step requires NADH which is oxidized to NAD^+. In order to follow the NADH decay and hence the ATPase activity of the LmrA reconstituted in different lipids environments, the absorbance of NADH at 340 nm is measured with time at different pressures.

2.9.1 Experimental Part – Sample Preparation for ATPase Activity Assay

The ATPase activity was determined at 30 °C in an assay medium containing 20 mM HEPES, pH 7.2, 130 mM NaCl, 20 mM KCl, 0.1 mM EDTA, 4 mM $MgCl_2$, 30 units/mL of phosphokinase (PK), 90 units/mL of lactosedehydrogenase (LDH), 3 mM phosphoenolpyruvate (PEP), 0.4 mM NADH, 0.11 µM Ethidium bromide, 5 µg of LmrA in different lipid environment. The reaction was started by adding 3 mM Mg-ATP and the consumption of NADH was followed by its absorbance decrease at 340 nm with time at different pressures of 1 atm, 500 bar, 1 kbar, 1.5 kbar, and 2 kbar. The total volume of 1.15 mL content is taken in a small quartz glass bottle, covered with laboratory stretch film and closed with an o-ring made from fluorinated rubber (VI563/FPM70, Otto Gehrckens GmbH, Germany).

In order to measure the absorbance of NADH as a function of pressure, all the experiments were carried out on a K2 multifrequency phase and modulation fluorometer (ISS, Inc., Champaign, IL) using transmission mode. In the transmission

mode, I_o and I were measured separately using liposomes and proteoliposomes as blank and sample, respectively. All the other components of the assay mixture were kept constant. For each pressure, the absorbance is defined as $A_{340} = \log_{10} (I_0 / I)$, where I_o and I are, respectively, the transmission intensity measured with liposome and proteoliposome along with all other assay mixture. The proteoliposome solution contains an equal amount of lipids (0.1 mg/mL) as in the case of liposome. The temperature was controlled to ±0.1 °C by a circulating water bath. The sample was pressured by ethanol in a high pressure cell system made by the ISS Company. The high pressure cell construction is presented in Figure 2.5.

3 Results and Discussion

3.1 Part I: Lipid–Peptide Interactions

3.1.1 Influence of Temperature on the Phase Behavior of Ternary POPC:SM:Chol Lipid Systems

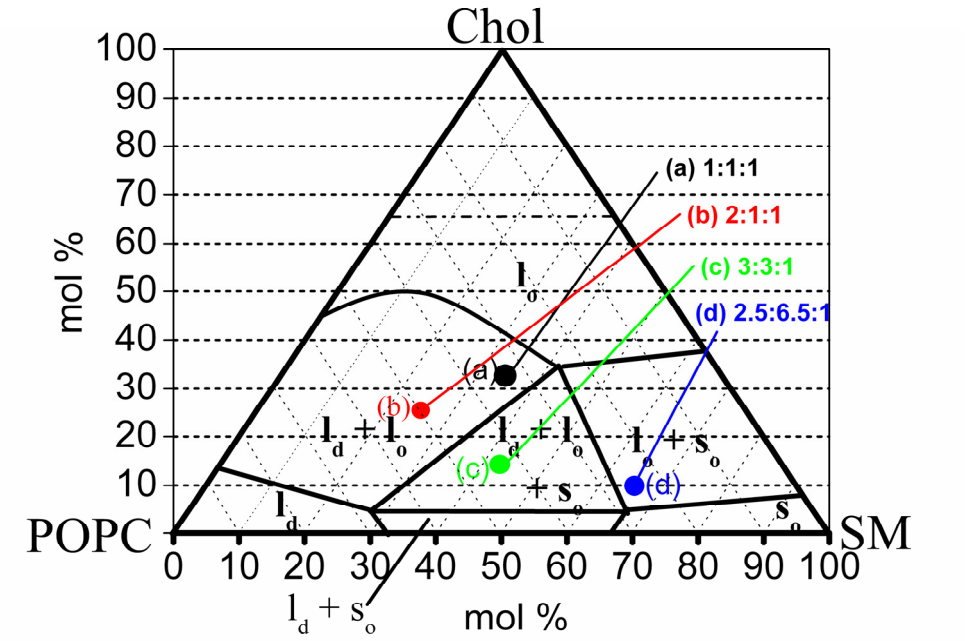

Figure 3.1: Phase diagram of the ternary system POPC:SM:Chol (Almeida et al. 2003).

The temperature dependence of the generalized polarization of Laurdan labelled ternary lipid mixtures at ambient pressure is shown in Fig 3.2, which depicts *GP* values of the system POPC:SM:Chol consisting of different compositions of its constituent lipids (with molar ratios 1:1:1, 2:1:1, 3:3:1, and 2.5:6.5:1), which were measured over a temperature range from 3 to 75 °C. According to the phase diagram of the ternary system POPC:SM:Chol as given by Almeida et al. [80], all the above mixtures have coexisting domains of different phases at room temperature (23 °C), which is shown in Fig. 3.1. The 1:1:1 and 2:1:1 mixtures contain l_o and l_d domains, the 3:3:1 mixture l_d, l_o and s_o domains, and the 2.5:6.5:1 mixture contains l_o and s_o domains (l_d, l_o and s_o denotes liquid-disordered (fluid), liquid-ordered and solid-ordered, respectively). All measurements were carried out at least three times and the average value and respective error bars of the *GP* values are given.

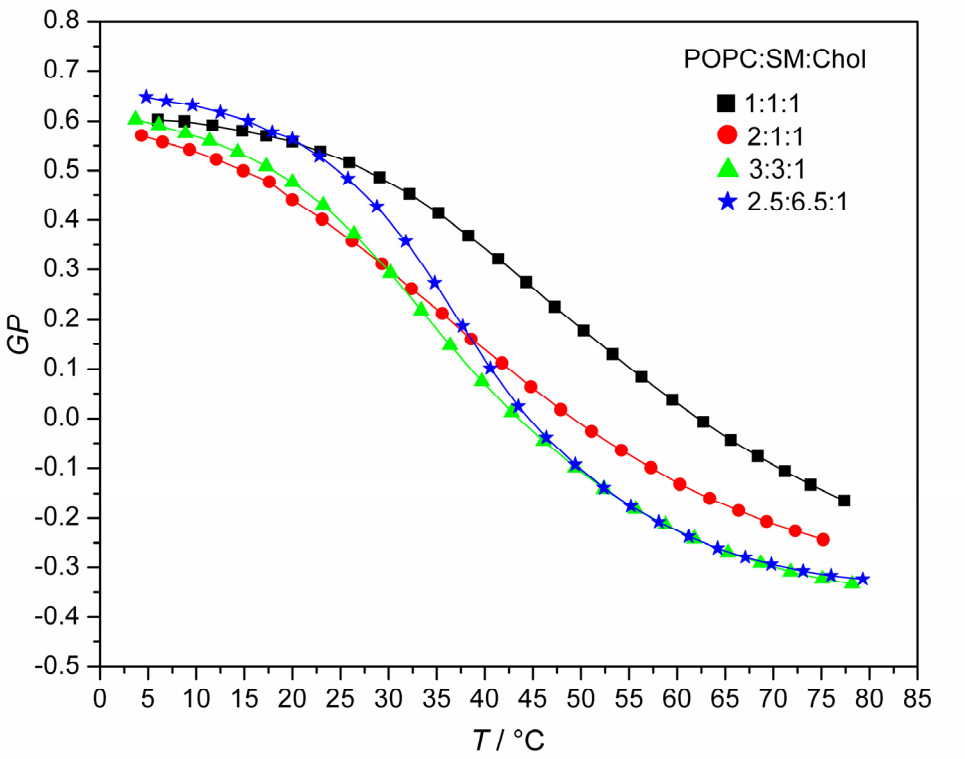

Figure 3.2: Temperature dependence of the generalized polarization-*GP* of Laurdan labelled ternary POPC:SM:Chol lipid bilayer systems.

As can be clearly seen in Fig. 3.2, the generalized polarization value gradually decreases with increasing temperature for all four compositions measured, with a sigmoidal kind of shape in the temperature interval between about 15 and 65 ^{o}C. In fact, such a smooth behavior is expected from Gibbs' phase rule for such three-component lipid mixtures, which is very different from one-component lipid bilayer systems, which generally exhibit several sharp gel-to-gel and a gel-to-fluid phase transitions in the temperature range covered [14, 81]. Hence, by a more or less continuous increase of liquid-disordered domains, the fluidity and conformational disorder of the membrane gradually increases with increasing temperature, and *GP* values typical for pure fluid phases are reached above about 65 ^{o}C for the 3:3:1 and 2.5:6.5:1 POPC:SM:Chol mixtures. These conclusions are in good agreement with TMA-DPH steady state fluorescence anisotropy data, which directly reflect the mean order parameter of the lipid acyl chains in these ternary systems. No clear-cut value for the transition temperature to the overall fluid phase can be given owing to the continuous nature of the *GP* curves. The population of individual domains (l_o, l_d, or s_o) depends on the molecular composition of the mixture and on the temperature. As

expected, and owing to the disordering effect of the lipid POPC (with a gel-to-fluid transition temperature of about -5 °C [81]), the *GP* value over the whole temperature range is lower in the case of the 2:1:1 mixture compared to the less POPC containing 1:1:1 mixture. Vesicles made up of 2.5:6.5:1 POPC:SM:Chol, containing only l_o+s_o domains at room temperature [80], exhibit more ordered domains at 20 °C as the *GP* value (0.56) is higher than that of the other mixtures (*GP* = 0.55 for 1:1:1, *GP* = 0.44 for 2:1:1, and *GP* = 0.47 for 3:3:1), thus pointing to the marked rigidifying effect of SM. Due to its lower POPC content, the *GP*(*T*) curve of the 1:1:1 mixture is shifted by ~12 °C to higher temperatures with respect to the 2:1:1 mixture. For the vesicles made up of 1:1:1 POPC:SM:Chol, fluid-like *GP* values are not reached even up to ~80 °C.

3.1.2 Influence of Pressure on the Phase Behavior of Ternary POPC:SM:Chol Lipid Systems

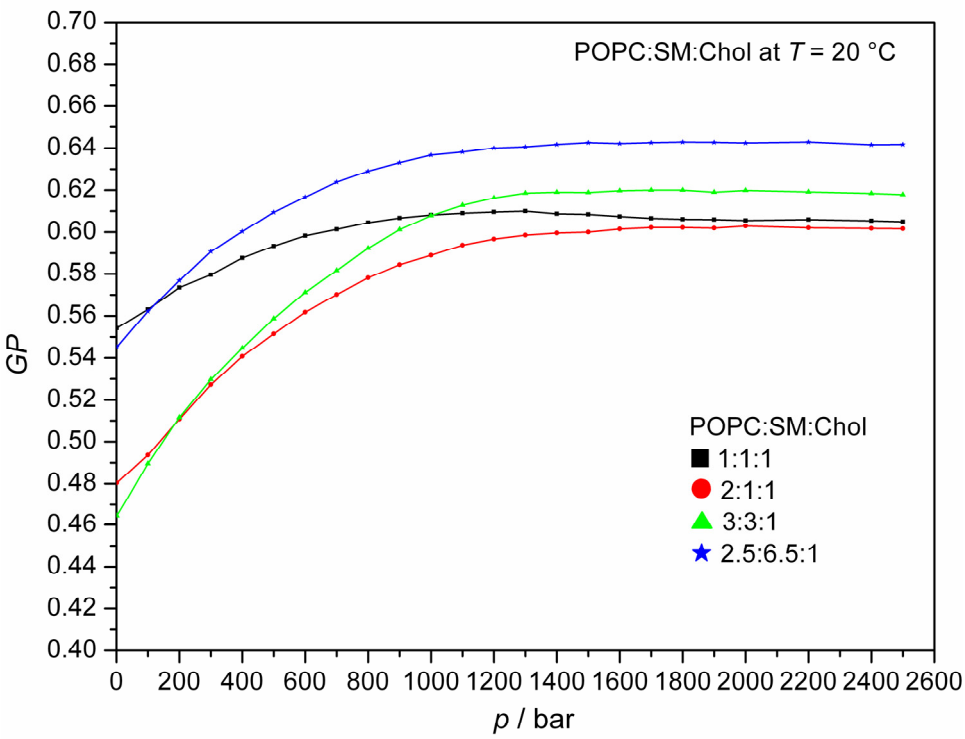

Figure 3.3: Pressure dependence of the generalized polarization *GP* of Laurdan labelled ternary POPC:SM:Chol lipid bilayer systems at *T* = 20 °C.

The effect of pressure on the generalized polarization data of the Laurdan labelled POPC:SM:Chol mixtures is shown in Fig. 3.3, which exhibits *GP* data at room temperature (20 °C) as a function of pressure, from ambient pressure up to 2500 bar. In

the case of the 1:1:1 composition, the *GP* values increase steadily with increasing pressure up to about 800-900 bar, where a plateau value of about 0.6 is reached, indicating that a rather ordered (probably an s_o+l_o) state is reached which is not affected upon further application of higher pressures (up to 2.5 kbar) any more. At much higher pressures, the transition to all s_o phase could be envisaged. However, as the lipid mixture contains cholesterol and sphingomyelin, which might not pack well against *cis*-unsaturated lipids, this could be prohibited. A corresponding *GP* plateau value is reached at about 1100-1200 bar for all other compositions, with maximal *GP* values of 0.60 for the 1:1:1, 0.64 for the 2.5:6.5:1, 0.60 for the 2:1:1, and 0.62 for the 3:3:1 mixture, respectively. These data indicate that for all model raft mixtures, an overall (liquid or solid) ordered membrane state, i.e., a maximal ordering of their acyl chains, is reached at pressures of about 800 to 1200 bar. The maximal *GP* values reached upon pressurization are only slightly larger than those at the lowest temperatures (~5 ^{o}C) of the corresponding system. Hence, a temperature decrease of about 50 ^{o}C has a similar effect on membrane ordering and lateral organization as a pressure increase of about 1 kbar at room temperature.

3.1.3 The Effect of Gramicidin D (GD) Incorporation

Figures 3.4 and 3.5 show the effect of incorporating 5 mol% GD on the temperature and pressure dependencies of *GP* for the 1:1:1 POPC:SM:Chol mixture, respectively. Addition of the polypeptide leads to a small, but readily reproducible increase of *GP* over the whole temperature range covered. The larger *GP* values indicate that the polypeptide is incorporated into the l_d domains of the lipid mixture, thus increasing the orientational order of their acyl chains, in a similar manner as it has been observed for one-component phospholipid bilayer systems in their respective fluid phases [30]. Apart from that, no markedly different phase behavior is observed. An increase of pressure at constant temperature (40 ^{o}C) has a similar effect. The overall *GP* values of the peptide containing membrane are slightly larger than those of the pure lipid mixture up to ~1400 bar, and the same limiting plateau value of *GP* = 0.62 is reached above about 2000 bar.

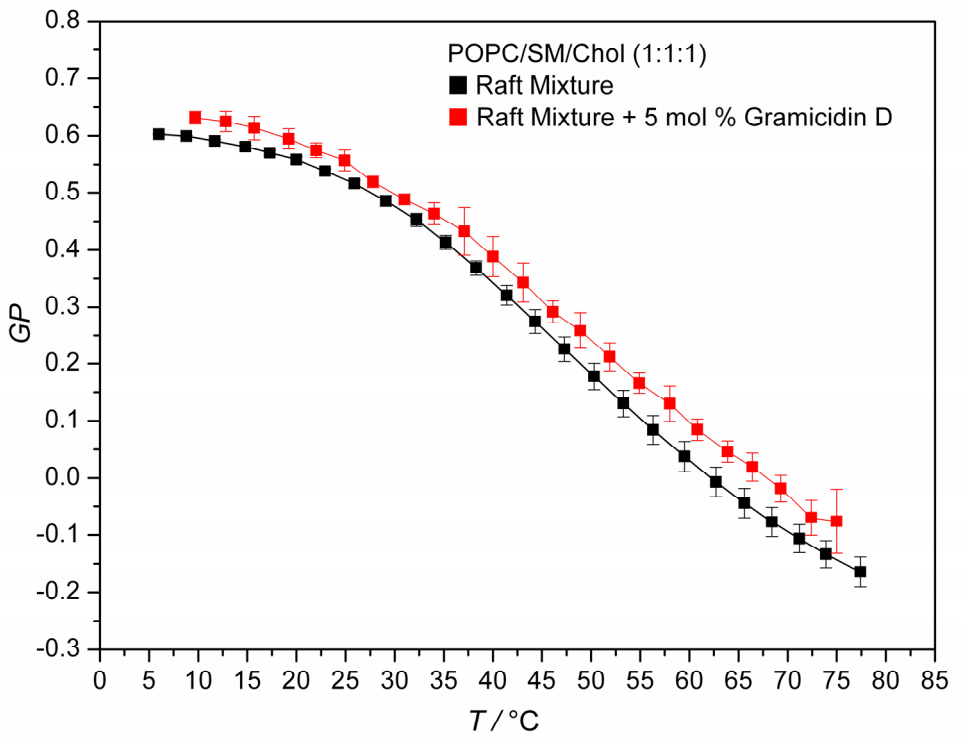

Figure 3.4: Temperature dependence of Laurdan *GP* values of the lipid mixture POPC:SM:Chol 1:1:1 without and with addition of 5 mol% GD.

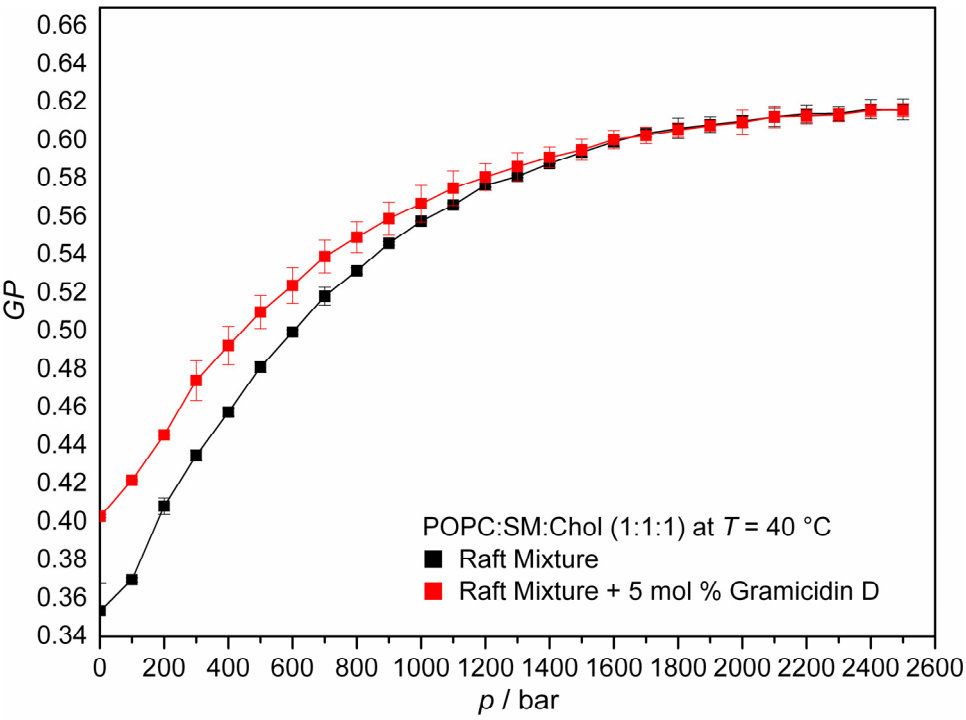

Figure 3.5: Pressure (at $T = 40\ ^{o}C$) dependence of Laurdan *GP* values the of lipid mixture POPC:SM:Chol 1:1:1 without and with addition of 5 mol% GD.

3.1.4 Summary Part-I: Lipid-Peptide Interactions

In conclusion, it is shown that the liquid-disordered/liquid-ordered phase coexistence region of POPC:SM:Chol model raft mixtures extends over a very wide temperature range of about 50 ^{o}C. An overall fluid phase is reached at rather high temperatures (above ~65 ^{o}C), only. Upon pressurization at room temperature (20 ^{o}C), an overall (liquid- and/or solid-) ordered membrane state with maximal ordering of their acyl chains is reached at pressures of about 1 kbar. A temperature decrease of about 50 ^{o}C has a similar effect on membrane ordering and lateral organization as a pressure increase of 1 kbar. At 40 ^{o}C, the overall (according to the Gibbs phase rule, probably l_o+s_o) ordered lipid state of the 1:1:1 POPC:SM:Chol mixture is reached at ~2 kbar. Essentially, the fluid phase lipids will become ordered. A purely solid-ordered state might not be reached until very high pressures (if at all), owing to the fact that cholesterol and sphingomyelin are not expected to pack well against the *cis*-unsaturated POPC. Interestingly, in this pressure range of 2 kbar, ceasing of membrane protein function in natural membrane environments has been observed for a variety of systems [24, 29, 31, 34, 35], which might be correlated with the membrane matrix reaching a physiologically unacceptable overall ordered state at these pressures. These data may be compared with the slope of ~20 ^{o}C/kbar for the pressure-induced fluid to gel phase transition of one-component lipid bilayer systems [22, 24-26, 28].

Incorporation of *GD* slightly increases the overall order parameter profile in the l_o+l_d two-phase coexistence regions, probably by selectively partitioning into l_d domains, which is indicated by the increased *GP* values with respect to the pure lipid mixture. This behavior is in contrast to the effect of *GD* incorporation into simple, one-component phospholipid bilayer systems, where no different coexisting domains are offered and no lipid sorting mechanism is feasible. As revealed by recent ^{2}H-NMR measurements [82], in these one-component phospholipid systems the mean order of the acyl chains decreases markedly in the gel phases and more or less broad fluid-gel and gel-gel two-phase regions may be induced, but the chain order parameter also slightly increases in the fluid-like state of the phospholipid bilayer systems. Incorporation of 5 mol% of the peptide into the 1:1:1 model raft mixture does not markedly change the pressure range where an overall ordered membrane state is reached. Please note that with an increase of pressure, which increasingly orders the fluid phase lipids, a decreasing mismatch in lipid length of the l_d and l_o domains

(which is ~0.8 nm at ambient conditions) is expected. A developing hydrophobic mismatch between the lipid bilayer and protein hydrophobic lengths will have drastic consequences for the energetics of protein insertion into the lipid bilayer system.

3.2 Part II: Lipid–Protein Interactions

3.2.1 Phase Behavior of the DMPC Lipid System with and without LmrA

As seen in Fig. 3.6, pure DMPC lipid bilayers exhibit a rather sharp gel-to-fluid ($P_{\beta'}/L_{\alpha}$) phase transition around T_m = 24°C. Reconstitution of LmrA protein leads to a broad gel-fluid phase coexistence region with an increased conformational order of the lipid acyl chains above the gel-liquid phase transition temperature of DMPC. Below T_m, LmrA slightly disturbs the packing order and hence the *GP* values are reduced. The effect of pressure on the generalized polarization data of Laurdan labelled DMPC bilayers with and without LmrA is shown in Fig. 3.7. Upon pressurization, the pressure-induced fluid-to-gel phase transition takes place around 700 bar at 37 °C in pure DMPC. Reconstitution of LmrA leads to an increasing overall conformational order of the membrane in the whole pressure range covered, i.e., from 1 to 2000 bar. The pressure dependent phase behavior does not change markedly upon the reconstitution of LmrA. Above 900 bar, a plateau *GP* value is reached in both pure (*GP* = 0.44) and reconstituted *(GP* = 0.49) DMPC vesicles. All the graphs presented here are the average of three independent measurements.

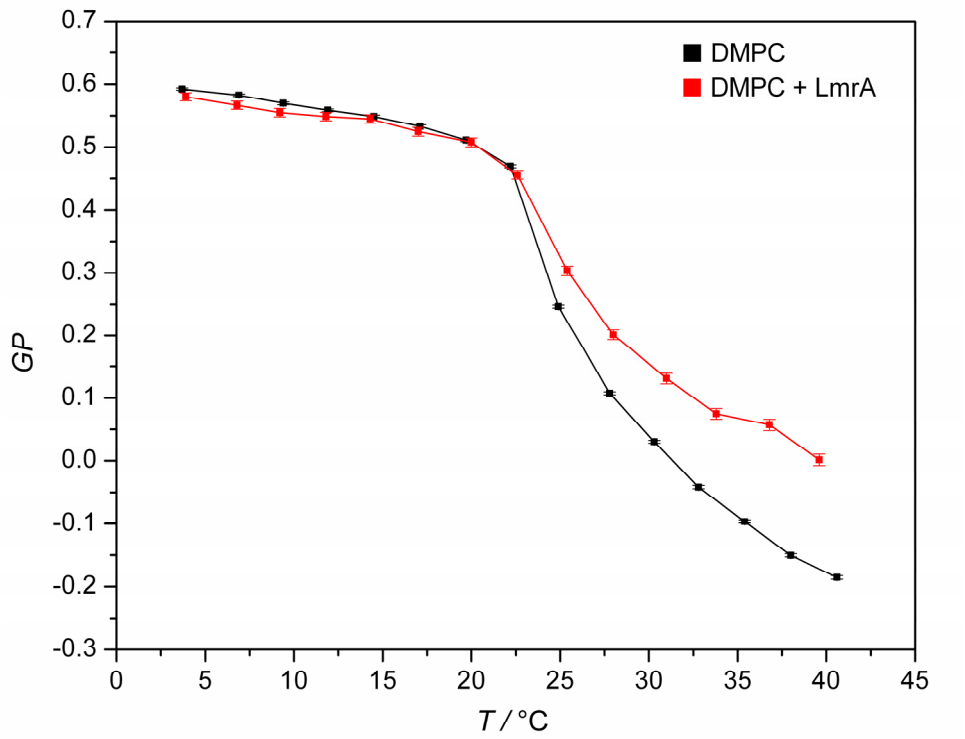

Figure 3.6: Temperature dependence of Laurdan *GP* values of DMPC vesicles with and without reconstitution of LmrA**.**

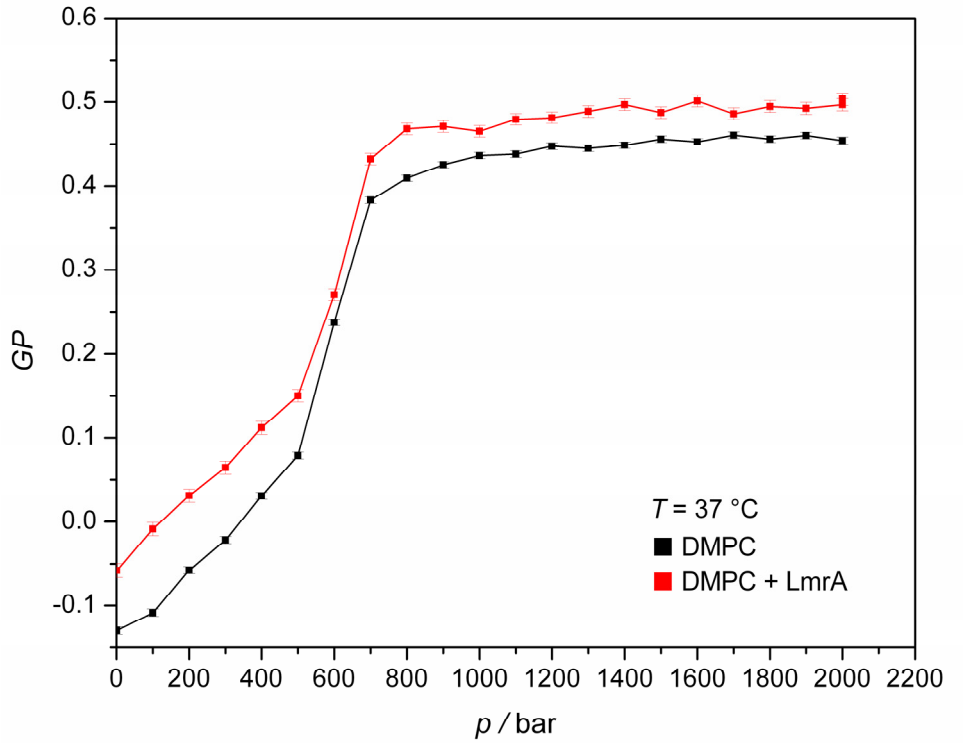

Figure 3.7: Pressure dependence (at $T = 37$ ºC) of Laurdan *GP* values of DMPC vesicles with and without reconstitution of LmrA.

3.2.2 Phase Behavior of the DOPC Lipid System with and without LmrA

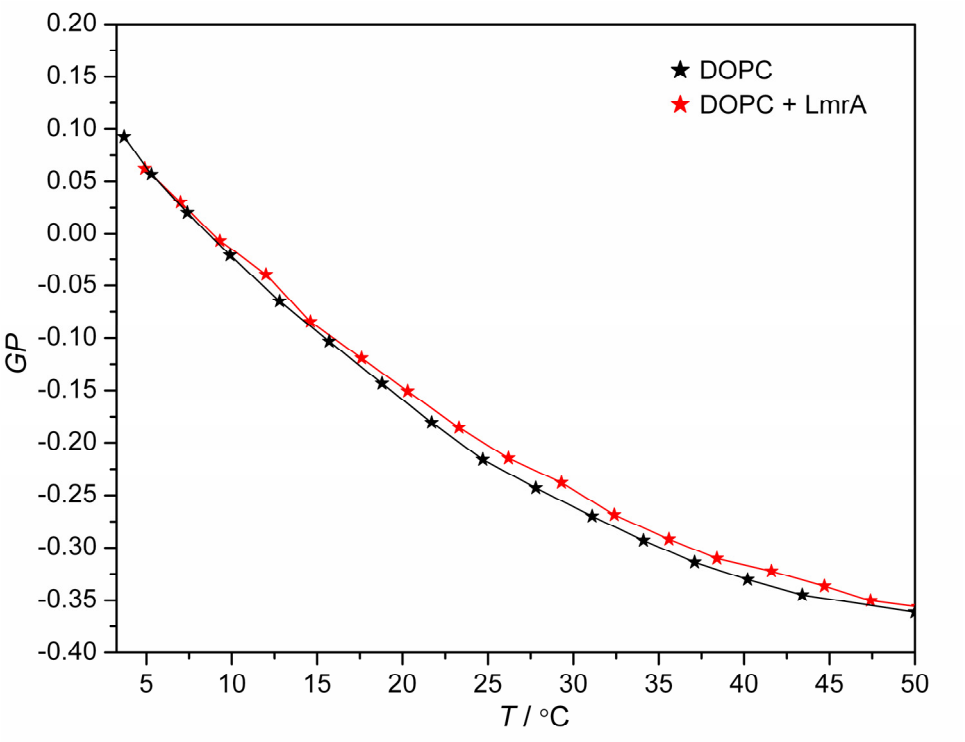

Figure 3.8: Temperature dependence of Laurdan *GP* values of DOPC vesicles with and without reconstitution of LmrA**.**

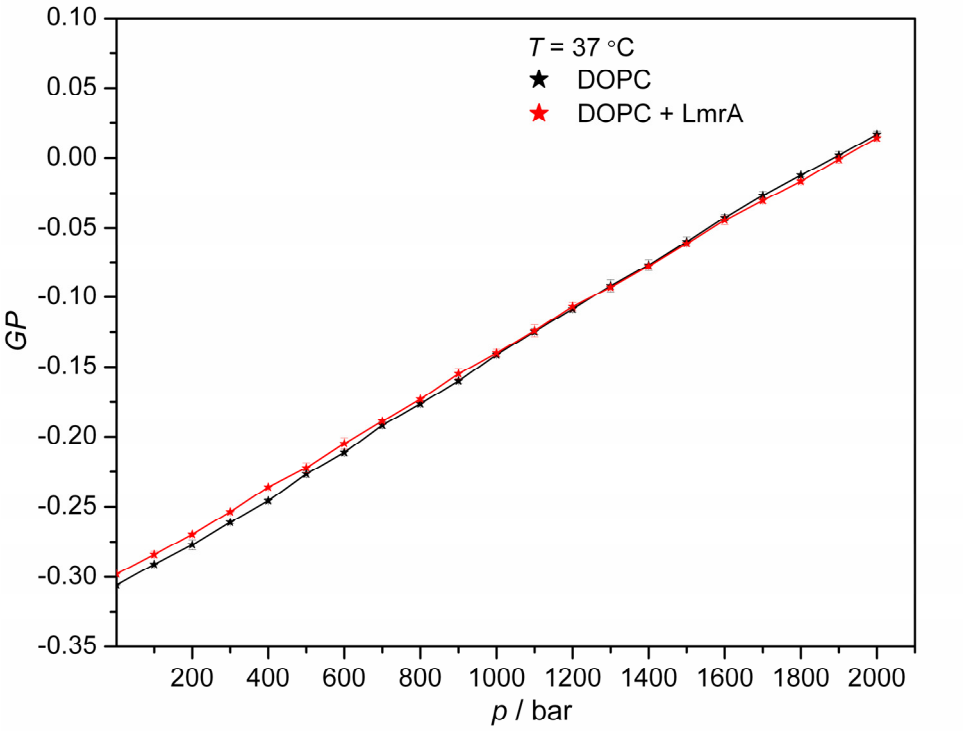

Figure 3.9: Pressure dependence (at $T = 37$ ºC) of Laurdan *GP* values of DOPC vesicles with and without reconstitution of LmrA.

The effect of temperature and pressure on the generalized polarization data of Laurdan labelled DOPC bilayer with and without LmrA is shown in Figs. 3.8 and 3.9, respectively. Due to the presence of two unsaturated acyl chain, the transition temperature of DOPC is -20 ºC. Hence throughout the measurement range (3 to 50 ºC) the DOPC bilayers are in the liquid-disordered state, which is characterized by very low *GP* values. By increasing the temperature, the fluidity of the acyl chains are still increased which leads to further slight reduction in the *GP* value. Pure DOPC bilayer at 3.7 ºC exhibits a *GP* value of 0.09, which gradually reduced to -0.36 at 50 ºC. Reconstitution of LmrA does not significantly increase the order parameter, still there is a very small increase of *GP* value throughout the temperature range covered. LmrA reconstituted in DOPC bilayer exhibits a *GP* value of 0.06 at 4.9 ºC, which gradually declines with increasing temperature; at 50.2 ºC, the *GP* value is -0.35. In pressure dependent *GP* measurements, the mean order parameter linearly increases with increasing pressure, as seen in Fig. 3.9. The *GP* value of pure DOPC bilayer at 1 atm is -0.31 and linearly increases to 0.02 at 2000 bar. As in the case of temperature dependent measurement, the reconstitution of LmrA did not markedly change the phase behaviour of the DOPC bilayer. The mean order parameter of LmrA reconstituted in DOPC system is slightly higher than that of the pure DOPC bilayer up to 1200 bar and it slightly reduced in higher (>1200 bar) pressure measurements carried out at 37 ºC. At 1 atm, the *GP* value of the LmrA reconstituted DOPC bilayer is -0.29 and at 2000 bar it increases to 0.01, only.

3.2.3 Phase Behavior of the DMPC + 10 Mol% Cholesterol Lipid System with and without LmrA

It is clearly evident from the Fig. 3.10, that the incorporation of 10 mol% of cholesterol into pure DMPC lipid bilayers largely abolishes the sharp gel-to-fluid ($P_{\beta'}/L_{\alpha}$) phase transition, due to the fact, that the incorporation of cholesterol in five to ten mol percentages in any pure lipid bilayer reduces the disorder in the liquid-crystalline state. This is evident by a slight increase of *GP* in the cholesterol incorporated system compared to that of the pure DMPC lipid system at all temperatures. Reconstitution of LmrA in the 10 mol% cholesterol containing DMPC lipid system leads to an increase in the conformational order of the lipid acyl chains

above the gel-liquid phase transition temperature of DMPC, and leads to no changes in the order parameter below T_m.

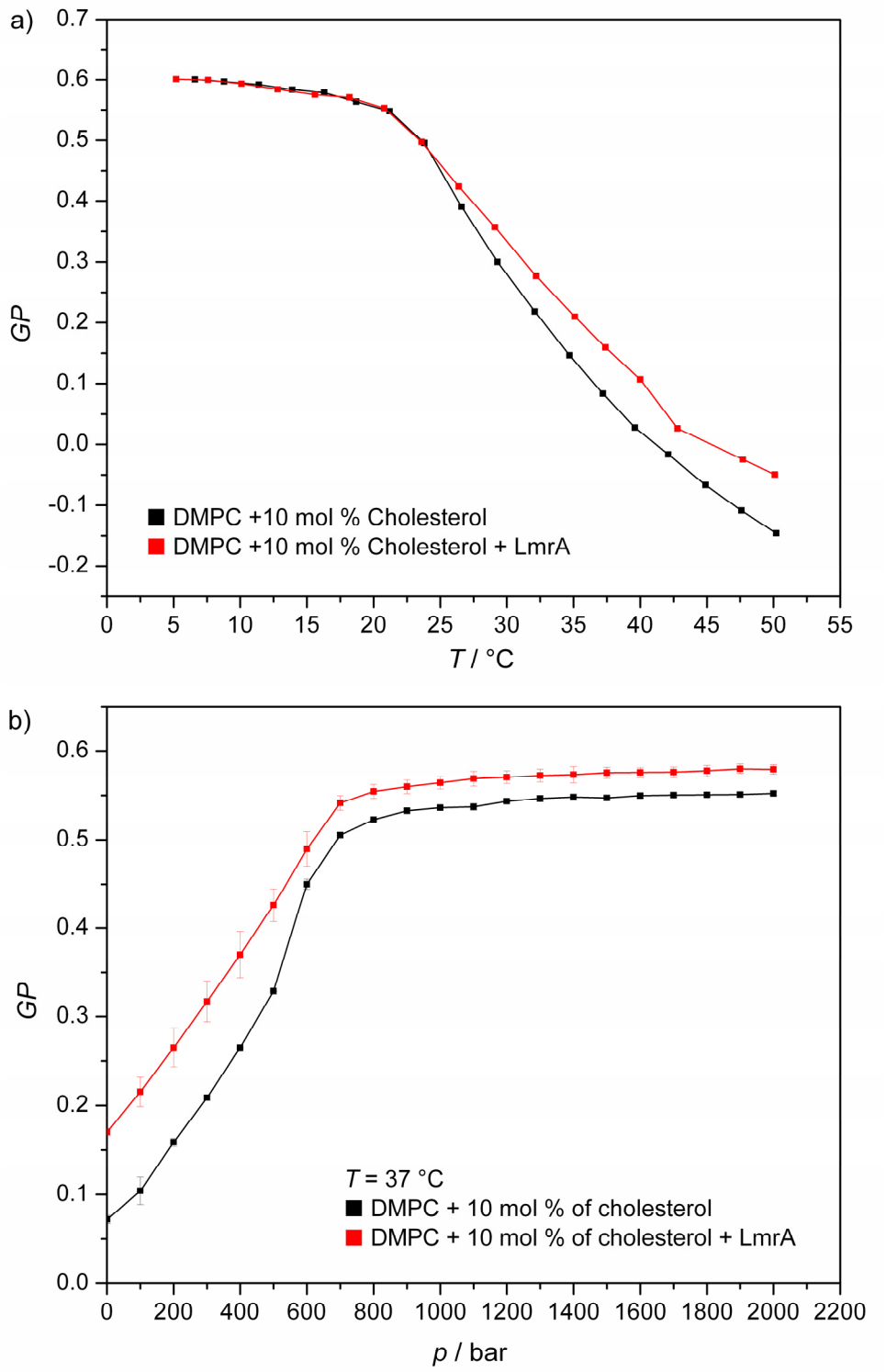

Figure 3.10(a): Temperature dependence of Laurdan *GP* values of lipid vesicles made of DMPC + 10 mol% cholesterol with and without reconstitution of LmrA. (b) Pressure dependence (at T = 37 ºC) of Laurdan *GP* values of vesicles made of DMPC + 10 mol% cholesterol with and without reconstitution of LmrA.

Upon pressurization, the pressure-induced fluid-to-gel phase transition takes place around 700 bar at 37 °C as we have observed in the pure DMPC system before. Reconstitution of LmrA leads to an increasing overall conformational order of the acyl chains in the membrane in the entire pressure range studied (1 to 2000 bar). The pressure dependent phase behavior does not change markedly upon the reconstitution with LmrA. A plateau *GP* value of 0.54 is reached in the case of DMPC + 10 mol% cholesterol and (*GP* = 0.57) in the case of LmrA reconstituted in cholesterol containing DMPC system at about 900 bar.

3.2.4 Phase Behavior of the Raft Lipid System with and without LmrA

Fig. 3.11(a) depicts the *GP* value of the DOPC/DPPC/Chol-1:2:1 system. The measurement was taken over a temperature range from 5 to 65 ºC. This system exhibits a physiologically more relevant l_o and l_d domain coexistence [21]. As can be clearly seen in Fig. 3.11(a), the generalized polarization value gradually decreases with increasing temperature with a sigmoidal kind of shape in the temperature interval between about 15 ºC (*GP* = 0.58) and 65 ºC (*GP* = -0.05). By a more or less continuous increase of liquid-disordered domains, the fluidity and conformational disorder of the membrane gradually increases with increasing temperature, and *GP* values typical for pure fluid phases are reached at about 60 ^{o}C. No clear-cut value for the transition temperature to the overall fluid phase can be given owing to the continuous nature of the transition and hence *GP* curve. The population of individual domains (l_o, l_d) depends on the temperature measured. Reconstitution of LmrA leads to a very small, but readily reproducible increase of *GP* in the lower temperature range from 5 to 35 ^{o}C. Above 30 ^{o}C, the LmrA has no effect on the orientational order of their acyl chains, which may be due to an even incorporation of LmrA in both, l_o- and l_d-domains. This was clearly observed in the AFM studies as well.

The effect of pressure on the generalized polarization data of Laurdan labelled DOPC/DPPC/Chol mixtures is shown in Fig. 3.11(b), which exhibits *GP* data at 40 ^{o}C as a function of pressure, from ambient pressure up to 2000 bar. In both, the pure and the LmrA reconstituted raft system, the *GP* value increases steadily with increasing pressure up to about 500 bar; from 500 to 1400 bar the *GP* value increases very slowly

and thereafter it reaches a plateau value of about 0.55 and 0.58, respectively, indicating that a rather ordered (probably an s_o+l_o) state is reached which is not affected upon application of higher pressures any more.

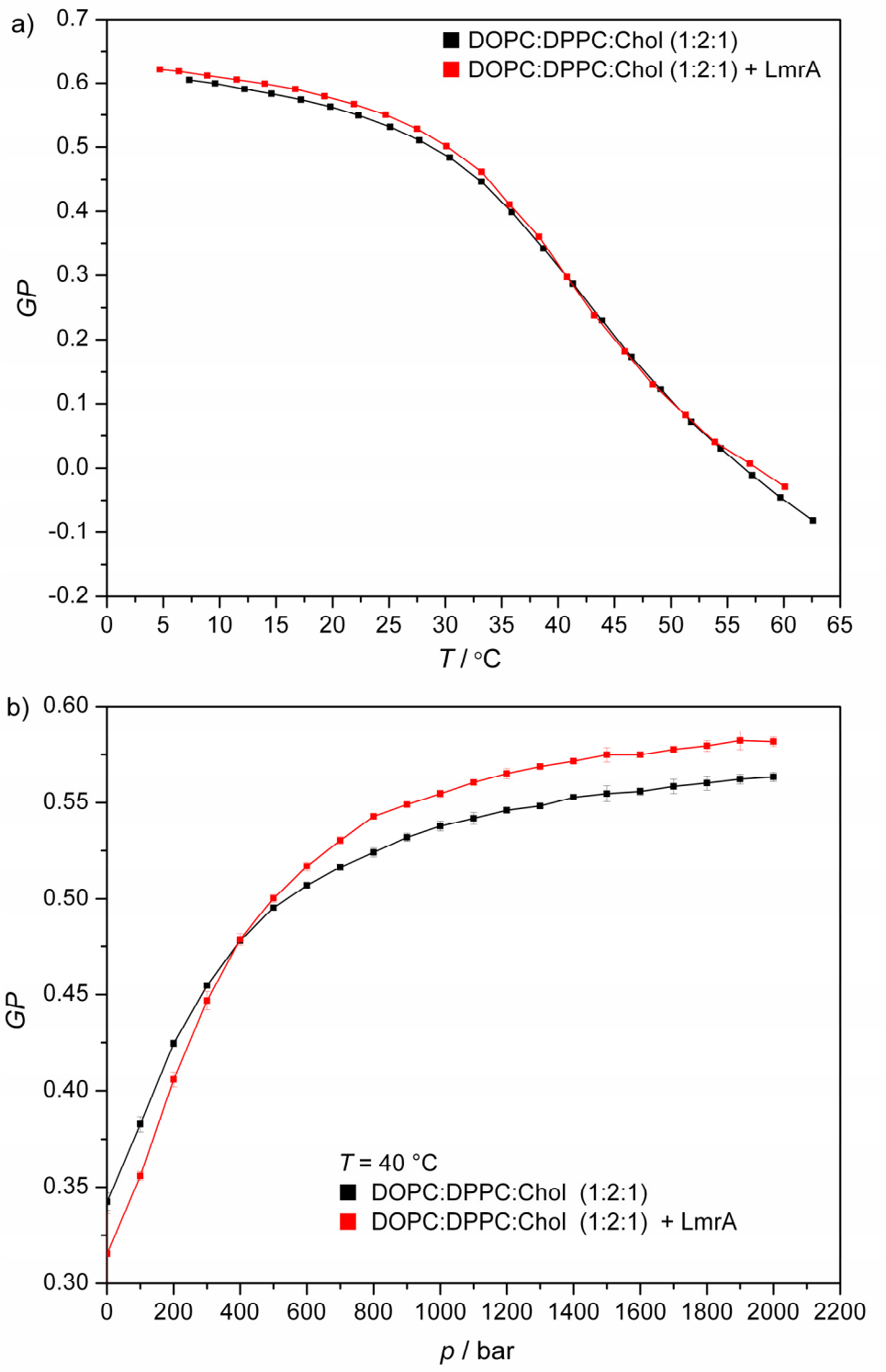

Figure 3.11(a): Temperature dependence of Laurdan *GP* values of vesicles made of the raft lipid system with and without reconstitution of LmrA. (b) Pressure dependence (at $T = 40$ ºC) of Laurdan *GP* values of vesicles made of the raft lipid system with and without reconstitution of LmrA.

At much higher pressures, the transition to an all s_o phase could be envisaged. However, as the lipid mixture contains cholesterol and DPPC, which might not pack well against *cis*-unsaturated lipids, this could be prohibited. *GP* values up to 400 bar in the reconstituted system are slightly smaller than those of the pure system, and above 400 bar *GP* values exhibits slightly higher values. Hence, it is clearly seen that the reconstitution of LmrA into the raft system does not drastically affect the overall behavior of the pressure dependent *GP* values.

3.2.5 Phase Behavior of the Natural Lipid System with and without LmrA

Lipids extracted from *Lactobacillus plantarum* TMW 1.460 mainly contain phosphatidylglycerol along with diphosphatidylglycerol (cardiolipin). Other phospholipids seen in decreasing amounts include shpingomyelin, lyso-phosphatidylglycerol, diacylglycerol and free fatty acids. The effect of temperature and pressure on the generalized polarization data of the Laurdan labelled natural lipid bilayer system with and without LmrA is shown in Figs. 3.12(a) and 3.12(b), respectively. Owing to the complex nature of the natural lipid extract, no sharp phase transition is observed, rather a continuous decrease of *GP* with increasing temperature. Around 50 ºC, a plateau *GP* value of 0.2 is reached. This value represents a significantly higher order of the acyl chains compared to all model membrane systems studied at this temperature. Reconstitution of LmrA profoundly increases the acyl chain order of the membrane. The effect is stronger at temperatures higher than 37 ºC. Above 37 ºC, the reconstituted system reached a maximum *GP* value of 0.43. Upon pressurization in the non reconstituted natural membrane system, the overall conformational order of the membrane increases continuously in the whole pressure range covered, i.e., from1 to 2000 bar. Over this pressure range, the *GP* value gradually increases from 0.24 to 0.44. Reconstitution of LmrA into the natural lipid environment leads to an overall increase in the conformational order of the acyl chains throughout the whole pressure range studied. However, the reconstituted system is less sensitive to environmental hydrostatic pressure changes. The *GP* value of the reconstituted system increases from 0.41 to 0.49 from ambient pressure to 2000 bar, respectively. The standard deviation of three separate readings was used for the error bar calculation.

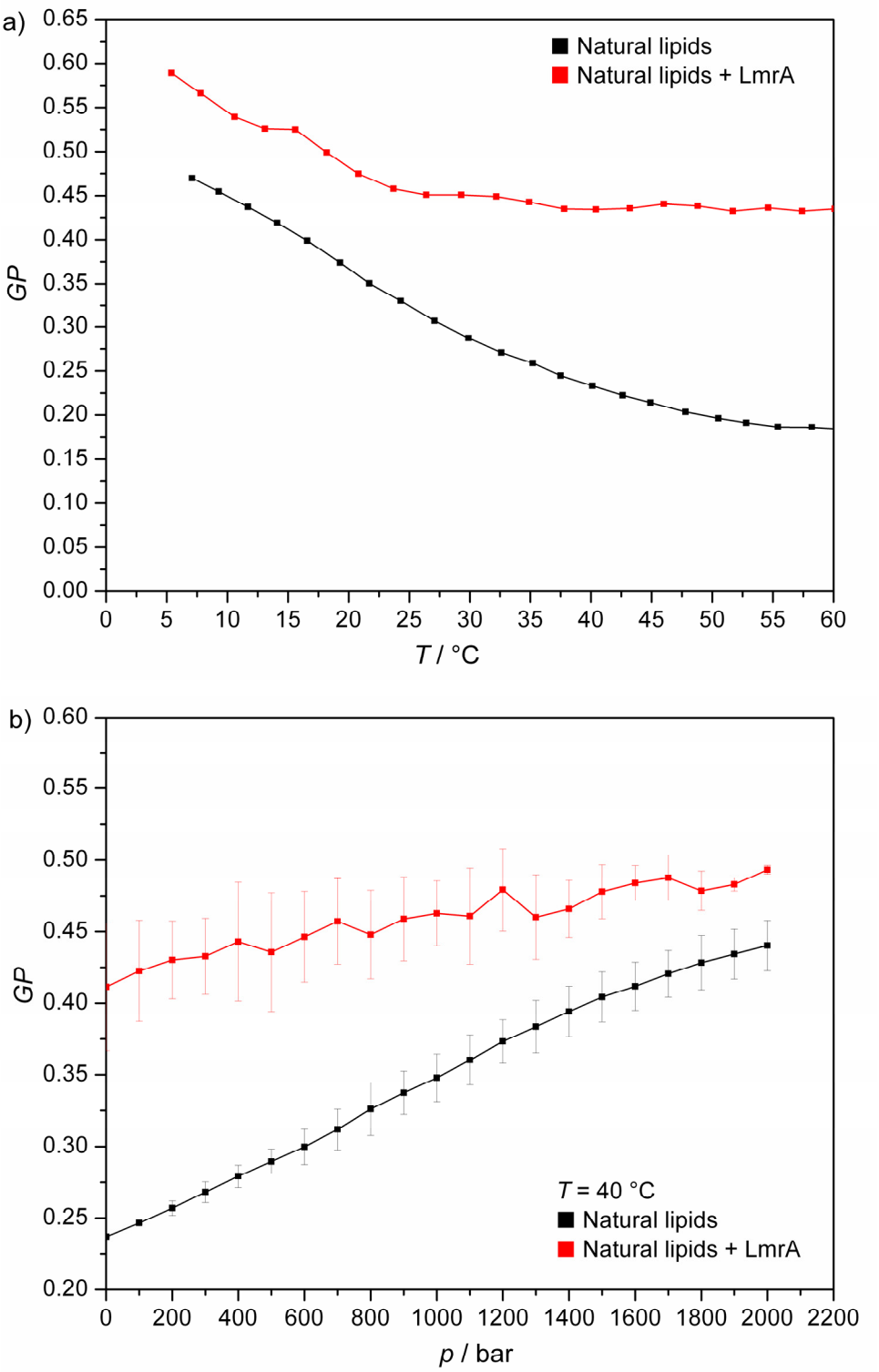

Figure 3.12(a): Temperature dependence of Laurdan *GP* values of vesicles made of natural lipid extract from *Lactobacillus plantarum* with and without reconstitution of LmrA. (b) Pressure dependence (at $T = 40$ ºC) of Laurdan *GP* values of vesicles made of the natural lipid system with and without reconstitution of LmrA.

3.2.6 AFM Measurements on Model Membrane Systems.

Using AFM experiments, the previously described three model membrane systems (DMPC, DMPC+Chol, DOPC:DPPC:Chol) were also examined. In all these systems, an extensive lipid bilayer area was detected on the mica, over which three small areas of lipid bilayers are located. In the LmrA reconstituted DMPC sample, three lipid bilayers were detected (Fig. 3.13A). The first lipid bilayer with incorporated LmrA protein shows a thickness of ~6.2 nm (red arrows in the section analysis), the second ~6.0 nm and the third bilayer ~6.6 nm. The black areas in the figure are defects in the first lipid bilayer so that the underlying mica can be seen. A few vesicles (e.g., two on the lower right side), which had not fused on the mica surface appear as big white spots. The LmrA protein is spread nearly homogeneous over the whole membrane (light brown small dots, black arrows in the section analysis), but there are also small domains present without incorporated protein. The incorporation of the protein leads to an ordering effect in the membrane which is reflected by a height difference of about 1.8 nm (green arrows in the section analysis), i.e., the membrane domains without protein show a thickness of around 4.5 nm which would correspond to a pure DMPC membrane in the gel phase [83, 84]. The extramembraneous domains of the incorporated LmrA protein protruding from the bilayer vary from 0.7 nm to 6.7 nm in size with a median of 3.1 nm (histogram in Fig. 3.13A). This particle size distribution may be explained by the membrane topology of the LmrA protein [53, 85]. The six membrane-spanning regions cause the N- and C-terminus of the protein being located at the same side of the membrane. The LmrA protein is located in the supported lipid membranes preferentially in a way that the termini will reside at the membrane surface facing the buffer solution and not the mica. However, the orientation of the incorporated protein can not be controlled. The particles possessing a smaller size could be due to the membrane protruding part of 34 amino acids of the N-terminus and the loops (5-65 amino acids) connecting the transmembrane domains. On the other hand, it is likely that the larger particles represent the hydrophilic C-terminal containing the nucleotide-binding domain (NBD, 278 amino acids). Finally, the particle size is also influenced by the orientation of the membrane protruding parts with respect to the bilayer.

In the liposomes consisting of DMPC with 10 mol% cholesterol and being reconstituted with LmrA protein, up to four lipid bilayers were measured (Fig. 3.13B).

The thickness of the lipid bilayers are ~6.4 nm for the first (green arrows in the section analysis), ~6.3 nm for the second, ~6.4 nm for the third, and ~6.6 nm for the fourth lipid bilayer. Again, the protein is spread nearly homogeneously over the whole membrane, but there are also some domains without or less incorporated protein (dark brown region on the right side of the image). Similar to the pure DMPC membrane system, the incorporation of the protein leads to an ordering effect in the membrane which is reflected by a height difference of about 1.7 nm (red arrows in the section analysis), i.e., the membrane domains without protein show a thickness of around 4.7 nm, which is in agreement with the previously determined value of 4.5 nm for a pure DMPC membrane in the gel phase. A size distribution between 1.3 nm and 6.6 nm with a median of 2.9 nm was detected, corresponding to the membrane protruding parts of the LmrA protein being incorporated in DMPC/Chol membranes (histogram in Fig. 3.13B and black arrows in the section analysis).

In the proteoliposome of LmrA in the raft mixture consisting of DOPC:DPPC:Chol-1:2:1, up to three bilayers are observed (Fig. 3.13C). In the liquid-ordered (l_o) phase, the first lipid bilayer shows a thickness of ~7.0 nm (red arrows in the section analysis), the second of ~6.9 nm, and the third lipid bilayer of ~6.8 nm. The difference between the l_o- and l_d-phase is around 1.1 nm (green arrows in the section analysis), i.e., the bilayers show a thickness of around 5.8 nm in the liquid-disordered (l_d) phase. Similar to the previous membrane systems, the LmrA protein is spread nearly homogeneously in raft membrane system as well. Interestingly, the LmrA protein is incorporated in both, the l_o- and l_d-phases. The incorporation of the protein leads again to an ordering effect in the membrane which is reflected in a height difference of about 1.7 nm, i.e., the membrane domains without protein show a thickness of around 5.2 nm in the l_o-phase and of 4.1 nm in the l_d-phase. The membrane protruding parts of the incorporated LmrA protein possess a size between 0.7 nm and 6.4 nm with a median of 2.4 nm (histogram in Fig. 3.13C and black arrows in the section analysis).

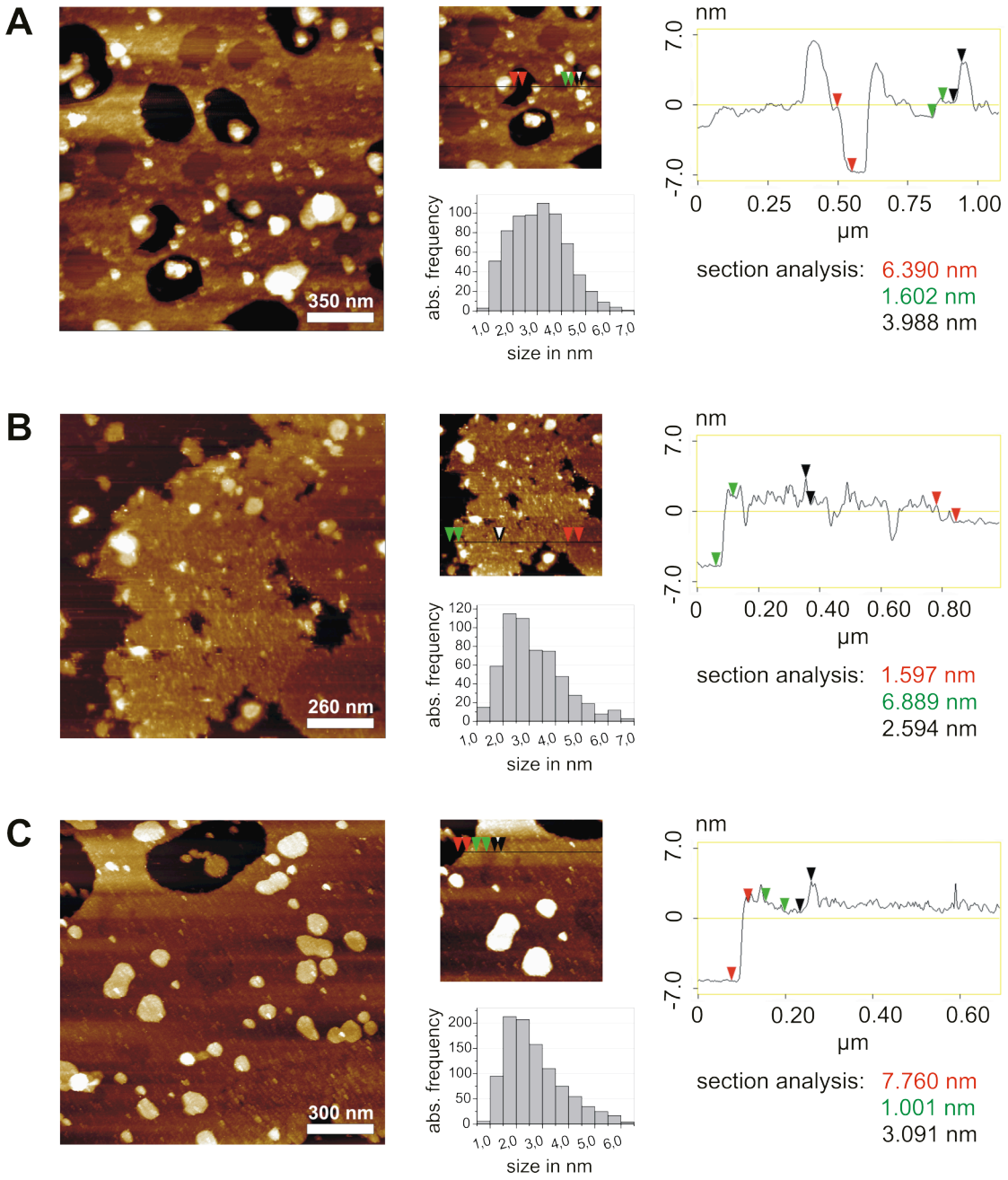

Figure 3.13: AFM measurements of proteoliposomes with the transmembrane protein LmrA incorporated into lipid bilayers composed of **(A)** DMPC, **(B)** DMPC with 10 mol % cholesterol, and **(C)** DOPC:DPPC:Chol-1:2:1. On the left hand side, the whole scan area is shown with a vertical color scale from dark brown to white corresponding to an overall height of 15 nm, 25 nm, and 25 nm for figure A, B, and C, respectively. The concomitant section profile of the AFM image is given on the right hand side. The horizontal black line in the middle figure is the localization of the section analysis shown on the right, indicating the vertical distances between pairs of arrows (black, green and red). The size distribution of the extramembraneous domains of the incorporated LmrA protein protruding from the bilayer is given in the concomitant histogram for each measurement.

3.3 Summary part II: Lipid–Protein Interactions

3.3.1 Temperature Dependent Generalized Polarization Measurements

The pure DMPC bilayers exhibit a sharp gel-to-fluid ($P_{\beta'}/L_{\alpha}$) phase transition which appears around T_m = 24°C. The incorporation of cholesterol (10 mol%) largely abolishes the sharp phase transition in DMPC bilayer and also increases the conformational order of the lipid acyl chains throughout the temperature range from 5 to 50 ^{o}C. Due to the negative transition temperature of DOPC (-20 ºC), throughout the measurement range the DOPC bilayer is in the liquid-disordered state, which is reflected by very low *GP*-values. By increasing the temperature, the fluidity of the acyl chains is still increased and leads to a further reduction in the *GP*-values. In ternary raft mixture (DOPC:DPPC:Chol) generalized polarization value gradually decreases with increasing temperature with a sigmoidal kind of shape. This type of phase behavior is consistent with an another model raft system composed of POPC:SM:Chol [23]. In fact, such a smooth behavior is expected from Gibbs' phase rule for such three-component lipid mixtures, which is very different from pure DMPC one-component lipid bilayer systems, which show sharp gel-to-gel and gel-to-fluid phase transitions in the temperature range covered [81]. Due to the complex nature of the natural lipid extract, no sharp phase transition is observed, leading to a continuous decrease of *GP* with increasing temperature up to 45 ^{o}C, finally reaching a plateau value around 0.2. Despite of the high dynamics of the lipid acyl chains at high temperatures (>45 ^{o}C), a significantly high conformational order of the acyl chains (higher *GP* values) are exhibited by the natural membrane system compared to all other model membrane system studied. This explains the highly dense packing of different lipid species present in the natural membrane system which is obviously quite different from simple and as well as more complex ternary model membrane systems.

Both LmrA and cholesterol exhibit the same effects of broadening the gel-fluid phase coexistence region and increasing the overall conformation order of the lipid acyl chains in DMPC bilayers above the phase transition temperature. Cholesterol (10 mol%) shows a larger ordering effect than LmrA. The effect is more pronounced

above the phase transition temperature. Reconstitution of LmrA into cholesterol containing DMPC bilayers further increases the ordering of the lipid acyl chains. Reconstitution of LmrA into DOPC bilayers did hardly increase the order of the acyl chains, however there is a very small increase of *GP* value throughout the temperature range covered. Due to the fact that DOPC has 18 CH_2 groups where as DMPC has only 14 in their lipid acyl chains, the hydrophobic thickness of the DOPC bilayer (27 Å) is larger compared to DMPC bilayer (22 Å) [86]. By observing the larger ordering effect of LmrA in DMPC bilayers but not in DOPC bilayers, one might conclude that a significant hydrophobic mismatch is present between DMPC bilayers and the LmrA protein's hydrophobic transmembrane segment. Reconstitution of LmrA into the raft mixture (DOPC:DPPC:Chol-1:2:1) leads to a very small, but readily reproducible increase of *GP* in the lower temperature range from 5 to 35 ^{o}C, whereas above 30 ^{o}C the LmrA have no effect on the orientational order of their acyl chains. This may be due to an even incorporation of LmrA into both l_o- and l_d-domains. This dual domain incorporation is further confirmed by AFM studies. Reconstitution of LmrA into the natural lipid environment leads to a large increase of the overall conformational order of the acyl chains in the whole temperature range covered.

3.3.2 Pressure Dependent Generalized Polarization Measurements

In case of the pure and cholesterol (10 mol%) containing DMPC bilayer systems, upon pressurization the pressure-induced fluid-to-gel phase transition takes place around 700 bar at 37 °C. Above 900 bar, both systems are insensitive to a further pressure change and a plateau *GP* value is reached. The mean order parameter of the DOPC bilayer linearly increases with increasing pressure at a constant temperature of 37 ºC. However, the *GP* value exhibited even at very high pressures of 2000 bar is less than the *GP* values of other model and natural membrane systems exhibited at 1 atm. This is due to the low transition temperature of DOPC bilayer (- 20 °C). In case of the lipid raft system (DOPC:DPPC:Chol-1:2:1), the *GP* value increases steadily with increasing pressure up to 500 bar and thereafter its rather insensitive to pressure. At 1 atm pressure (at T = 40 °C) the raft mixture exhibits a *GP* value of 0.34 and at 2000 bar it raises to 0.56, only. This small change (ΔGP = 0.22) in the *GP* value indicates that the system already exists in a relatively ordered state (liquid-ordered) throughout the pressure range covered. The lipid mixture containing cholesterol and DPPC, which

might not pack well against *cis*-unsaturated lipid (DOPC), could prohibit the system to reach a fully ordered s_o phase. Remarkably, lipids extracted from the natural membrane are less sensitive to pressure and exhibit a *GP* value of 0.24 at 1 atm and 0.44 at 2000 bar. This indicates that this system exists in a relatively ordered state (liquid-ordered) throughout the pressure range studied at $T = 40$ ºC.

Reconstitution of LmrA into the pure and cholesterol containing DMPC system leads to an increase in the overall conformational order of the membrane in the whole pressure range studied (1 to 2000 bar) at 37 ºC. The pressure dependent phase behavior does not change markedly upon the reconstitution of LmrA. The mean order parameter of the LmrA reconstituted DOPC system is slightly higher than that of the pure DOPC bilayer up to 1200 bar and it slightly reduced in higher pressures (>1200 bar) measurements carried out at a constant temperature of 37 ºC. In case of the lipid raft system, up to 400 bar, the system exhibits slightly less acyl chain order than that of the pure system, and above 400 bar, *GP* values exhibits a slightly higher order at a constant temperature of 40 ºC. However, the reconstitution of LmrA into the raft system does not affect the overall behavior of the pressure dependent *GP* measurement. Reconstitution of LmrA into the natural lipid environment leads to an increase in the overall conformational order of the acyl chains throughout the pressure range studied. However, the reconstituted system is less sensitive to environmental hydrostatic pressure changes, as the total change in the *GP* value of the reconstituted system is very low. (*GP* = 0.41 at 1 atm and *GP* = 0.49 at 2000 bar).

3.3.3 AFM Measurements

The AFM experiments demonstrate that the described reconstitution method is indeed suitable to reconstitute the purified protein in model membrane systems. It is shown that the incorporation of the transmembrane LmrA protein leads to an ordering effect in the membrane, which is reflected in an increase in membrane thickness of about 1.7 nm. Furthermore, the LmrA protein shows no phase preference in a canonical raft mixture, i.e., the protein is located in both the l_o- and l_d-phase of the DOPC:DPPC: Chol membrane. Finally, the size distribution of the LmrA protruding from the membrane's surface points towards a different orientation with respect to the lipid

bilayer, i.e., the 34 amino acid N-terminal domain, the loops and the huge hydrophilic C-terminal ATP-binding domain.

3.4 Part III: Secondary Structure of LmrA as a Function of Temperature

The LmrA transporter is a homodimer, each unit consisting of a 590 amino acids residue monomer containing 6 transmembrane helixes in the amino terminal hydrophobic domain, followed by a large hydrophilic domain containing an ATP binding site. In the functional unit of LmrA-homodimer, there are four core domains consisting of 2 transmembrane domains (one from each monomer unit) and 2 nucleotide binding domains. The structure and dynamics of the membrane embedded domains of LmrA was already investigated in the work of Erik Goormaghtigh *et al.,* [85, 87, 88]. It is reported that the reconstituted LmrA alone or in the presence of ADP has 35% α-helix, 24% β-sheets, 28% β-turn and 13% random coil [87]. Here we report the temperature dependent secondary structural change of non-reconstituted LmrA in dodecyl maltoside (DDM) micelles. Fig. 3.14 shows the temperature-dependent CD scans carried out from 30 ºC to 70 ºC with 5 ºC intervals.

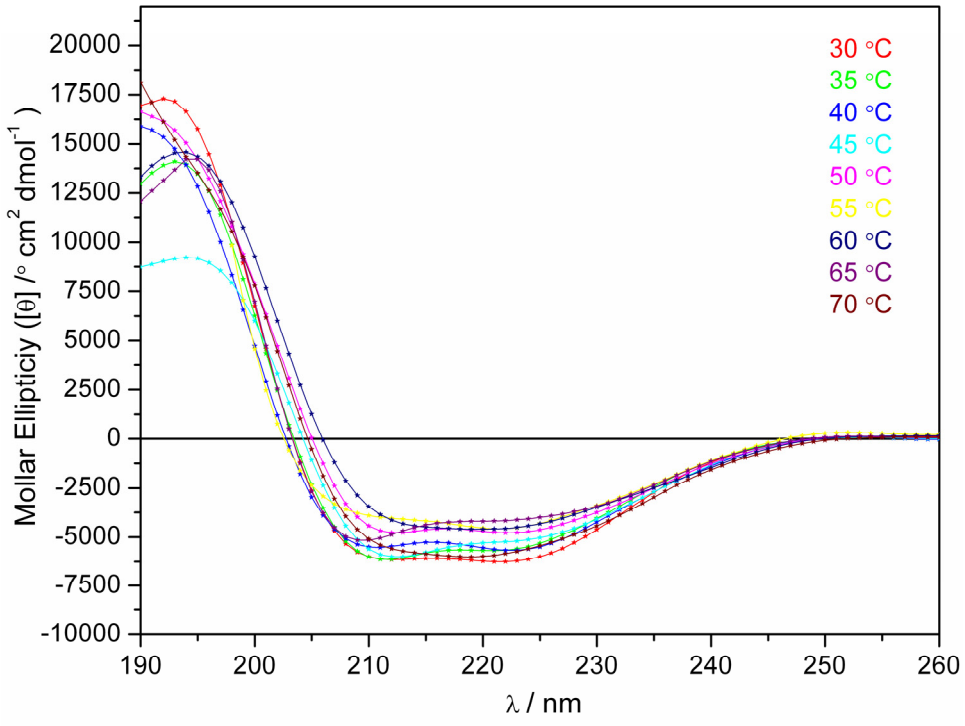

Figure 3.14: CD spectrum of LmrA in DDM micelles as a function of temperature.

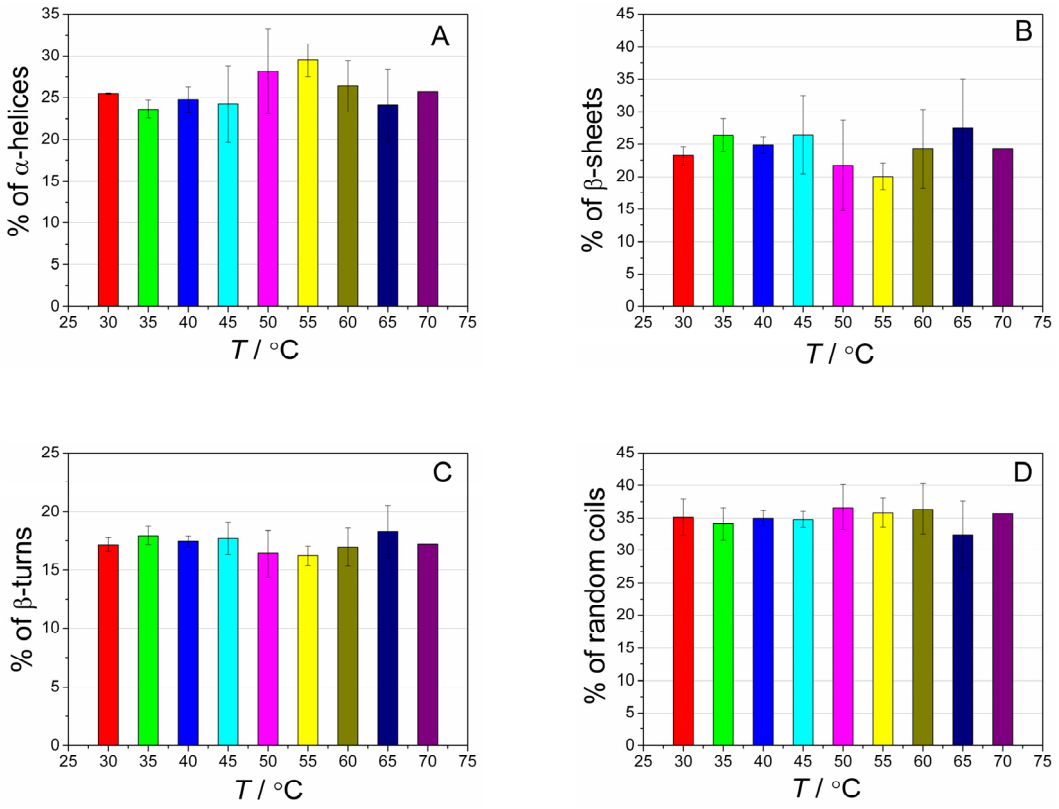

Figure 3.15: Percentage of different secondary structural contents as a function of temperature. 5.2(A) α-helices, 5.2(B) β-sheets, 5.2(C) β-turns, 5.2(D) random coils

All the spectra depict a similar shape consisting of a double minimum band at ~210 nm and at ~222 nm, and one maximum between 192 nm to 194 nm, which is characteristic of α-helices. For almost all temperatures, the molar ellipticity value falls in the negative region between 210 and 225 nm, indicates the presence of β-sheet structures. All the spectra were deconvoluted by CDNN software and the percentage of individual secondary structures was determined. Generally, the overall shape of the CD spectra and hence the proportion of the secondary structure elements did not change markedly with increasing temperature. Non-reconstituted LmrA protein present in the DDM vesicles has 26% α-helix, 24% β-sheets, 17% β-turn and 33% random coil. The α-helix and β-turn contents decrease in the non-reconstituted system compared to those of the membrane embedded environment. A decrease of 9% α-helices and 11% β-turns, is found in the micellar environment, whereas the random coil structure is more predominant in the micelle than bilayer. In the bilayer environment, the random coil constitute only 14 % whereas this conformation is increased to 33% in micellar system and the proportion of β-sheets is not affected by

the environment with about 24% in both micelles and bilayers. Fig. 3.15 depicts the changes if at all present in the secondary structural element of LmrA with increasing temperature. Obviously the protein is extremely temperature stable, nonsignificant unfolding occurs up to 70 ºC.

By deconvoluting the molar ellipticity into the secondary structure with two different softwares, namely CDNN and DicroWeb, as a function of temperature, the pattern of changes is consistence, however, the absolute percentage of α-helices is decreased to 12%and β-sheets is increased to 36% in case the of DicroWeb analysis. The turns and random coil percentage are quite close in both the analysis.

3.4.1 Summary Part III: Secondary Structure of LmrA as a Function of Temperature

The temperature dependent secondary structure of the non-reconstituted LmrA in DDM micelles were carried out from 30 to 70 ºC with 5 ºC intervals by circular dichroism spectroscopy. Overall, the shape of CD spectra did not change markedly with increasing temperature. The average proportion of the secondary structure of the non-reconstituted LmrA in DDM micelles has 26% α-helices, 24% β-sheets, 17% β-turns and 33% random coil. The α-helix and β-turns contents decrease in the non-reconstituted system compared to those of the membrane embedded environment, whereas the random coil structure is more predominant in the micelle than bilayer. The proportion of secondary structures of LmrA does not change considerably with increasing temperature; this may be explained partially due to the stability of the LmrA protein over the temperature range from 30 to 70 ºC and partially due to the protection of the secondary structures by DDM micelles.

3.5 Part-IV: Lateral Inhomogeneity of Model Raft Mixtures

3.5.1 Two-Photon Excitation Fluorescence Microscopy

Biomembranes made of multicomponent lipid system exhibit a strong heterogeneity and phase segregation originating from compositional fluctuations. To understand the role of lipid complexes and lipid domains in regulating the membrane properties, ternary mixture containing cholesterol and a saturated and an unsaturated phospholipid are often chosen in model membrane studies of lipid rafts. Even though, a number of techniques have been used to study the membrane heterogeneity, important contributions have come form fluorescence microscopy and atomic force microcopy. Fluorescence microscopy has enabled the direct visualization and analysis of phase separation in giant unilamellar vesicles (GUVs). Phases can be identified as ordered or disordered, on the basis of the known partition behavior of selective fluorescence probes. Fluorophore-Lissamine rhodamine B, (rhodamine DHPE) serves as a well-known marker of the liquid-disordered phase (red channel) and Bodipy labeled fatty acid analogue C_5-ganglioside G_{M1} were used as a raft (liquid-ordered phase) marker. In this work, GUVs formed from the ternary mixture of DOPC (di(18:1)PC), DPPC (di(16:0)PC) and cholesterol in 1:2:1 molar ratio has been chosen. Unsaturated DOPC prefers a disordered (l_d) phase whereas the saturated DPPC and cholesterol enrich in an ordered phase. The GUV images around 30 μm in diameter are shown in Fig. 3.16. The images (false color representation) are taken at various temperatures from the bottom view of the GUV. The fluorescence intensity was collected in two channels; the green channel collects the Ganglioside G_{M1} fluorescence intensity and the red channel collects the *N*–Rh-DHPE fluorescence intensity. We could clearly visualize the GUV images in both channels and the spatial distribution of two fluorophores could be examined.

In the fluid phase of the lipid bilayer system, at $T > 41$ °C (chain melting temperature of DPPC), the images in both channels coincide, indicating all vesicles are in one uniform liquid phase and both fluorophores are distributed homogeneously on the vesicle surface (Fig. 3.16A).

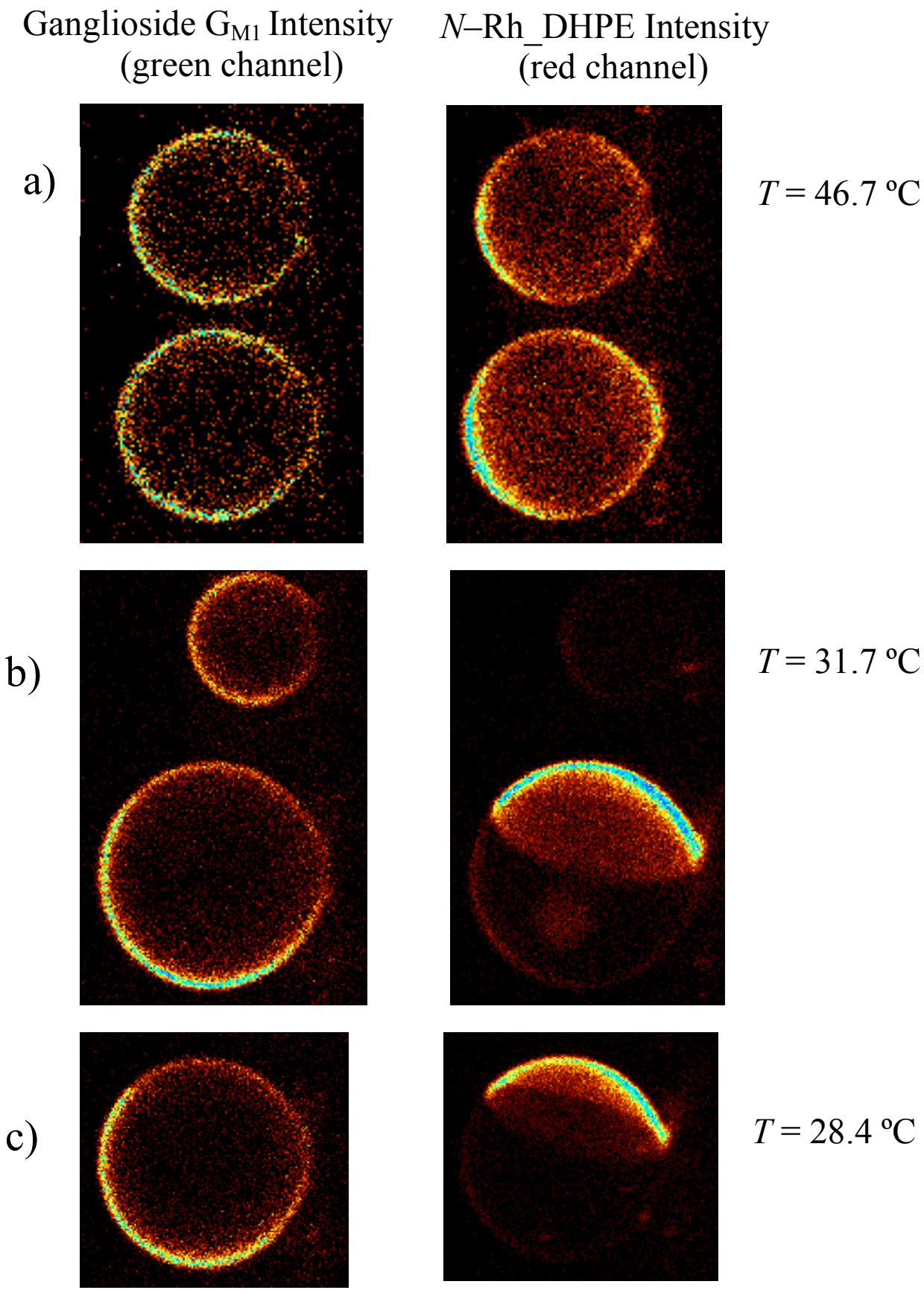

Figure 6.1: Two-photon excitation fluorescence intensity images (false color representation) of GUVs (size ~ 30 μm) consisting of DOPC:DPPC:Chol -1:2:1.

When the temperature is slowly decreased to about 30 °C, the vesicles reach a region of coexisting liquid phases. In the fluid like coexistence region, fluorophores have their choice of phases and start segregating in their favored phase. In Fig. 3.16B in the red channel the bright areas with embedded rhodamine-DHPE correspond to liquid-disordered (l_d) domains. Whereas the dark domains mainly consist of liquid-ordered (l_o) domain, which can be clearly visualized as the bright area in the green channel. It is interesting to note that the small vesicle located on the top is clearly visible in the green channel, indicating that the liquid-ordered phase is predominant at 31.7 ºC.

Further decrease in the temperature results in the growth of the domains, by colliding and merging with other domains of the same phase. From Fig. 3.16C, it is clear that all the l_o and l_d domains merge with their respective domains, and the lipids in the whole vesicle segregate into two clear separate domains.

3.5.2 Steady-State Fluorescence Polarization Measurements of Raft Mixtures

The steady-state fluorescence anisotropy data were taken in the temperature range between 3 and 75 ºC. Figure 3.17 depicts the steady-state fluorescence anisotropy data of TMA-DPH in the POPC:SM:Chol (1:1:1) and DOPC:DPPC:Chol (1:2:1) mixtures as a function of temperature. Data are very well reproducible and the errors in the r_{ss} values are negligible. As can be clearly seen in Fig. 3.17, in both lipid mixtures, the steady-state fluorescence anisotropy r_{ss} of TMA-DPH in the high temperature (liquid-crystalline) phase is significantly lower than that in the low temperature (ordered) phase, indicating that a greater dynamic molecular disorder is present in the liquid-crystalline phase of the bilayer. In case of the POPC raft mixture, the r_{ss} value reduces gradually with increasing temperature, whereas in the DOPC raft mixture there is a sharp decrease in the r_{ss} value around the chain melting temperature (41 ºC) of DPPC, indicating an increased molecular disorder above 41 ºC. In spite of having a 2:1 mole ratio of saturated DPPC in the DOPC:DPPC:Chol raft mixture, the overall r_{ss} value of this system is lower than the POPC raft mixture, which indicates that the molecular disorder in the DOPC raft system is higher in comparison to the POPC raft system. This result can be rationalized, based on the presence of two unsaturated acyl chains in

the DOPC raft system, which increases the molecular disorder by reducing the packing and order parameter.

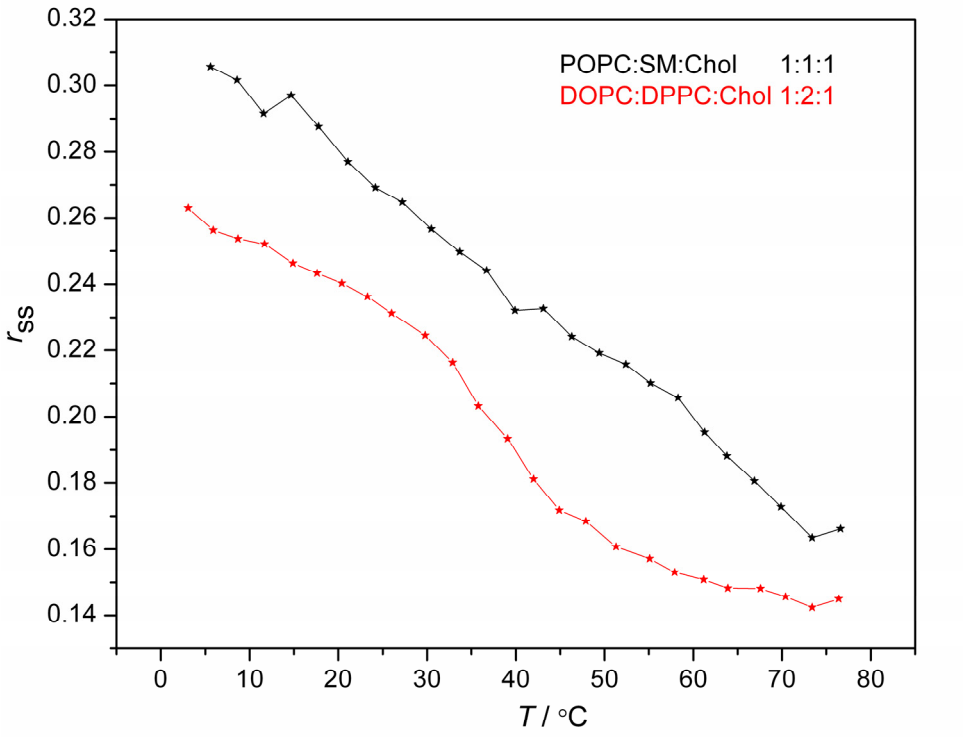

Figure 3.17: Temperature dependence of the steady-state fluorescence anisotropy r_{ss} of TMA-DPH in POPC:SM:Chol-1:1:1 and DOPC:DPPC:Chol-1:2:1 raft systems.

3.5.3 Summary Part IV: Lateral Inhomogeneity of Raft Mixtures

The steady-state fluorescence anisotropy data of TMA-DPH in the DOPC:DPPC:Chol (1:2:1) mixture as a function of temperature suggest that the acyl chain order of the canonical raft mixture depends on the temperature. Similar behavior was observed in the POPC:SM:Chol (1:1:1) raft mixture as well. Interestingly, at temperatures above the main transition temperature of DPPC, the steady-state fluorescence anisotropy data exhibit only a small change with further increase in the temperature. From the fluorescence microscopic image (Fig. 3.16A) of the DOPC:DPPC:Chol-1:2:1 raft system, it is clear that above the main transition temperature of DPPC (>41 ºC), the whole system exists in a homogenous liquid-disordered phase. All temperature below 41 ºC the system exhibits in a liquid phase coexistence region as clearly seen in Figs. 3.16B and 3.16C. This also explains the increase in the r_{ss} value below 41 ºC. The difference in acyl chain conformational order creates a difference in the bilayer thickness of the raft system, which is also quantified (1.1 nm) in AFM studies (Fig.

3.13C). Taken together, all observations from these different studies, i.e., steady-state fluorescence anisotropy measurement, generalized polarization measurement of Laurdan, fluorescence microscopic studies of GUVs and AFM measurements confirm the later inhomogeneity present in DOPC:DPPC:Chol (1:2:1) raft mixture.

3.6 Part-V: Activity Measurements of the Reconstituted LmrA Systems

3.6.1 Hoechst-33342 Transport in Proteoliposomes

The fluorescent substrate Hoechst-33342 was used to assess the transport activity of the reconstituted LmrA system. The Hoechst-33342 transport activity in proteoliposomes made of DMPC vesicles with LmrA is shown in Fig. 3.18. Hoechst-33342 is non fluorescent in aqueous environment while in the membrane environment it displays a strong fluorescence signal [51]. After collecting the background signal for around 75 s, 1.25 μM fluorophore-Hoechst was added. As we can see clearly from the Fig. 7.1, the Hoechst binds to the membrane immediately and increases the fluorescence signal several fold. Since LmrA uses the free energy of ATP hydrolysis to expel a wide variety of structurally unrelated compounds from the membrane, Mg-ATP (final concentration 1.6 mM) was added after around 100 s from the addition of Hoechst-33342. In case of LmrA non-reconstituted DMPC vesicles, the Hoechst signal did not change markedly even after 2 additions of Mg-ATP indicating that the fluorophore continuously stays in the membrane. But in case of LmrA reconstituted in DMPC vesicles after addition of Mg-ATP, the fluorescence intensity of Hoechst kept declining, suggesting that the LmrA protein is expelling the fluorescence probe Hoechst-33342 from DMPC membrane in an ATP dependent manner. From these data, it is clear that the LmrA protein is functionally reconstituted in DDM destabilized DMPC vesicles. The orientation of the LmrA in the membrane is expected to be 50% in, 50% out orientation of purified LmrA in the proteoliposomes [51].

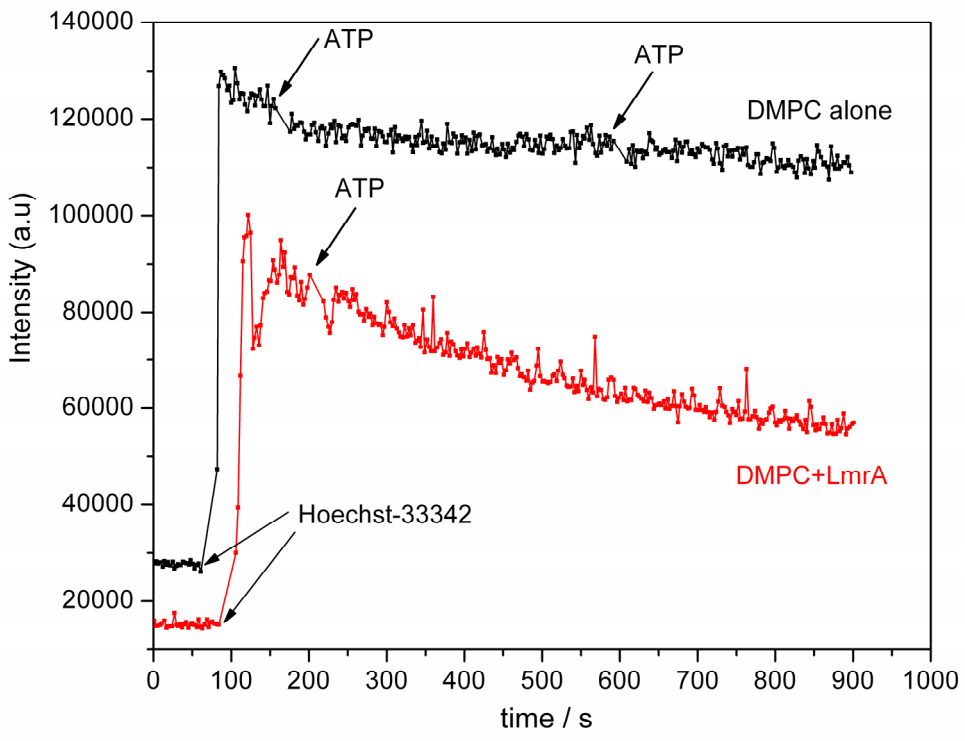

Figure 3.18: Hoechst-33342 transport in proteoliposomes.

3.6.2 ATPase Activity Using Coupled Enzyme ATPase Assay

ATP hydrolysis by the action of LmrA is also checked by the coupled ATPase enzyme assay [78, 79]. The coupled enzyme ATPase assay is based on the conversion of phosphoenolpyruvate (PEP) to pyruvate by pyruvate kinase (PK) coupled to the conversion of pyruvate to lactate by lactate dehydrogenase (LDH). The latter step requires the oxidation of NADH to NAD^+. NADH absorbs strongly at 340 nm but NAD^+ does not absorb, enabling the utilisation of following the absorbance of NADH at 340 nm with time. A decrease in NADH absorbance indicates the presence of the ATPase activity of the reconstituted system (the lower the absorbance, the higher the activity of the protein). The slope of the absorbance decay curve is inversely proportional to the dissociation rate of NADH (the higher the slope, the lower the dissociation rate of NADH). The pressure effect on the activity of LmrA is followed by checking the ATPase activity of LmrA using a coupled assay in different lipid environments at different pressures, range from 1 atm to 2000 bar. The scheme of the coupled enzyme assay is depicted as follows:

$$ATP + H_20 \xrightarrow[LmrA]{} P_i + ADP \quad (1)$$

$$ADP + PEP \xrightarrow[PK]{} Pyruvate + ATP \quad (2)$$

$$Pyruvate + NADH + H^+ \xrightarrow[LDH]{} Lactate + NAD^+ \quad (3)$$

3.6.3 Pressure Effect on the ATPase Activity of LmrA Reconstituted in DMPC Vesicles

The ATPase activity of LmrA reconstituted in the DMPC vesicles at different pressures is shown in Fig. 3.19. Experimental data are shown after performing the line fit using the Origin software. The same concentration of the reconstituted LmrA protein was used for all the pressure measurements. From the Fig. 3.19, it is clear that the LmrA reconstituted in DMPC vesicle shows a high ATPase activity at 1 atm pressure. As described in the coupled enzyme assay scheme, the absorbance of NADH decreases with time, which indicate the conversion of NADH to NAD^+. The low slope of the absorbance curve also explains the increased dissociation rate of NADH. There is no marked change in the NADH absorbance at 500 bar, which indicates that the activity of LmrA is inhibited by the pressure. The high slope of the curve also reflects the low dissociation rate of NADH at 500 bar. In the case of 1000 bar, the absorbance of NADH slightly decreased with time and the rate of dissociation of NADH is lower compared to that of 1 atm pressure. At pressures higher than 1000 bar, absorbance curve exhibits rather complex behavior. At 1500 bar, the absorbance of NADH initially decreases and after 2.5 h it increases. In case of 2000 bar, the absorbance of NADH first increases up to 2 h and then decreases. However, in comparison with the other pressures, the absorbance value of NADH is higher, indicating that the activity of LmrA is greatly decreased at these high hydrostatic pressures.

It is important to note that it takes a few minutes to seal the pressure vessel and to slowly pressurize the system before starting the measurements. So it is not possible to measure the absorbance from time zero when the ATPase reaction is started by addition of 3 mM ATP. The difference in the behavior at high pressures (>1000 bar)

indicate that the pressure-induced reaction involves two or more rate-limiting steps, which certainly is not unexpected because the ATPase reaction proceeds via several intermediate steps, which might be sensitive to pressure if significant changes in volume are involved.

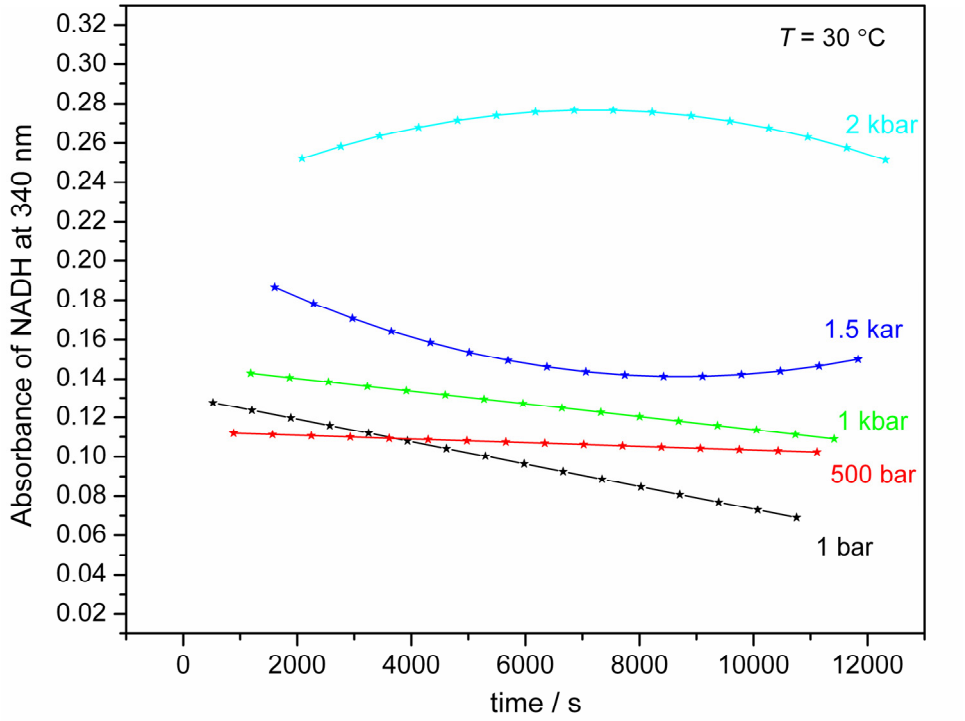

Figure 3.19: The effect of pressure on the ATPase activity of LmrA reconstituted in DMPC vesicles.

3.6.4 Pressure Effect on the ATPase Activity of LmrA Reconstituted in Raft Mixtures

The ATPase activity of LmrA reconstituted in DOPC:DPPC:Chol-1:2:1 vesicles at different pressures is shown in Fig. 3.20. From the Fig. 3.20, it is clear that the LmrA reconstituted in the raft mixture exhibits a relatively low ATPase activity at 1 atm pressure, as the absorbance of NADH did not decrease markedly with time and also the rate of NADH dissociation is low. Interestingly, the absorbance of NADH at 500 bar, decreases with time, which indicates the increased activity of LmrA. Also at 1000 bar, the activity of LmrA was retained; hence the absorbance of NADH decreases with time.

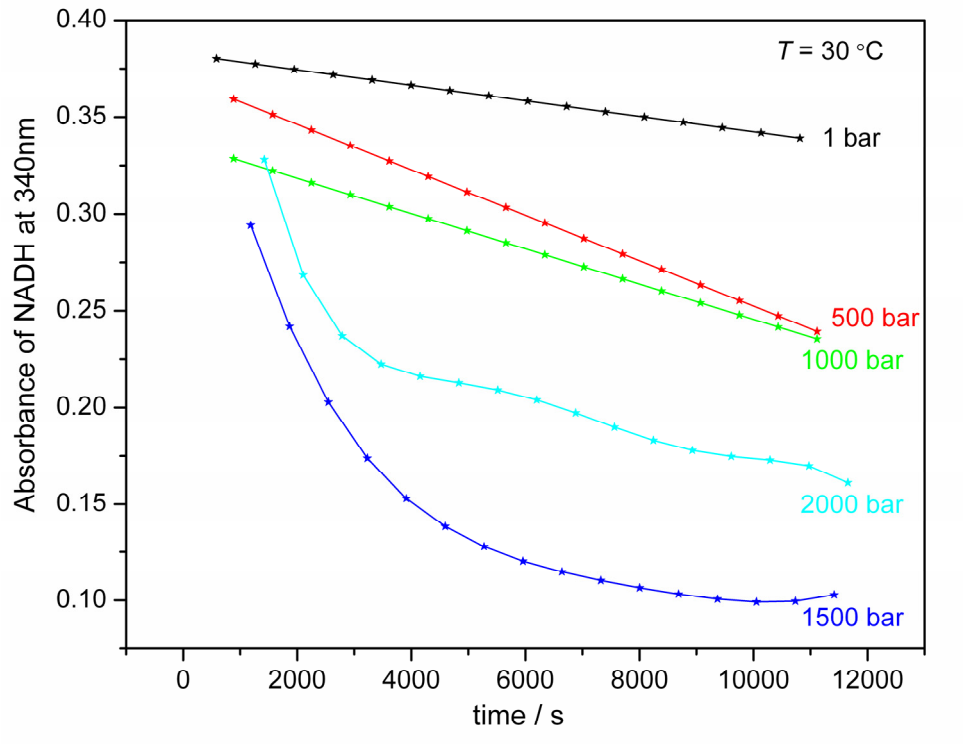

Figure 3.20: The effect of pressure on the ATPase activity of LmrA reconstituted in the model raft mixture (DOPC:DPPC:Chol).

Similar to the DMPC system, in the high pressure range (>1000 bar) the model raft system responds in a complex manner. At 1500 bar and 2000 bar the absorbance of NADH reduces very rapidly in the first hour and then it is rather insensitive to pressure. The complex behavior of the absorbance of NADH at high hydrostatic pressure can be due to the dissociation of the protein subunits, and pressure-induced conformational changes of protein. Moreover, at high hydrostatic pressure, the dissociation of the ATP itself occurs. Also, at high pressure the functionally active dimeric form of LmrA and/or the enzymes used in the assay might be dissociated [89]. However, in the low pressure range (1 atm pressure up to 1000 bar), this assay works very well and reproducible.

3.6.5 Summary Part V: Effect of Pressure on the Activity of Reconstituted LmrA in Different Lipid Environments.

The protein-LmrA belongs to an ATP-binding cassette (ABC)-type multidrug transporter which uses the free energy of ATP hydrolysis to pump structurally

unrelated compounds/drugs out of the cell membrane. The transport activity of the purified and reconstituted LmrA protein in DMPC membrane was checked by the Heochst-3342 transport assay. It is shown that the reconstituted LmrA protein expels the membrane bound fluorophore-Heochst-33342 in an ATP dependent manner, which confirms that the reconstitution protocol indeed works well with the model membrane lipid system. In order to understand the influence of lateral membrane organization on the activity of the protein, the ATPase activity of LmrA reconstituted in to pure DMPC and a model raft mixture composed of DOPC:DPPC:Chol-1:2:1 was measured by monitoring the decrease in NADH absorbance using a coupled enzyme assay method at different pressures. It is shown that the functionally reconstituted LmrA in the DMPC bilayers, exhibit a decreased activity with increasing hydrostatic pressure. This assay was carried out at 30 ºC, where the lipid acyl chains of DMPC bilayers are in a conformationally disordered state. At 1 atm pressure, the reconstituted LmrA shows considerable ATPase activity by exhibiting a decrease of NADH absorbance with time. However, with increasing pressure the activity of LmrA decreases. This activity decrease probably arises by the decreased fluidity of the DMPC lipid bilayer. The pressure-induced fluid-to-gel phase transition in LmrA reconstituted in the DMPC bilayer takes place around 700 bar at 37 ºC, and this transition takes place at a lower pressure (p = 270 bar) at 30 ºC [27]. Hence, the decreased ATPase activity of LmrA with increasing pressure can be rationalized based on the decrease in fluidity of the DMPC lipid bilayer with a subsequent decrease of the protein's conformational flexibility.

Interestingly, it is found that the ATPase activity of the reconstituted LmrA protein increases with increasing pressure in the model raft mixture composed of DOPC:DPPC:Chol-1:2:1 at 30 ºC. At this temperature, the raft system exists in the onset region of the liquid-ordered (l_o)/liquid-disordered (l_d) two phase co-existence region. By Laurdan generalized polarization measurements, it has been shown that an increase of pressure takes the system more to the l_o phase. It is worth to note that the ATPase activity of LmrA reconstituted in the raft system increases with increasing pressure. This increase in the activity with increasing pressure may be rationalized based on the ordering of the lipid acyl chains in the raft mixture, while still remaining in the l_o state with high rotational and translational mobility.

Pressure and temperature are important factors responsible for inducing phase transitions in lipid bilayers, which are accompanied by alterations in the thickness and cross-sectional area of the hydrocarbon region [25, 90-92]. These changes would be expected to alter the environment of transmembrane protein in the contact surfaces of the protein and lipid bilayer and/or the protein and water. An increase in the thickness of the lipid bilayer may partially cover the water soluble region of the transmembrane proteins and thus leading to an alteration of the function of the protein.

At high pressure above 1000 bar, the coupled assay behaves in a complex manner, which indicates that the pressure-induced reaction involves two or more rate-limiting steps, which certainly is not unexpected because the ATPase reaction proceeds via several intermediate steps. One or more steps might be sensitive to pressure if significant changes in the volume are involved. Moreover, pressure-induced conformational changes of protein, and the dissociation of the ATP itself may occur at high hydrostatic pressure. Also, at high hydrostatic pressure the functionally active dimeric form of LmrA and/or the enzymes used in the assay might be dissociated.

Taken together, the ATPase activity of functionally reconstituted LmrA is more active in the model raft mixture composed of DOPC:DPPC:Chol-1:2:1 than in a DMPC bilayer at different pressures up to 1000 bar. The reliability of the coupled assay under very high pressure above 1000 bar is questionable, however this assay works well at pressures below 1000 bar. The ATPase activity was measured for 3 h in total volume of 1.15 mL at different pressures without stirring in the high-pressure cell, so the kinetics of these reactions may be quite different in continuously mixing environments.

4. Conclusions

Cell membranes constitute one of the fundamental structural and functional elements of living organisms. In membranes, lipids and proteins are often organized into microdomains called lipid rafts. These lipid rafts (l_o lipid domains) may play a vital role in many important biological processes. Membrane proteins and lipidated peptides or proteins would either reside in or be excluded from these rafts, depending on their physio-chemical properties. Hence, it is important to study their properties, such as the lateral organization and structure of lipid rafts and their influence on the conformation and activity of membrane proteins/membrane associated proteins. In order to understand how proteins function in membranes, it is necessary to determine the ways in which proteins interact with the lipid bilayer, specifically how the proteins influence the local structure and composition of the bilayer, and on the other hand, how changes in the lipid-bilayer physical properties modulate the functional state of the proteins.

The lateral membrane organization of pure lipids, and peptide or protein incorporated lipid membranes, were studied by Laurdan fluorescence spectroscopy. Laurdan is a naphthalene-based membrane probe that displays spectral sensitivity to the polarity of the environment. Laurdan distributes equally into fluid and gel phase lipid membranes. The change in the emission spectrum of Laurdan is generally quantified by the so-called generalized polarization function (*GP*). Such values range from -1 to +1. High positive values correspond to a gel phase and high negative values correspond to a fluid like phase. Hence the measured *GP* value of a system reflects the overall phase behavior and fluidity of the membrane as a function of lipid concentration, temperature, and pressure.

In this work, lipid-peptide and lipid-protein interactions have been studied using different lipids of synthetic and natural origin. These lipids were reconstituted with a polypeptide, Gramicidin (GD), and a transmembrane multidrug transporter protein, LmrA, which is of biological and biotechnological interest.

In the scope of lipid-peptide interactions, the *GP* values of POPC:SM:Chol-1:1:1 were determined with 5 mol% of gramicidin as a function of temperature and pressure. To reveal the effect of compositional changes, the generalized polarization of Laurdan

labeled ternary lipid mixtures composed of POPC:SM:Chol, in different molar ratios (1:1:1, 2:1:1, 3:3:1, and 2.5:6.5:1) was determined as a function of temperature (3 to 75 °C) and pressure (ambient pressure up to 2500 bar at a constant temperature of 20°C). All the above mixtures have coexisting domains of different phases at room temperature. In temperature dependent studies, it was shown that the liquid-disordered /liquid-ordered phase coexistence region of POPC:SM:Chol model raft mixtures extends over a wide temperature range of about 50 ^{o}C. An overall fluid phase is reached at rather high temperatures (only above ~65 ^{o}C). Due to the disordering effect of the lipid POPC, the *GP* value over the whole temperature range is lower in the case of the 2:1:1 mixture compared to the less POPC containing 1:1:1 mixture. Vesicles made up of 2.5:6.5:1 mixture exhibit more ordered domains at 20 °C, as the *GP* value (0.56) is higher compared to all the other mixtures, thus pointing to the marked rigidifying effect of sphingomyelin. Upon pressurization at room temperature (20 ^{o}C), an overall (liquid- and/or solid-) ordered membrane state with maximal ordering of their acyl chains is reached at pressures of about 1 kbar. At 40 ^{o}C, the overall ordered lipid state of the POPC:SM:Chol-1:1:1 mixture is reached at ~2 kbar (according to the Gibbs phase rule probably l_o+s_o). Essentially, the fluid phase lipids will become ordered. A purely solid-ordered state might not be reached (if at all) until very high pressures, due to the fact that cholesterol and sphingomyelin are not expected to pack well against the *cis*-unsaturated POPC. A temperature decrease of about 50 ^{o}C has a similar effect on membrane ordering and lateral organization as a pressure increase of 1 kbar. Interestingly, in this pressure range of 2 kbar, ceasing of membrane protein function in natural membrane environments has been observed for a variety of systems [24, 29, 31, 34, 35], which might be correlated with the membrane matrix reaching a physiologically unacceptable overall ordered state at these pressures.

Incorporation of GD into the POPC:SM:Chol-1:1:1 mixture slightly increases the overall order parameter profile in the l_o+l_d two-phase coexistence region, probably by selectively partitioning into l_d domains. This is indicated by the increased *GP* values with respect to the lipid mixture without GD. The observed behavior is in contrast to the effect of GD incorporation into simple, one-component phospholipid bilayer systems. Incorporation of 5 mol% of GD has no marked effect on the phase behavior of the ternary mixture.

In the scope of lipid-protein interactions, the *GP* values of five different lipid systems were studied with and without reconstitution of LmrA protein as a function of temperature and pressure. These systems are composed of DMPC, DOPC, DMPC+10 mol% cholesterol, DOPC:DPPC:Chol-1:2:1 and natural membrane lipids extracted from *Lactobacillus plantarum.*

In temperature dependent studies, it is shown that the pure DMPC bilayer exhibits a sharp gel-to-fluid ($P_{\beta'}/L_{\alpha}$) phase transition around 24 °C. By incorporating 10 mol% cholesterol, the sharp phase transition in the DMPC bilayer was abolished with an increase of the conformational order of the lipid acyl chains was observed in the fluid phase. Due to the low transition temperature of DOPC (-20 ºC), the DOPC bilayer is in a liquid-disordered state throughout the whole temperature range (5 to 50 ºC). The ternary raft mixture (DOPC:DPPC:Chol) exhibits a phase behavior similar to the POPC:SM:Chol mixture, where the *GP* value gradually decreases with increasing temperature, following a sigmoidal kind of shape. Due to the complex nature of the natural lipid extract, no phase transitions are observed. The *GP* values continuously decrease with increasing temperature up to 50 ^{o}C and thereafter reach a rather high plateau value of around +0.2. Despite of high dynamics of lipid acyl chains at high temperatures, significantly high order of acyl chains (higher *GP* values) are exhibited by the natural membrane system compared to all other model membrane system studied. This explains the high dense packing of different lipid species present in the natural membrane system which is obviously quite different from simple and as well as more complex ternary model membrane systems.

Both LmrA and cholesterol have similar effects regarding the broadening of the gel-fluid phase coexistence region and the increase of the overall conformational order of the fluid acyl chains in the DMPC bilayers above the phase transition temperature. Reconstitution of LmrA into cholesterol containing DMPC bilayers further increases the conformational order of the lipid acyl chains. Conversely, reconstitution of LmrA into DOPC bilayer hardly increased the order of the acyl chain. Due to the fact that DOPC has 18 CH_2 groups whereas DMPC has only 14 of them in the lipid acyl chains, the DOPC bilayer has a larger hydrophobic thickness (27 Å) in comparison to the DMPC bilayer (22 Å) [86]. By noticing the higher ordering effect of LmrA in DMPC bilayers, but not in DOPC bilayers, one could conclude that a considerable

hydrophobic mismatch exists between the DMPC bilayers and the LmrA protein's hydrophobic transmembrane segment. Reconstitution of LmrA into the raft mixture (DOPC:DPPC:Chol-1:2:1) leads to a small, but readily reproducible increase of *GP* values in the lower temperature range from 5 to 35 ^{o}C, whereas above 35 ^{o}C the LmrA incorporation has no effect on the membrane conformational order. This may be due to either an even incorporation of LmrA in both l_o and l_d domains or an incorporation in the domain boundaries. Interestingly, such dual domain incorporation of the large transmembrane protein is quite different from small peptides like gramicidin which selectively incorporates only into the l_d phase. Reconstitution of LmrA into the natural lipid environment leads to a marked increase in the overall conformational order of the acyl chains in the whole temperature range studied.

In pressure dependent studies, it was shown that the pressure-induced fluid-to-gel phase transition takes place around 700 bar at 37 °C in case of both pure and cholesterol containing DMPC bilayer systems. Above 900 bar, regarding conformation -al order, both systems are insensitive to further pressure changes. A plateau *GP* value is reached in both pure (*GP* = 0.44) and cholesterol containing DMPC vesicles (*GP* = 0.54). The mean order parameter of DOPC bilayers linearly increases with increasing pressure at a constant temperature of 37 ºC. However, the *GP* value exhibited even at very high pressure of 2000 bar (*GP* = 0.02) is lower than the observed *GP* value of other model and natural membrane systems at 1 atm. Upon pressurization, both the raft mixture and the natural membrane system exhibit only a small change in the *GP* value (0.22 and 0.2 respectively) in the whole pressure range (1-2000 bar) studied. This indicates that these systems already exist in a relatively ordered phase (probably liquid-ordered) throughout the whole pressure range. A purely solid-ordered state might not be reached (if at all) until very high pressures, due to the fact that cholesterol and DPPC are not expected to pack well against the *cis*-unsaturated DOPC.

Reconstitution of LmrA into pure, and cholesterol containing DMPC system, led to an overall increase in the conformational order of the membrane in the whole pressure range studied at 37 ºC. The mean order parameter of LmrA reconstituted in the DOPC system is slightly higher than that of the pure DOPC system at all pressures. In the case of lipid raft system, up to 400 bar, the system exhibits a lower acyl chain order than that of the pure system. Above 400 bar *GP* values exhibits a slightly higher order

at a constant temperature of 40 ºC. Reconstitution of LmrA into the natural lipid environment leads to an increasing overall conformational order of the acyl chains throughout the whole pressure range. The reconstituted system is remarkably insensitive to environmental hydrostatic pressure changes from 1 atm to 2000 bar (ΔGP = 0.08 only). This reflects the fact that the membrane system already exists in a highly ordered state.

The lateral membrane organization and lipid-protein interactions were also studied by atomic force microscopy (AFM) in the case of the pure DMPC, DMPC containing 10 mol% cholesterol and the raft mixture composed of DOPC:DPPC:Chol-1:2:1. To the best of our knowledge, this is the first AFM study of the LmrA protein reconstituted in model membrane systems. From these studies it was confirmed that lateral inhomogeneity exists in the DOPC:DPPC:Chol system in the nanometer range. Reconstitution of LmrA leads to an ordering effect of the membrane thereby increasing the thickness of the membrane by about 1.7 nm in all the three systems studied. Furthermore, we found that the LmrA protein partitions into both, the l_o- and l_d -phases of the DOPC:DPPC:Chol model raft mixture.

In order to obtain a consensus description of the lateral inhomogeneity of the DOPC:DPPC:Chol mixture, fluorescence anisotropy measurements and two-photon excitation fluorescence microscopy measurements were carried out. The steady-state fluorescence anisotropy data of TMA-DPH, as a function of temperature, suggest that the acyl chain orientational order of the canonical raft mixture depends on the temperature up to 41 ºC (T_m of DPPC). Thereafter no marked change was observed. Two-photon excitation fluorescence microscopy measurements also confirmed the presence of a phase co-existence of l_o and l_d domains in this raft mixture in micrometer range below 30 ºC. It has been shown that the molecular disorder in the DOPC:DPPC: Chol-1:2:1 raft system is higher in comparison to the POPC:SM:Chol-1:1:1 model raft system.

The changes in the secondary structure of non-reconstituted LmrA in dodecyl maltoside (DDM)-micelles was measured as a function of temperature (from 30 to 70 ºC with 5 ºC intervals) using circular dichroism spectroscopy. It has been shown that the average proportion of the secondary structure over this temperature range has 26%

α-helices, 24% β-sheets, 17% β-turns and 33% random coil. The proportion of the secondary structural contents of the LmrA does not change markedly with increasing temperature, which may be partially due to the stability of the LmrA protein and partially due to the stabilization of the secondary structures surrounded by the DDM micelles.

Finally, the transport activity of the LmrA reconstituted system was checked by the Hoechst-33342 transport assay and was confirmed that the reconstituted LmrA functions in an ATP dependent manner. From this assay, it is also evident that the reconstitution protocol works and LmrA is functionally active in the reconstituted system. The ATPase activity of the LmrA reconstituted in DMPC and DOPC:DPPC:Chol raft systems were also studied at different pressures using coupled enzyme assay. It was shown that the LmrA reconstituted into the DMPC bilayers is very pressure sensitive and the ATPase activity decreases with increasing pressure. On the contrary, the LmrA reconstituted into the DOPC:DPPC:Chol-1:2:1 raft mixture exhibits an increased activity with increasing pressure. This increased activity observed with increasing pressure can be rationalized based on the increasing conformational order of the lipid acyl chains, which results in more l_o phase. In the case of the DMPC bilayer, the lipid acyl chains are in an all-gel phase ($P_{\beta'}$) at high pressures.

Hence, from these studies it has become clear that environmental factor such as high hydrostatic pressure, have a marked effect on the lipid matrix, even leading to phase transformations at a few hundred bar, which in turn, can have a significant effect on the activity of embedded membrane proteins. Finally, pressure in excess of ~ 2 kbar arrest protein function in a membranous environment, but low pressures- in a suitable membrane matrix -may even accelerate enzyme function as has been shown for LmrA in model raft mixture.

5 Zusammenfassung

Zellmembranen stellen eines der fundamentalen strukturellen und funktionellen Elemente von lebenden Organismen dar. Lipide und Proteine sind in Membranen oft in Mikrodomänen, sogenannten „lipid rafts“ organisiert. Diese „lipid rafts“ (Phasenzustand l_o in der Membran) können eine bedeutende Rolle in vielen wichtigen biologischen Prozessen spielen. Membranproteine und Lipoproteine oder –peptide reichern sich in Abhängigkeit ihrer physikalisch-chemischen Eigenschaften entweder innerhalb oder außerhalb der Rafts an. Daher ist es wichtig, Eigenschaften, wie z.B. die laterale Organisation und die Struktur von „lipid rafts“, sowie deren Einfluss auf die Konformation und Aktivität von Membranproteinen oder Proteinen, die mit Membranen im Zusammenhang stehen, zu untersuchen. Um die Funktion von Proteinen in der Membran zu verstehen, ist es notwendig die Mechanismen der Wechselwirkung von Proteinen mit Lipiddoppelschichten herauszufinden, insbesondere den Einfluss der Proteine auf die lokale Struktur und Zusammensetzung der Doppelschicht, aber auch wie Änderungen der physikalischen Eigenschaften der Lipid-Doppelschicht den funktionellen Zustand des Proteins modifizieren.

Die laterale Organisation von Membranen aus reinen Lipiden und von Membranen, in denen Peptide oder Proteine eingelagert sind, wurde mit Hilfe der Laurdan-Fluoreszenz-Spektroskopie untersucht. Laurdan ist eine Naphtalin-basierte Membransonde, welche eine spektrale Empfindlichkeit auf die Polarität der Umgebung aufweist. Laurdan verteilt sich gleichmäßig auf die fluide und die Gel-Phase der Lipidmembranen. Die Änderung des Emissions-Spektrums von Laurdan wird üblicherweise anhand der sogenannten generalisierten Polarisationsfunktion (*GP*) quantifiziert. *GP*-Werte nehmen Größen zwischen -1 und +1 an. Große positive Werte entsprechen der Gel-Phase und große negative Werte werden der fluiden Phase zugeordnet. Daher spiegelt der gemessene *GP*-Wert eines Systems das gesamte Phasenverhalten und die Fluidität der Membran als Funktion der Lipidkonzentration, der Temperatur und des Druckes wider.

In dieser Arbeit wurden Lipid-Peptid- und Lipid-Protein-Wechselwirkungen untersucht, wobei verschiedene Lipide von sowohl natürlicher, als auch synthetischer Herkunft eingesetzt wurden. Diese Lipide wurden mit einem Polypeptid, mit

Gramicidin (GD) und mit dem Multidrug-Transporter Protein LmrA rekonstituiert, wobei letzteres von biologischem und biotechnischen Interesse ist.

Im Hinblick auf die Lipid-Peptid-Wechselwirkung wurden die *GP*-Werte von POPC:SM:Chol-l:1:1 mit 5 mol% Gramicidin als Funktion der Temperatur und des Druckes untersucht. Um den Effekt von Änderungen in der Zusammensetzung aufzuklären, wurde die generalisierte Polarisation von mit Laurdan markierten, ternären Lipidmischungen, bestehend aus POPC:SM:Chol, in verschiedenen molaren Verhältnissen (1:1:1, 2:1:1, 3:3:1 und 2,5:6,5:1) als eine Funktion der Temperatur (3 bis 75 °C bei 1 atm Druck) und des Druckes (Umgebungsdruck bis 2500 bar bei einer konstanten Temperatur von 20 °C) untersucht. Alle genannten Lipidmischungen weisen ko-existierende Domänen verschiedener Phasenzustände bei Raumtemperatur auf. In temperaturabhängigen Untersuchungen wurde gezeigt, dass sich der flüssig-ungeordnete/flüssig-geordnete Phasen-Koexistenz-Bereich von POPC:SM:Chol-Modell-Raft-Mischungen über einen sehr weiten Temperaturbereich von ca. 50 °C erstreckt. Eine ausschließlich fluide Phase wird bei sehr hohen Temperaturen (nur oberhalb von ~65 °C) erreicht. Durch den unordnenden Effekt, verursacht durch das Lipid POPC, ist der *GP*-Wert über den ganzen angewandten Temperaturbereich in Bezug auf die Lipidmischung 2:1:1 niedriger im Vergleich zur Mischung 1:1:1, welche weniger POPC enthält. Vesikel, die aus der Lipidmischung 2,5:6,5:1 bestehen, weisen mehr geordnete Domänen bei 20 °C auf im Vergleich zu allen anderen verwendeten Lipidmischungen. Dies kann durch den versteifenden Effekt von Sphingomyelin erklärt werden. Unter Ausübung von Druck bei Raumtemperatur (20 °C) entsteht ein kompletter (flüssig- und/oder fest-) geordneter Membranzustand mit maximaler Ordnung der Acyl-Ketten bei einem Druck von ca.1 kbar. Bei 40 °C wird der vollständig geordnete Lipidzustand der 1:1:1 POPC:SM:Chol-Mischung bei ~2 kbar erreicht (gemäß der Gibbs'schen Phasenregel wahrscheinlich l_o+ s_o). Im Wesentlichen werden die Lipide der fluiden Phase geordnet. Ein ausschließlich fest-geordneter Zustand wird möglicherweise bis zu sehr hohen Drücken nicht erreicht (wenn überhaupt), was sich dadurch begründet, dass sich Cholesterin und Sphingomyelin zusammen mit dem cis-ungesättigten POPC erwartungsgemäß nicht sehr gut packen lassen. Eine Temperatursenkung von ca. 50 °C hat einen ähnlichen Effekt auf die Membranordnung und die laterale Organisation wie eine Druckerhöhung um 1 kbar. Interessanterweise wurde das Erlöschen der Membran-

Protein-Funktion in natürlicher Membranumgebung im Druckbereich von 2 kbar bei einer Vielzahl von Systemen beobachtet [23, 28, 30, 33, 34]. Dies könnte darauf zurückzuführen sein, dass die Matrix der Membran bei diesen Drücken einen physiologisch nicht akzeptablen gesamt-geordneten Zustand einnimmt.

Die Einlagerung von GD in die POPC:SM:Chol-1:1:1-Mischung erhöht geringfügig das Gesamt-Ordnungsparameter-Profil in der l_o+l_d Zweiphasenkoexistenzregion, möglicherweise durch selektive Aufteilung in die l_d-Domänen. Dieses macht sich durch erhöhte *GP*-Werte in Bezug auf die Lipidmischung ohne GD bemerkbar. Das beobachtete Verhalten steht im Kontrast zu dem Effekt der GD-Einlagerung in einfache, Ein-komponenten-Phospholipiddoppelschicht-Systeme. Eine Einlagerung von 5 mol% GD hat keinen signifikanten Effekt auf das Phasenverhalten der ternären Mischung.

In Hinblick auf die Lipid-Protein-Wechselwirkung wurden die *GP*-Werte von fünf verschiedenen Lipidsystemen mit und ohne Rekonstitution des Proteins LmrA in Abhängigkeit von der Temperatur und des Druckes bestimmt. Diese Systeme bestehen jeweils aus DMPC, DOPC, DMPC+10 mol% Cholesterin, DOPC:DPPC:Chol-1:2:1 und natürlichen Membranlipiden, welche aus *Lactobacillus plantarum* extrahiert wurden.

Bei temperaturabhängigen Untersuchungen wird gezeigt, dass die reine DMPC-Doppelschicht einen scharfen Gel-flüssig ($P_{\beta'}/L_\alpha$) Phasenübergang um ~24 °C aufweist. Bei Einlagerung von 10 mol % Cholesterin verschwindet dieser scharfe Phasenübergang der DMPC-Doppelschicht und die konformelle Ordnung der Lipid-Acyl-Ketten wird erhöht. Infolge der niedrigen Übergangstemperatur von DOPC (-20 °C), befindet sich die DOPC Doppelschicht über den ganzen Temperaturbereich (5 bis 50 °C) im flüssig-ungeordneten Zustand. Die ternäre Raft-Mischung (DOPC:DPPC: Chol) besitzt ein ähnliches Phasenverhalten wie die POPC:SM:Chol-Mischung. Hierbei sinkt der *GP*-Wert ebenfalls mit zunehmender Temperatur mit einem sigmoidalen Kurvenverlauf. Aufgrund der komplexen Zusammensetzung des natürlichen Lipidextraktes, werden keine Phasenübergänge beobachtet. Der *GP*-Wert nimmt gleichmäßig mit zunehmender Temperatur bis hin zu 50 °C ab, und erreicht danach einen relativ hohen Plateau-Wert von ungefähr +0.2. Trotz der hohen Dynamik

der Lipid-Acyl-Ketten bei hoheren Temperaturen kann eine signifikant höhere konformelle Ordnung der Acyl-Ketten im natürlichen Membransystem beobachtet werden im Vergleich zu allen anderen untersuchten Modell-Membran-Systemen. Dies erklärt die hohe Packungsdichte der verschiedenen Lipidarten, die in dem natürlichen Membran-System vorkommen, welche sich von einfachen und auch komplexeren ternären Modell-Membranen unterscheidet.

Sowohl LmrA, als auch Cholesterin besitzen den gleichen Effekt hinsichtlich der Verbreiterung der gel-flüssig-Phasenkoexistenzregion und erhöhen insgesamt die konformelle Ordnung der Lipid-Acyl-Ketten in der DMPC-Doppelschicht oberhalb der Phasenübergangstemperatur. Rekonstitution von LmrA in Cholesterin enthaltenden DMPC-Doppelschichten erhöht die Ordnung der Lipid-Acyl-Ketten noch weiter. Die Rekonstitution von LmrA in DOPC-Doppelschichten hingegen erhöht die Ordnung der Acyl-Ketten nicht nennenswert. Aufgrund der Tatsache, dass DOPC 18 CH_2-Gruppen besitzt, wohingegen DMPC nur 14 CH_2-Gruppen in den Lipid-Acyl-Ketten besitzt, ist die hydrophobe Dicke der DOPC-Doppelschicht (27 Å) grösser als bei der DMPC Doppelschicht (22 Å) [85]. Die Kenntnis des stärker ordnenden Effekts von LmrA in DMPC-Doppelschichten, jedoch nicht in DOPC-Doppelschichten, legt den Schluss nahe, dass eine beträchtliche hydrophobe Unverträglichkeit zwischen der DMPC-Doppelschicht und dem hydrophoben Transmembransegment von LmrA herrscht. Die Rekonstitution von LmrA in die Raft-Mischung (DOPC:DPPC:Chol-1:2:1) führt zu einer geringfügigen, aber vollständig reproduzierbaren Zunahme des *GP*-Werts im niedrigen Temperaturbereich zwischen 5 und 35 °C, wobei die Einlagerung von LmrA oberhalb von 30 °C keinen Effekt mehr auf die konformelle Ordnung der Membran hat. Dieses könnte entweder auf eine gleichmäßige Einlagerung von LmrA sowohl in die l_o- als auch in die l_d-Domänen, oder eine Einlagerung in die Domänengrenzen zurückzuführen sein. Interessanterweise ist diese Domäneneinlagerung der großen Transmembranproteine völlig anders als bei kleinen Peptiden wie Gramicidin, welches sich selektiv in die l_d-Phase einlagert. Rekonstitution von LmrA in die natürliche Lipidumgebung führt zu einer starken Zunahme der gesamten konformellen Ordnung der Acyl-Ketten im gesamten Temperaturbereich, der abgedeckt wurde.

In druckabhängigen Untersuchungen wurde gezeigt, dass der druckinduzierte flüssig-gel Phasenübergang sowohl im Falle von reinen, als auch im Falle von cholesterinhaltigen DMPC-Doppelschicht-Systemen bei ~700 bar bei 37 °C stattfindet. Oberhalb von 900 bar verhalten sich beide Systeme hinsichtlich der konformellen Ordnung unempfindlich gegenüber weiteren Druckänderungen. Sowohl in reinen (*GP* = 0,44) als auch in cholesterinhaltigen DMPC-Vesikeln (*GP* = 0,54) wird ein Plateau-*GP*-Wert erreicht. Der mittlere Ordnungsparameter der DOPC-Doppelschicht erhöht sich linear mit zunehmendem Druck bei einer konstanten Temperatur von 37 °C. Der *GP*-Wert ist jedoch auch bei sehr hohem Druck von 2000 bar (*GP* = 0,02) kleiner als bei anderen synthetischen und natürlichen Membransystemen bei 1 atm. Unter Druckerhöhung weisen sowohl die Raft-Mischung, als auch das natürliche Membransystem lediglich eine kleine Änderung des *GP*-Wertes (0,22 und 0,2 entsprechend) im gesamten angewendeten Druckbereich (1-2000 bar) auf. Das deutet darauf hin, dass diese Systeme bereits in einem relativ geordneten Zustand (möglicherweise flüssig-geordnet) im untersuchten Druckbereich vorliegen. Da sich Cholesterin und DPPC-Moleküle schlecht mit dem cis-ungesättigten Lipid (DOPC) packen lassen, dürfte ein rein fest-geordneter Zustand bis zu sehr hohen Drücken nicht erreicht werden.

Rekonstitution von LmrA in reinen und cholesterinhaltigen DMPC-Systemen führte zu einem allgemeinen Anstieg der konformellen Ordnung der Membran im gesamten untersuchten Druckbereich bei 37 °C. Der mittlere Ordnungsparameter von LmrA, welches im DOPC-System rekonstituiert wurde, ist bei allen Drücken geringfügig größer als der im reinen DOPC-System. Bei den Lipid-Rafts zeigt das System bis zu 400 bar eine etwas geringere Ordnung der Acyl-Ketten als im reinen System. Oberhalb von 400 bar nimmt es bei einer konstanten Temperatur von 40 °C eine geringfügig höhere Ordnung an. Rekonstitution von LmrA in die natürliche Membranumgebung führt zu einer Zunahme der konformellen Gesamtordnung der Acyl-Ketten über den gesamten untersuchten Druckbereich. Das rekonstituierte System ist bedeutend unempfindlicher gegenüber Änderungen des hydrostatischen Umgebungsdruckes von 1 atm bis 2000 bar (ΔGP = 0,08). Das bedeutet, dass das System bereits in einem maximal geordneten Zustand vorliegt.

Die laterale Membranorganisation und die Lipid-Protein-Wechselwirkung wurde außerdem mit Rasterkraftmikroskopie (AFM) für reines DMPC, eine DMPC-Mischung, welche 10 mol-% Cholesterin enthält, sowie eine Raft-Mischung, bestehend aus DOPC:DPPC:Chol-1:2:1, analysiert. Unseres Wissens nach ist dies die erste AFM-Untersuchung des in Modellmembranen rekonstituierten LmrA-Proteins. Anhand dieser Studien konnte gezeigt werden, dass eine laterale Inhomogenität in dem DOPC:DPPC:Chol-System im Nanometer-Bereich existiert. Die Rekonstitution von LmrA führt zu einem ordnenden Effekt auf die Membran und die Dicke der Membran wird um ungefähr 1.7 nm in allen drei untersuchten Systemen verstärkt. Es wurde auch bestätigt, dass das LmrA-Protein sich sowohl in der l_o-, als auch in der l_d-Phase der DOPC:DPPC:Chol-Mischung befindet.

Um ein einvernehmlicheres Bild über die laterale Inhomogenität der DOPC:DPPC:Chol-Mischung zu erhalten, wurden Fluoreszenz-Anisotropie-Messungen und Zwei-Photonen-Anregungs-Fluoreszenz-Mikroskopie-Messungen durchgeführt. Die stationären Fluoreszenz-Anisotropie-Daten des Fluorophors TMA-DPH als Funktion der Temperatur lassen vermuten, dass die Orientierungsordnung der Acyl-Ketten der kanonischen Raft-Mischung bis zu 41 °C von der Temperatur abhängt (T_m von DPPC). Darüber hinaus wurde keine signifikante Änderung mehr festgestellt. Zwei-Photonen-Anregungs-Fluoreszenz-Mikroskopie-Messungen bestätigten ebenfalls die Gegenwart einer Phasen-Koexistenz von l_o- und l_d-Domänen in dieser Raft-Mischung im Mikrometerbereich unterhalb von 30 °C. Es wurde weiterhin gezeigt, dass die molekulare Unordnung im DOPC:DPPC:Chol-1:2:1- Raftsystem im Vergleich zum POPC:SM:Chol-1:1:1-Modell-Raftsystem höher ist.

Die Änderungen der Sekundärstruktur von nicht-rekonstituiertem LmrA in dodecyl maltoside (DDM)-Mizellen wurden als Funktion der Temperatur (von 30 bis 70 °C in 5 °C Intervallen) mit Hilfe Zirkulardichroismus-Spektroskopie bestimmt. Es wurde gezeigt, dass die durchschnittliche Zusammensetzung der Sekundärstruktur über diesen Temperaturbereich aus 26% α-Helices, 24% β-Faltblättern, 17% β-turns und 33% Zufallsknäueln besteht. Die Zusammensetzung der Sekundärstrukturanteile von LmrA ändert sich nicht beachtenswert mit ansteigender Temperatur, was sich teilweise durch die Stabilität des LmrA Proteins, teilweise aber auch durch die Stabilisierung der Sekundärstrukturen durch die sie umgebenden DDM-Mizellen erklären lässt.

Schließlich wurde die Transportaktivität des rekonstituierten LmrA mit dem Hoechst-33342 Transportassay überprüft, und es wurde bestätigt, dass rekonstituiertes LmrA ATP-getrieben funktioniert. Anhand des Assays ist auch ersichtlich, dass das Rekonstitutionsprotokoll funktioniert, und dass LmrA im rekonstituierten System funktionell aktiv ist. Die ATPase-Aktivität des in DMPC und DOPC:DPPC:Chol-Raftsystemen rekonstituierten LmrA wurde auch unter Verwendung eines gekoppelten Enzym-Assays bei verschieden Drücken untersucht. Es wurde gezeigt, dass das in DMPC-Doppelschichten rekonstituierte LmrA sehr druckempfindlich ist, und dass die ATPase-Aktivität mit zunehmendem Druck nachlässt. Im Kontrast dazu zeigt das in DOPC:DPPC:Chol-1:2:1-Raftmischungen rekonstituierte LmrA eine Zunahme der Aktivität mit zunehmendem Druck. Diese Zunahme lässt sich durch die Ordnung der Lipid-Acyl-Ketten in der Raft-Mischung erklären, welche einem l_o-Zustand gleichkommt. In der DMPC-Doppelschicht liegen die Lipid-Acyl-Ketten unter hohem Druck alle in der Gelphase ($P_{\beta'}$) vor.

Demzufolge wurde aus diesen Studien deutlich, dass Umgebungsfaktoren wie hoher hydrostatischer Druck, einen signifikanten Einfluss auf die Lipidmatrix ausüben, und sogar zu Phasenübergängen bei wenigen hundert bar führen, welche wiederum einen merklichen Einfluss auf die Aktivität der eingebetteten Membranproteine haben. Letztlich blockieren Drücke über ~2 kbar hinaus die Proteinfunktion in einer Membranumgebung, niedrige Drücke jedoch - in einer passenden Membranmatrix - können die Enzymfunktion sogar beschleunigen, wie es für LmrA in der Modell-Raft-Mischung gezeigt wurde.

6. References

1. Singer, S.J. and G.L. Nicolson, The fluid mosaic model of the structure of cell membranes. *Science*, 1972. **175**(23): p. 720-31.

2. Pietzsch, J. *Mind the membrane*. in *A living frontier – exploring the dynamics of the cell membrane*. 2004. Palazzo Arzaga in Italy

3. Bretscher, M.S., Membrane structure: some general principles. *Science*, 1973. **181**(100): p. 622-9.

4. Anderson, R.G. and K. Jacobson, A role for lipid shells in targeting proteins to caveolae, rafts, and other lipid domains. *Science*, 2002. **296**(5574): p. 1821-5.

5. Edidin, M., The state of lipid rafts: from model membranes to cells. *Annu Rev Biophys Biomol Struct*, 2003. **32**: p. 257-83.

6. Janosch, S., C. Nicolini, B. Ludolph, C. Peters, M. Volkert, T.L. Hazlet, E. Gratton, H. Waldmann, and R. Winter, Partitioning of dual-lipidated peptides into membrane microdomains: lipid sorting vs peptide aggregation. *J Am Chem Soc*, 2004. **126**(24): p. 7496-503.

7. London, E. and D.A. Brown, Insolubility of lipids in triton X-100: physical origin and relationship to sphingolipid/cholesterol membrane domains (rafts). *Biochim Biophys Acta*, 2000. **1508**(1-2): p. 182-95.

8. Mukherjee, S. and F.R. Maxfield, Membrane domains. *Annu Rev Cell Dev Biol*, 2004. **20**: p. 839-66.

9. Munro, S., Lipid rafts: elusive or illusive? *Cell*, 2003. **115**(4): p. 377-88.

10. Simons, K. and E. Ikonen, Functional rafts in cell membranes. *Nature*, 1997. **387**(6633): p. 569-72.

11. Simons, K. and W.L. Vaz, Model systems, lipid rafts, and cell membranes. *Annu Rev Biophys Biomol Struct*, 2004. **33**: p. 269-95.

12. Fantini, J., N. Garmy, R. Mahfoud, and N. Yahi, Lipid rafts: structure, function and role in HIV, Alzheimer's and prion diseases. *Expert Rev Mol Med*, 2002. **4**(27): p. 1-22.

13. Israelachvili, J.N., S. Marcelja, and R.G. Horn, Physical principles of membrane organization. *Q Rev Biophys*, 1980. **13**(2): p. 121-200.

14. Mouritsen, O.G., *Life as a matter of fat, The emerging science of lipidomics*. 2005: Springer-Verlage, Heidelberg.

15. Ipsen, J.H., G. Karlstrom, O.G. Mouritsen, H. Wennerstrom, and M.J. Zuckermann, Phase equilibria in the phosphatidylcholine-cholesterol system. *Biochim Biophys Acta*, 1987. **905**(1): p. 162-72.

16. Needham, D. and R.S. Nunn, Elastic deformation and failure of lipid bilayer membranes containing cholesterol. *Biophys J*, 1990. **58**(4): p. 997-1009.

17. Bloom, M., E. Evans, and O.G. Mouritsen, Physical properties of the fluid lipid-bilayer component of cell membranes: a perspective. *Q Rev Biophys*, 1991. **24**(3): p. 293-397.

18. Jensen, M.O. and O.G. Mouritsen, Lipids do influence protein function-the hydrophobic matching hypothesis revisited. *Biochim Biophys Acta*, 2004. **1666**(1-2): p. 205-26.

19. Lee, A.G., How lipids affect the activities of integral membrane proteins. *Biochim Biophys Acta*, 2004. **1666**(1-2): p. 62-87.

20. Mouritsen, O.G. and K. Jorgensen, A new look at lipid-membrane structure in relation to drug research. *Pharm Res*, 1998. **15**(10): p. 1507-19.

21. Veatch, S.L. and S.L. Keller, Separation of liquid phases in giant vesicles of ternary mixtures of phospholipids and cholesterol. *Biophys J*, 2003. **85**(5): p. 3074-83.

22. Czeslik., C., O. Reis., R. Winter., and G. Rapp., Effect of high pressure on the structure of dipalmitoylphosphatidylcholine bilayer membranes: A synchrotron-X-ray diffraction and FT-IR spectroscopy study using the diamond anvil technique. *Chem. Phys. Lip*, 1998. **91**: p. 135-144.

23. Periasamy, N. and R. Winter, The effects of temperature, pressure and peptide incorporation on ternary model raft mixtures--a Laurdan fluorescence spectroscopy study. *Biochim Biophys Acta*, 2006. **1764**(3): p. 398-404.

24. R. Winter (Ed.), *Advances in High Pressure Bioscience and Biotechnology*. 2003: Springer-Verlag, Heidelberg.

25. R. Winter, W.C.P., A SANS study of high pressure phase transitions in model biomembranes. *Ber. Bunsenges. Phys. Chem*, 1989. **93** p. 708-717.

26. Winter, R. and C. Czeslik., Pressure effects on the structure of lyotropic lipid mesophases and model biomembrane systems. *Z. Kristallogr*, 2000. **215**: p. 454-474.

27. Winter, R. and W. Dzwolak, Exploring the temperature-pressure configurational landscape of biomolecules: from lipid membranes to proteins. *Philos Transact A Math Phys Eng Sci*, 2005. **363**(1827): p. 537-62; discussion 562-3.

28. Winter, R. and W. Dzwolak, Temperature-pressure configurational landscape of lipid bilayers and proteins. *Cell Mol Biol (Noisy-le-grand)*, 2004. **50**(4): p. 397-417.

29. Balny, C., P. Masson, and K. Heremans, High pressure effects on biological macromolecules: from structural changes to alteration of cellular processes. *Biochim Biophys Acta*, 2002. **1595**(1-2): p. 3-10.

30. Zein, M. and R. Winter, Effect of temperature, pressure and lipid acyl-chain length on the structure and phase behaviour of phospholipid-gramicidin bilayers. *Phys. Chem. Chem. Phys*, 2000. **2**: p. 4545-4551.

31. Ulmer, H.M., H. Herberhold, S. Fahsel, M.G. Ganzle, R. Winter, and R.F. Vogel, Effects of pressure-induced membrane phase transitions on inactivation of HorA, an ATP-dependent multidrug resistance transporter, in Lactobacillus plantarum. *Appl Environ Microbiol*, 2002. **68**(3): p. 1088-95.

32. Scarlata, S., The effect of hydrostatic pressure on membrane-bound proteins. *Braz J Med Biol Res*, 2005. **38**(8): p. 1203-8.

33. Scarlata, S., Determination of the activation volume of PLCbeta by Gbeta gamma-subunits through the use of high hydrostatic pressure. *Biophys J*, 2005. **88**(4): p. 2867-74.

34. S. Janosch, E. Kinne-Saffran, R.K.H. Kinne, and R. Winter, *Inhibition of Na+, K+-ATPase by hydrostatic pressure*. Advances in High Pressure Bioscience and Biotechnology II, ed. R. Winter. 2003: Springer-Verlag, Heidelberg. 215-219.

35. Chong, P.L., P.A. Fortes, and D.M. Jameson, Mechanisms of inhibition of (Na,K)-ATPase by hydrostatic pressure studied with fluorescent probes. *J Biol Chem*, 1985. **260**(27): p. 14484-90.

36. Powalska, E., S. Janosch, E. Kinne-Saffran, R.K. Kinne, C.F. Fontes, J.A. Mignaco, and R. Winter, Fluorescence spectroscopic studies of pressure effects on Na+,K(+)-ATPase reconstituted into phospholipid bilayers and model raft mixtures. *Biochemistry*, 2007. **46**(6): p. 1672-83.

37. Wallace, B.A., Gramicidin channels and pores. *Annu Rev Biophys Biophys Chem*, 1990. **19**: p. 127-57.

38. Koeppe, R.E., 2nd and O.S. Anderson, Engineering the gramicidin channel. *Annu Rev Biophys Biomol Struct*, 1996. **25**: p. 231-58.

39. Sarges, R. and B. Witkop, Gramicidin a. V. the Structure of Valine- and Isoleucine-Gramicidin A. *J Am Chem Soc*, 1965. **87**: p. 2011-20.

40. Neu, H.C., The crisis in antibiotic resistance. *Science*, 1992. **257**(5073): p. 1064-73.

41. Hayes, J.D. and C.R. Wolf, Molecular mechanisms of drug resistance. *Biochem J*, 1990. **272**(2): p. 281-95.

42. Speer, B.S., N.B. Shoemaker, and A.A. Salyers, Bacterial resistance to tetracycline: mechanisms, transfer, and clinical significance. *Clin Microbiol Rev*, 1992. **5**(4): p. 387-99.

43. Roberts, M.C., Tetracycline resistance determinants: mechanisms of action, regulation of expression, genetic mobility, and distribution. *FEMS Microbiol Rev*, 1996. **19**(1): p. 1-24.

44. van Veen, H.W., R. Callaghan, L. Soceneantu, A. Sardini, W.N. Konings, and C.F. Higgins, A bacterial antibiotic-resistance gene that complements the human multidrug-resistance P-glycoprotein gene. *Nature*, 1998. **391**(6664): p. 291-5.

45. Paulsen, I.T., M.H. Brown, and R.A. Skurray, Proton-dependent multidrug efflux systems. *Microbiol Rev*, 1996. **60**(4): p. 575-608.

46. Nikaido, H., Multidrug efflux pumps of gram-negative bacteria. *J Bacteriol*, 1996. **178**(20): p. 5853-9.

47. Lewis, k., D.C. Hooper., and M. Ouellette., Multidrug Resistance Pumps Provide Broad Defense. *ASM News* 1997. **63**: p. 605–610.

48. Putman, M., H.W. van Veen, and W.N. Konings, Molecular properties of bacterial multidrug transporters. *Microbiol Mol Biol Rev*, 2000. **64**(4): p. 672-93.

49. Sakamoto, K. and W.N. Konings, Beer spoilage bacteria and hop resistance. *Int J Food Microbiol*, 2003. **89**(2-3): p. 105-24.

50. Mazurkiewicz, P., A.J. Driessen, and W.N. Konings, Energetics of wild-type and mutant multidrug resistance secondary transporter LmrP of Lactococcus lactis. *Biochim Biophys Acta*, 2004. **1658**(3): p. 252-61.

51. Margolles, A., M. Putman, H.W. van Veen, and W.N. Konings, The purified and functionally reconstituted multidrug transporter LmrA of Lactococcus

lactis mediates the transbilayer movement of specific fluorescent phospholipids. *Biochemistry*, 1999. **38**(49): p. 16298-306.

52. Sakamoto, K., A. Margolles, H.W. van Veen, and W.N. Konings, Hop resistance in the beer spoilage bacterium Lactobacillus brevis is mediated by the ATP-binding cassette multidrug transporter HorA. *J Bacteriol*, 2001. **183**(18): p. 5371-5.

53. van Veen, H.W., K. Venema, H. Bolhuis, I. Oussenko, J. Kok, B. Poolman, A.J. Driessen, and W.N. Konings, Multidrug resistance mediated by a bacterial homolog of the human multidrug transporter MDR1. *Proc Natl Acad Sci U S A*, 1996. **93**(20): p. 10668-72.

54. Bolhuis, H., H.W. van Veen, D. Molenaar, B. Poolman, A.J. Driessen, and W.N. Konings, Multidrug resistance in Lactococcus lactis: evidence for ATP-dependent drug extrusion from the inner leaflet of the cytoplasmic membrane. *Embo J*, 1996. **15**(16): p. 4239-45.

55. Bolhuis, H., D. Molenaar, G. Poelarends, H.W. van Veen, B. Poolman, A.J. Driessen, and W.N. Konings, Proton motive force-driven and ATP-dependent drug extrusion systems in multidrug-resistant Lactococcus lactis. *J Bacteriol*, 1994. **176**(22): p. 6957-64.

56. Higgins, C.F., ABC transporters: from microorganisms to man. *Annu Rev Cell Biol*, 1992. **8**: p. 67-113.

57. van Veen, H.W., A. Margolles, M. Muller, C.F. Higgins, and W.N. Konings, The homodimeric ATP-binding cassette transporter LmrA mediates multidrug transport by an alternating two-site (two-cylinder engine) mechanism. *Embo J*, 2000. **19**(11): p. 2503-14.

58. Royer, C.A., Probing protein folding and conformational transitions with fluorescence. *Chem Rev*, 2006. **106**(5): p. 1769-84.

59. Parasassi, T., E. Gratton, W.M. Yu, P. Wilson, and M. Levi, Two-photon fluorescence microscopy of laurdan generalized polarization domains in model and natural membranes. *Biophys J*, 1997. **72**(6): p. 2413-29.

60. Parasassi, T., G. De Stasio, A. d'Ubaldo, and E. Gratton, Phase fluctuation in phospholipid membranes revealed by Laurdan fluorescence. *Biophys J*, 1990. **57**(6): p. 1179-86.

61. Bagatolli, L.A., S.A. Sanchez, T. Hazlett, and E. Gratton, Giant vesicles, Laurdan, and two-photon fluorescence microscopy: evidence of lipid lateral separation in bilayers. *Methods Enzymol*, 2003. **360**: p. 481-500.

62. Rigaud, J.L., B. Pitard, and D. Levy, Reconstitution of membrane proteins into liposomes: application to energy-transducing membrane proteins. *Biochim Biophys Acta*, 1995. **1231**(3): p. 223-46.

63. Gratton, E. and M. Limkeman, A continuously variable frequency cross-correlation phase fluorometer with picosecond resolution. *Biophys J*, 1983. **44**(3): p. 315-24.

64. Spencer, R.D. and G. Weber, Influence of Brownian rotations and energy transfer upon the measurements of fluorescence lifetimes. *J. Chem. Phys.*, 1970. **52**: p. 1654-1663.

65. Pauling, L. and R.B. Corey, Configurations of Polypeptide Chains With Favored Orientations Around Single Bonds: Two New Pleated Sheets. *Proc Natl Acad Sci U S A*, 1951. **37**(11): p. 729-40.

66. Wu, J., J.T. Yang, and C.-S.C. Wu, Beta-II conformations of all beta proteins can be distinguished from unordered form by circular dishcroism. *Anal.Biochem*, 1992. **200**: p. 359-364.

67. Manavalan, P. and W.C. Johnson, Jr., sensitivity of circular dichroism to protein tertiary structure class. *Nature*, 1983. **305**: p. 831-832.

68. Bohm, G., R. Muhr, and R. Jaenicke, Quantitative analysis of protein far UV circular dichroism spectra by neural networks. *Protein Eng*, 1992. **5**(3): p. 191-5.

69. Whitmore, L. and B.A. Wallace, DICHROWEB, an online server for protein secondary structure analyses from circular dichroism spectroscopic data. *Nucleic Acids Res*, 2004. **32**(Web Server issue): p. W668-673.

70. Lobley, A., L. Whitmore, and B.A. Wallace, DICHROWEB: an interactive website for the analysis of protein secondary structure from circular dichroism spectra. *Bioinformatics*, 2002. **18**(1): p. 211-212.

71. Birge, R.R., Two-photon spectroscopy of protein bound chromophores. *Acc. Chem. Res*, 1986. **19**: p. 138-146.

72. Dietrich, C., L.A. Bagatolli, Z.N. Volovyk, N.L. Thompson, M. Levi, K. Jacobson, and E. Gratton, Lipid rafts reconstituted in model membranes. *Biophys J*, 2001. **80**(3): p. 1417-28.

73. Angelova, M.I. and D.S. Dimitrov, Liposome electroformation. *Faraday Discuss. Chem. Soc.* , 1986. **81:**: p. 303-311.

74. Bagatolli, L.A. and E. Gratton, Two-Photon Fluorescence Microscopy Observation of Shape Changes at the Phase Transition in Phospholipid Giant Unilamellar Vesicles. *Biophys J,* , 1999. **77**(4): p. 2090-2101,.

75. So, P.T.C., T. French, W. Yu, K.M. Berland, C.Y. Dong, and G. E., Time-resolved Fluorescence Microscopy Using Two-photon Excitation. *Bioimaging*, 1995. **3**: p. 49-63

76. Shapiro, A.B. and V. Ling, Reconstitution of drug transport by purified P-glycoprotein. *J Biol Chem*, 1995. **270**(27): p. 16167-75.

77. Putman, M., H.W. van Veen, B. Poolman, and W.N. Konings, Restrictive use of detergents in the functional reconstitution of the secondary multidrug transporter LmrP. *Biochemistry*, 1999. **38**(3): p. 1002-8.

78. Nørby, J.G., *Coupled Assay of Na+,K+-ATPase Activity*. Methods in Enzymology Vol. 156. 1988.

79. Norby, J.G., Studies on a coupled enzyme assay for rate measurements of ATPase reactions. *Acta Chem Scand*, 1971. **25**(7): p. 2717-26.

80. de Almeida, R.F., A. Fedorov, and M. Prieto, Sphingomyelin/phosphatidylcholine/cholesterol phase diagram: boundaries and composition of lipid rafts. *Biophys J*, 2003. **85**(4): p. 2406-16.

81. G. Cevc (Ed.), Phospholipids Handbook, . *Marcel Dekkar, New York.*, 1993.

82. Eisenblatter, J. and R. Winter, Pressure effects on the structure and phase behavior of DMPC-gramicidin lipid bilayers: a synchrotron SAXS and 2H-NMR spectroscopy study. *Biophys J*, 2006. **90**(3): p. 956-66.

83. Wieland, J.A., A.A. Gewirth, and D.E. Leckband, Single-molecule measurements of the impact of lipid phase behavior on anchor strengths. *J Phys Chem B*, 2005. **109**(12): p. 5985-93.

84. Feng, Z.V., T.A. Spurlin, and A.A. Gewirth, Direct visualization of asymmetric behavior in supported lipid bilayers at the gel-fluid phase transition. *Biophys J*, 2005. **88**(3): p. 2154-64.

85. Siarheyeva, A., J.J. Lopez, I. Lehner, U.A. Hellmich, H.W. van Veen, and C. Glaubitz, Probing the molecular dynamics of the ABC multidrug transporter LmrA by deuterium solid-state nuclear magnetic resonance. *Biochemistry*, 2007. **46**(11): p. 3075-83.

86. Koert, U., Synthetic ion channels: Functional analysis and structural studies. *Phys.Chem.Chem.Phys.*, 2005. **7**: p. 1501-1506.

87. Vigano, C., A. Margolles, H.W. van Veen, W.N. Konings, and J.M. Ruysschaert, Secondary and tertiary structure changes of reconstituted LmrA induced by nucleotide binding or hydrolysis. A fourier transform attenuated total reflection infrared spectroscopy and tryptophan fluorescence quenching analysis. *J Biol Chem*, 2000. **275**(15): p. 10962-7.

88. Grimard, V., C. Vigano, A. Margolles, R. Wattiez, H.W. van Veen, W.N. Konings, J.M. Ruysschaert, and E. Goormaghtigh, Structure and dynamics of the membrane-embedded domain of LmrAinvestigated by coupling polarized ATR-FTIR spectroscopy and $^{1}H/^{2}H$ exchange. *Biochemistry*, 2001. **40**(39): p. 11876-86.

89. Schmid, G., H.D. Ludemann, and R. Jaenicke, Dissociation and aggregation of lactic dehydrogenase by high hydrostatic pressure. *Eur J Biochem*, 1979. **97**(2): p. 407-13.

90. Kato, M. and R. Hayashi, Effects of high pressure on lipids and biomembranes for understanding high-pressure-induced biological phenomena. *Biosci Biotechnol Biochem*, 1999. **63**(8): p. 1321-8.

91. Braganza, L.F. and D.L. Worcester, Hydrostatic pressure induces hydrocarbon chain interdigitation in single-component phospholipid bilayers. *Biochemistry*, 1986. **25**(9): p. 2591-6.

92. Kato, M., R. Hayashi, T. Tsuda, and K. Taniguchi, High pressure-induced changes of biological membrane. Study on the membrane-bound Na(+)/K(+)-ATPase as a model system. *Eur J Biochem*, 2002. **269**(1): p. 110-8.